FCT
Fundação para a Ciência e a Tecnologia
MINISTÉRIO DA EDUCAÇÃO E CIÊNCIA

POPH
QUALIFICAR É CRESCER.

QREN
QUADRO DE REFERÊNCIA ESTRATÉGICO NACIONAL
PORTUGAL 2007.2013

Governo da República Portuguesa

UNIÃO EUROPEIA
Fundo Social Europeu

João Carlos Lima Gonçalves Dissecting the mechanisms of dynein recruitment to the nuclear envelope during neocortical development UMinho | 2019

Universidade do Minho
Escola de Medicina

João Carlos Lima Gonçalves

Dissecting the mechanisms of dynein recruitment to the nuclear envelope during neocortical development

julho de 2019

Universidade do Minho
Escola de Medicina

João Carlos Lima Gonçalves

Dissecting the mechanisms of dynein recruitment to the nuclear envelope during neocortical development

Tese de Doutoramento em Medicina

Trabalho efetuado sob a orientação do
Doutor Richard Bert Vallee
e do
Doutor Tiago Gil Rodrigues Oliveira

julho de 2019

ACKNOWLEDGEMENTS

None of this work would have been possible without the continuous support from my two scientific mentors Richard and Tiago Gil. To Richard, for all the constant scientific inquiring and for giving me the opportunity to freely address my research questions. To Tiago Gil, for all of his enthusiasm and mentoring from a very early stage in my scientific career. Today, I am better scientist and a better person than before.

To my thesis committee members, Dr. Gregg Gundersen and Dr. Edmund Au, who thoughts and suggestions were very helpful.

To the faculty involved in the MD/PhD program, Professor Joana Palha, Professor Margarida Correia-Neves and Professor Nuno Sousa, whose efforts made this program possible. To Professor Michael Shelanski for his continuous support of the MD/PhD collaborative program.

To Tiago Dantas, for being a friend and the best bench mate that someone can ask for.

To Sebastián Quintremil, for all of his friendship and long-lasting scientific discussions.

To Dave Doobin, for being my guide in the first months in the Vallee laboratory.

To Noopur Khobrekar, for being always cheerful and supportive.

To all of the members of the Vallee and Oliveira laboratories.

To all the MD/PhD students from the program, who were like family in the US.

To all my friends, who always cheered for me.

To my mum and dad, for their unconditional support.

To my sister, my source of proudness.

To my grandad Feliciano, who educated me from an early age and nourish on me the idea of a constant search for knowledge.

Financial support for this PhD work was provided by FCT (Fundação para Ciência e Tecnologia) fellowship PD/BD/113782/2015, awarded through the University of Minho MD/PhD program.

STATEMENT OF INTEGRITY

I hereby declare having conducted this academic work with integrity. I confirm that I have not used plagiarism or any form of undue use of information or falsification of results along the process leading to its elaboration. I further declare that I have fully acknowledged the Code of Ethical Conduct of the University of Minho.

Dissecar os mecanismos de recrutamento de dineína para o invólucro nuclear durante o desenvolvimento do neocórtex.

A dineína citoplasmática-1 (dineína) é um complexo proteico composto por várias subunidades que desempenha a maioria do transporte retrógrado dependente de microtúbulos na célula. A dineína tem múltiplas funções durante o desenvolvimento cerebral, e no humano mutações em genes que codificam proteínas do complexo causam patologias graves associadas ao neurodesenvolvimento. Nas zonas mais internas do neocórtex embrionário, a proliferação de células estaminais neurais depende do recrutamento de dineína para o núcleo, durante a oscilação nuclear característica destas células. Além disso, a dineína é necessária para a transição morfológica de neurónios multipolares para bipolares, e a subsequente migração neuronal para o córtex requer o transporte do núcleo e do centrossoma pela dineína. Globalmente, os mecanismos da diversidade funcional da dineína não são bem entendidos. Neste trabalho, usamos eletroporação *in utero* para injetar plasmídeos no cérebro de embriões de ratos, que foram analisados por microscopia confocal 4 dias após a cirurgia. Com isto, descobrimos que a dineína que contém a subunidade *Light Intermediate Chain* 1 é necessária para a proliferação de células estaminais neurais, para a transição de neurónios multipolares para bipolares, e para a migração neuronal. Não encontramos nenhuma função relevante nos mecanismos anteriores para a subunidade *Light Intermediate Chain* 2, mas esta população de dineína é fundamental para a *terminal somal translocation* de neurónios, um processo em que se desconhecia o envolvimento de motores de microtúbulos. Encontramos também através de experiências com imunofluorescência em células e co-imunoprecipitações que a Nesprina-2, uma proteína do invólucro nuclear, recruta dineína através do seu adaptador BicD2. Esta cadeia de interações é importante para a migração neuronal, e quando afetada, os neurónios não conseguem entrar para a Placa Cortical, o precursor embrionário do neocórtex. A disrupção da função da Nesprina-2 ou da BicD2 interrompe o movimento nuclear, mas curiosamente não afeta o transporte do centrossoma. Então as células afectadas apresentam uma separação anormal do núcleo em relação ao centrossoma. Em suma, os nossos dados definem populações específicas de dineína que contribuem de diferente forma para o desenvolvimento cerebral, e ajudam a perceber os mecanimos envolvidos na migração neuronal. Isto é importante para ajudar a entender as patologias do neurodesenvolvimento decorrentes de mutações humanas em genes relacionados com a dineína.

Palavras-chave: BicD2, Dineína, Migração Neuronal, Nesprina-2, Neurogénese.

Dissecting the mechanisms of dynein recruitment to the nuclear envelope during neocortical development

The multi-subunit protein cytoplasmic dynein 1 (dynein) is the major retrograde microtubule motor in the cell. Dynein has multiple roles during brain development and human mutations in dynein-related genes lead to severe neurodevelopmental disorders. In the inner proliferative zones of the neocortex, division of neural stem cells depends on dynein recruitment to the nucleus during interkinetic nuclear migration. Moreover, dynein is required for the multipolar-to-bipolar transition of post-mitotic neurons, and subsequent neuronal migration requires dynein transport of both the nucleus and centrosome to form the layered neocortex. The mechanisms for dynein functional diversity in brain development and in general are unclear. In this work, we used *in utero* electroporation to deliver cDNAs and shRNAs into the developing rat brain. Analysis was performed by fixed and live imaging 4 days post injection. We found that dynein containing the Light Intermediate Chain 1 subunit is required for neural stem cell proliferation, multipolar-to-bipolar transition and glial-guided neuronal migration. We found no role in the previous mechanisms for Light Intermediate Chain 2-containing dynein, but this dynein population was required for terminal somal translocation of neurons, which was unknown to depend on microtubule motors. Further, our *in vitro* and *in vivo* evidence demonstrates that Nesprin-2, a resident protein at the nuclear envelope, recruits dynein via its adaptor BicD2, to mediate nuclear transport during glial-guided neuronal migration. Disruption of Nesprin-2 or BicD2 dynein recruitment caused a severe block in migration, as cells were arrested before reaching the cortical plate. Centrosomal movement appeared intact, but nuclear transport was impaired which led to an increase by more than 50 fold in nucleus-centrosome distance. Overall, our data define discrete dynein populations that contribute differentially to brain development. These data also elucidate the mechanisms for nuclear movement during glial-guided neuronal migration and terminal somal translocation. Ultimately, these advances might help to understand the neurodevelopmental pathologies arising from human mutations in dynein related genes.

Keywords: BicD2, Dynein, Nesprin-2, Neurogenesis, Neuronal Migration.

TABLE OF CONTENTS

ABBREVIATIONS

Adaptor domain (A-domain)

Cortical Interneurons (CINs)

Cortical Plate (CP)

Cortical Projection Neurons (CPN)

Dynein Heavy Chain (DHC or HC)

Interkinetic Nuclear Migration (INM)

Intermediate Chain (IC)

Intermediate Zone (IZ)

GTPase-like domain (G-domain)

Klarsicht, ANC-1, and Syne Homology (KASH)

Knockdown (KD)

Light Intermediate Chains (LIC)

Linker of the Nucleoskeleton and Cytoskeleton (LINC)

Microtubule Associated Protein 1C (MAP-1C)

Microtubule Associated Protein 7 (MAP-7)

Nesprin-2 Giant isoform (N2G)

Neural Stem Cells (NSC)

Nucleus-Centrosome (N-C)

Nuclear Envelope (NE)

Nuclear Pore Complexes (NPC)

Outer Radial Glia (oRG)

Radial Glial Progenitors (RG or RGPs)

Sad1 and UNC-84 (SUN)

Short Neural Precursor (SNP)

Spectrin Repeat (SR)

Subventricular Zone (SVZ)

Terminal Somal Translocation (TST)

Transmembrane Actin-associated Nuclear (TAN)

Ventricular Radial Glia (vRG)

Ventricular Surface (VS)

Ventricular Zone (VZ)

CHAPTER 1 - INTRODUCTION

1.1 Overview of the development of the neocortex

The human neocortex is the region of the brain responsible for complex cognitive behaviors. When compared to non-human primates, the neocortex in humans has more surface area, thickness and number of neurons proportional to the body size (Sousa et al., 2017). The neocortex is composed by six-layers of mostly excitatory neurons (around 80%) that make projections to the contralateral hemisphere, to deeper structures, such as the thalamus or basal ganglia, to the cerebellum, and to nuclei within the spinal cord (Marín and Müller, 2014). Neocortical development is extremely complex, and demands the fine orchestration of various cellular events. There are many fundamental questions regarding how the neocortex is developed at the molecular level and rodent models have been useful to understand mechanisms that govern brain formation, due to its similarities to neurodevelopment in humans (Figure 1) (Lui, Hansen and Kriegstein, 2011; Florio and Huttner, 2014).

By the 3rd week of gestation in humans, the neural plate folds and forms the neural tube, in which the brain is specified in the rostral region. Lining the lumen of the neural tube, neural stem cells (NSC) are organized in a pseudostratified epithelia with a highly elongated bipolar morphology. NSCs display a particular form of cell division, in which their nuclei oscillate in synchrony with the cell cycle (Kriegstein and Alvarez-buylla, 2009). After mitosis at the VS, NSCs enter the G1 phase of the cell cycle and initiate migration basally, away from the VS. Then cells enter the S phase, and in order to complete division they enter in the G2 phase, migrating apically, back toward the Ventricular Surface (VS). When NSCs reach the VS they enter mitosis. This behavior is called interkinetic nuclear migration (INM) and it was long known in the scientific community (Sauer, 1934, 1936; Sauer and Walker, 1959), but only in the recent years the mechanisms that govern it have been investigated (Bertipaglia, Gonçalves and Vallee, 2018).

In the earlier stages of neural development, NSC divide symmetrically, meaning that one mother NSC gives rise to two identical NSCs, and this serves to increase outstandingly their numbers. Later on, neurogenesis starts and NSCs acquire glial features and are now called Radial Glial Progenitors (RGPs) (Kriegstein and Alvarez-buylla, 2009). These cells display INM, but it is now restricted to the Ventricular Zone (VZ) of the developing neocortex. They maintain their apical process in contact with the ventricular lumen, and a basal process that reaches the pial surface, in the outermost region of the brain. RGPs are group of heterogeneous cells that persist during most of the late cortical development and can divide symmetrically, or asymmetrically to originate intermediate progenitors or neurons directly (Pinto and Götz, 2007; Kriegstein and Alvarez-buylla,

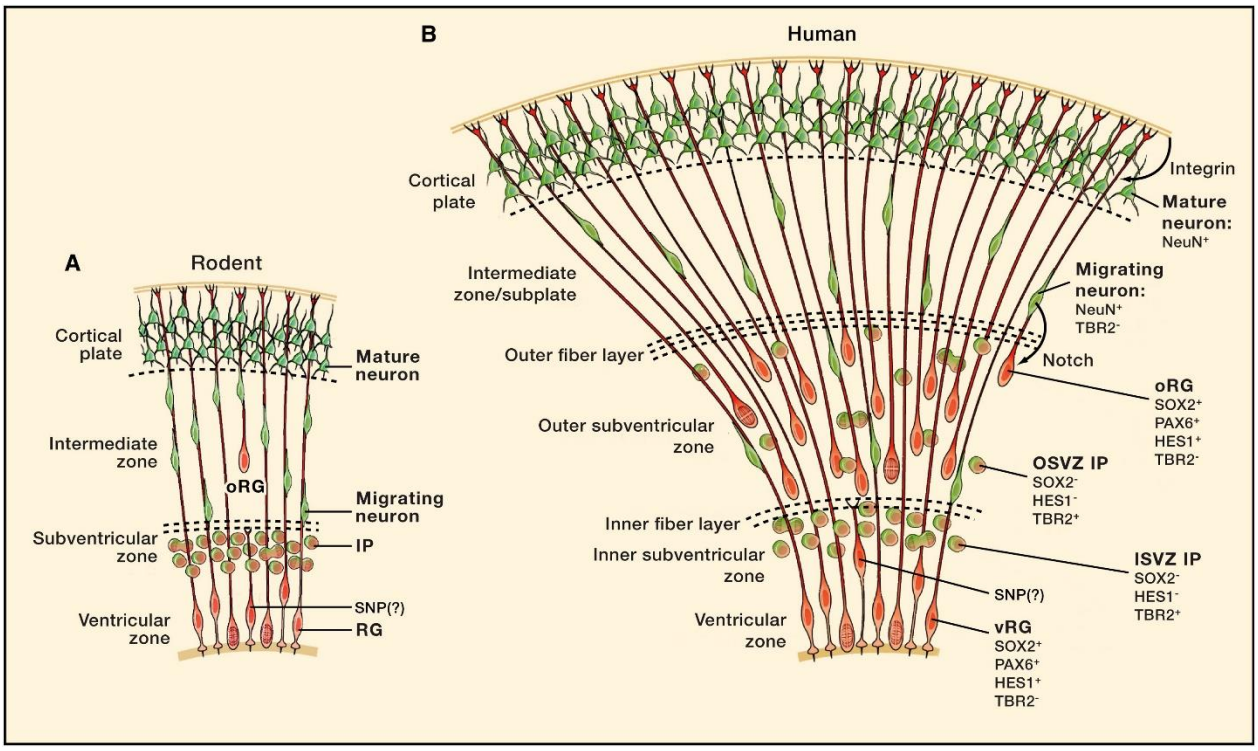

Figure 1: **Rodent and Human Neocortical Development**. Schematic illustrations of the corticogenesis in the rodent brain (A) and in the human brain (B). Radial Glial (RG) give rise to the Intermediate Progenitors (IPs), which undergo rounds of proliferation to give rise to neurons. Then neurons migrate along the RG fibers to establish the neocortical layers. In the human brain there are more outer Radial Glial (oRG) cells. Below the cell types are the cell markers that identified them. On the left, the neocortical layers are described. SNP, Short Neural Precursor; vRG, ventricular Radial Glia. Adapted from Lui, Hansen and Kriegstein, 2011.

2009; Johnson *et al.*, 2015). Intermediate progenitors undergo multiple rounds of division within the SVZ, increasing the capacity for the brain to originate post-mitotic neurons in high numbers (Haubensak *et al.*, 2004; Noctor *et al.*, 2004; Gao *et al.*, 2014). Most of the excitatory neurons in the brain, glia and the neural stem cell population in the adult are originated from RGPs (Merkle *et al.*, 2004; Noctor *et al.*, 2004; Kriegstein and Alvarez-buylla, 2009).

RGPs can also give rise to another type of progenitor population called outer radial glial (oRG), which have distinct morphology and cellular markers (Hansen *et al.*, 2010; Wang *et al.*, 2011; Pollen *et al.*, 2015; Nowakowski *et al.*, 2016). oRG cell number increases greatly from rodents to primates, so that in the primate brain they define an entire region known as outer subventricular zone (Figure 1). Morphologically, these cells

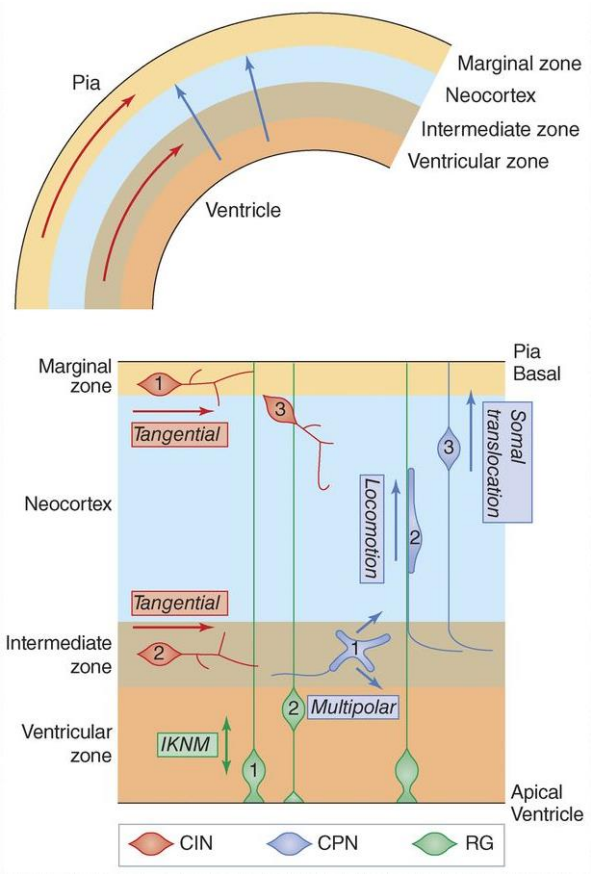

Figure 2: Major neuronal migration pathways in the developing rodent brain. Top panel shows the tangential (red) and radial (blue) modes of migration. The colors of arrows in the top panel correspond to the colors of cells in the bottom panel. **Cortical interneurons (CINs, red)** migrate tangentially along the marginal zone (1) and intermediate zone (2) from their origins in the basal forebrain. Later they migrate into the cortical plate (3). **RG (green)** undergo interkinetic nuclear migration (IKNM), with mitosis apically (1) and S phase basally (2). **Cortical projection neurons (CPN, blue)** migrate through three phases: multipolar (1), locomotion (2), and somal translocation (3). Adapted from Cooper 2013.

are not in contact with the VS, in contrast to the RGPs, but maintain a basal process that reaches the pial surface (Hansen et al., 2010). oRG cells retain the capacity to renew their population and to give rise to neurons, which underlies the ability of the primate brain to generate more neurons in comparison to rodents (Ostrem, Di Lullo and Kriegstein, 2017).

Neurons originated from RGP asymmetric divisions or from intermediate progenitors migrate from the inner proliferative layers to the outer neocortical layers (Noctor *et al.*, 2004; Lui, Hansen and Kriegstein, 2011)

(Figure 2). The first neurons to be produced form a transient layer called Preplate that contains the Cajal-Retzius cells (Govek, Hatten and Van Aelst, 2011), which secrete Reelin forming a gradient in the neocortex, essential for neuronal migration (Cooper, 2008, 2014). Before reaching the Cortical Plate (CP), neurons go through changes at a morphological and transcriptional factor level in the Intermediate Zone (IZ), in a process called multipolar-to-bipolar transition (Figure 2). Initially, neurons display a multipolar morphology, dynamically extending and retracting equally sized processes, in preparation for their migration journey (Tabata and Nakajima, 2003). These have been suggested to sense environmental clues to direct their migration toward the CP (Valiente and Marín, 2010).

Eventually, neurons become bipolar and project an axon toward deeper structures or the contralateral hemisphere, and a leading process toward the CP (Tsai *et al.*, 2005; de Anda *et al.*, 2010). Then, neurons initiate radial migration (Figure 2) to form the stratified layers of the neocortex in an inside-out fashion, in which deeper neocortical layers are formed first, and layers that are more superficial are the last ones to be formed. Neurons migrate from the IZ to the CP with the aid of the RGP cell fibers, which serve as scaffolds. Migrating neurons and RGPs establish multiple contact sites between both cytoplasmic membranes (Sidman and Rakic, 1973; Vallee, Rakic and Bhide, 2008; Solecki, 2012). Because of the close relationship between migrating neurons and RGPs, this migration mechanism is called glial-guided migration or locomotion.

Later, when neurons reach the surroundings of the Marginal Zone (MZ) they switch migration mode, and it is now called terminal somal translocation (TST) (Nadarajah *et al.*, 2001; Olson and Walsh, 2006; Franco *et al.*, 2011; Gil-Sanz *et al.*, 2013). At this stage, the neuronal leading process becomes detached from the glial fibers and extends toward the MZ. In this region of the brain, the leading process contacts with the Cajal-Retzius cells, which secrete Reelin and possibly promotes this type of migration (Franco *et al.*, 2011; Gil-Sanz *et al.*, 2013). Then cells, shorten their leading processes and the soma is translocated toward the pial surface. Interestingly, this mechanism of neuronal migration can also be used in the first stages of development when the first layers are formed (Nadarajah *et al.*, 2001). This is because the relatively small thickness of the neural tube allows neurons, which were newly generated, to directly touch the basal surface and translocate independently of the glial fibers.

As neurogenesis terminates, RGPs delaminate and give rise to astrocytes, ependymocytes, and oligodendrocytes in the brain (Kriegstein and Alvarez-buylla, 2009). The VZ ceases to exist and some RGP

cells conserve their stem cell-like properties and create the SVZ neurogenic niche in the adult (Doetsch, 2003; Merkle *et al.*, 2004; Pinto and Götz, 2007; Kriegstein and Alvarez-buylla, 2009; Gao *et al.*, 2014).

Besides the radial migration of cortical excitatory projection neurons, another type of migration occurs in the developing brain (Figure 2). Inhibitory interneurons originated from the medial, lateral and caudal ganglionic eminences in the brain, migrate tangentially long distances toward the neocortex (Wonders and Anderson, 2006), followed by a switch to radial migration into the developing cortical layers. Interneurons are incorporated into the neocortical circuits to provide crucial modulatory activity. The molecular mechanisms that govern the locomotion of excitatory neurons and the tangential migration of inhibitory neurons are comparable, and they will be described in the next section (Bellion *et al.*, 2005; Schaar and McConnell, 2005; Tsai, Bremner and Vallee, 2007).

1.2 The role of dynein in brain development, from INM through neuronal migration.

As it can be appreciated from the previous section, proper brain development requires massive cell migration and organelle displacement, and one could predict that these directly involve the cytoskeleton. In fact, mutations in cytoskeleton genes encoding molecular motors causes severe neurodevelopmental pathology (Reiner *et al.*, 1993; Lipka *et al.*, 2013; Poirier *et al.*, 2013). Mutations in cytoplasmic dynein 1 (hereafter "dynein"), the focus of most of this thesis work, or dynein related genes can lead to gross defects such as smaller brain (microcephaly), defects in neocortical layering (lissencephaly) or milder defects that may contribute for diseases such as autism or schizophrenia (Lipka *et al.*, 2013; Reiner *et al.*, 2016). Over the years, work performed in the Vallee laboratory and by others has determined the molecular mechanisms through which dynein and other microtubule motors contribute to brain development (Bertipaglia, Gonçalves and Vallee, 2018).

In the VZ of the developing brain, RGPs require microtubule motors for INM (Figure 3). The centrosome in these cells is located in the apical process, close to the VS throughout the cell cycle, and emanate microtubules toward the basal side. Consistent with this microtubule organization different microtubule motors mediate basal and apical INM. During G1 the kinesin Kif1A was shown to power basal migration, as knockdown (KD) of this protein arrests RGP nuclei close to the VS (Tsai *et al.*, 2010; Carabalona, Hu and Vallee, 2016). Although Kif1A KD does not cause a decrease in the number of cells undergoing mitosis, it favors symmetric divisions and reduces neurogenesis (Carabalona, Hu and Vallee, 2016). After migration toward the basal side of the VZ, RGPs go through S phase and enter in G2 phase of the cell cycle. Then these nuclei have to return to the VS in order to complete mitosis, and for that RGPs recruit dynein for nuclear transport. The requirement for dynein during this phase was first observed when the dynein heavy chain motor-containing subunit (DHC) or LIS1, a dynein regulator were targeted. Upon DHC or LIS1 KD using RNAi in the developing brain, there was a strong arrest in RGP nuclei away from the VS (Tsai *et al.*, 2005). Because the microtubule minus-end is located in the apical most part of the RPG cytoplasm it was proposed that dynein transports the nucleus along microtubules toward the centrosome through an interaction with the RGP nuclear envelope (NE) (Tsai *et al.*, 2010).

Subsequent work has confirmed the requirement for dynein and dynein-associated proteins in apical INM, as well as the recruitment factors and regulatory mechanisms involved in nuclear transport (Del Bene *et al.*, 2008; Tsai *et al.*, 2010; Hu *et al.*, 2013; Baffet, Hu and Vallee, 2015). In non-neuronal cultured cells, two

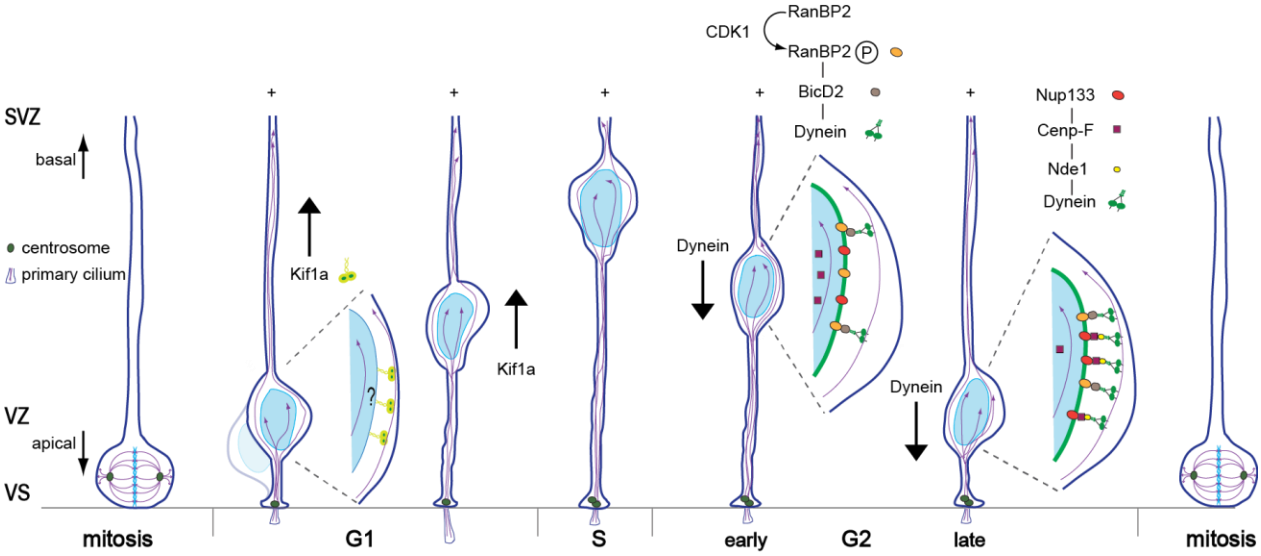

Figure 3: Molecular motors involved in INM. RGPs are polarized cells, with an apical process containing the centrosome and a basal process extending to the cortical plate. Most microtubules (purple arrows) are unidirectional (+ indicates orientation) and serve as tracks for nucleokinesis. From left to right. RGPs enter mitosis at the ventricular surface (VS). During G1 the RGP nucleus migrates basally toward the SVZ, a behavior mediated by the Kif1A plus-end directed microtubule motor protein. Whether Kif1A acts at the NE remains unknown (question mark). Following S-phase the nucleus moves toward the VS driven by cytoplasmic dynein. In early G2, Cdk1 phosphorylates the nucleoporin RanBP2, increasing its binding affinity for BicD2, which recruits dynein to the NE. During late G2, Cenp-F exits the nucleus and binds the nucleoporin Nup133 and Nde1, which, in turn, is able to recruit additional amounts of dynein. The RGP nucleus reaches the VS and divides. Adapted from Bertipaglia et al. 2018.

distinct Nuclear Pore Complexes (NPC) proteins, RanBP2 and Nup133, were shown to anchor dynein at the NE (Splinter *et al.*, 2010; Bolhy *et al.*, 2011). Interestingly, these two NPC proteins are part of two conserved sequential dynein recruitment pathways to the RGP NE (Hu *et al.*, 2013; Baffet, Hu and Vallee, 2015). The "early" dynein recruitment mechanism in apical INM involves the nucleoporin RanBP2, which recruits dynein via the dynein adaptor BicD2. *In utero* electroporation of RanBP2 or BicD2 shRNAs arrested apical INM, suggesting a role of these proteins in nuclear transport (Hu *et al.*, 2013). Analysis of the RGP nuclear distribution revealed that these accumulated in the basal side of the VZ, far from the VS (>30μm), which

indicated that this pathway is necessary for the initial displacement of the RGP nuclei upon G2 entry. However, this mechanism alone is not sufficient to complete apical migration and a "late" mechanism is used by RGP cells to recruit additional amounts of dynein to the NE. This second mechanism depends on the recruitment of CENP-F by Nup133. Then, CENP-F recruits dynein and the dynein regulator Nde1 to the NE. Notably, the late recruitment pathway appears to be essential for the final portion of apical INM, as KD of Nup133, CENP-F or Nde1 cause an arrest relatively close to the VS (<10μm). An important question is why cells evolved these two dynein recruitment pathways. A possible explanation comes from an experiment in which dynein is artificially targeted to the NE. Forced recruitment of dynein to NE is able to overcome the nuclear arrest observed with the KD of genes in the early and late pathways (Hu *et al.*, 2013; Doobin *et al.*, 2016). This argues in favor that these two pathways exist to recruit large amounts of dynein to the NE, and perhaps this allows RGP nuclei to navigate through the crowed VZ epithelia.

These two dynein recruitment mechanisms are only active during the G2 phase of the cell cycle (Splinter *et al.*, 2010; Bolhy *et al.*, 2011; Hu *et al.*, 2013), strongly suggesting a cell-cycle dependent regulation. In fact, the shift of dynein from its cytoplasmic functions to the NE was found to be under Cdk1 control (Baffet, Hu and Vallee, 2015). In G2, Cdk1 becomes more active and phosphorylates RanBP2, which increases its affinity for BicD2 targeting it to the NE. Pharmacological inhibition of Cdk1 in brain slices or expression of dominant negative constructs recapitulates the arrest seen with RanBP2 or BicD2 KD in RGPs. In support of these findings, experiments in cultured cells treated with Cdk1 pharmacological inhibitors have shown that BicD2 could no longer be targeted to the NE. This suggests that Cdk1 acts upstream of RanBP2 and BicD2, and that this regulatory mechanism is required during apical INM (Baffet, Hu and Vallee, 2015). The late pathway involving Nup133/CENP-F/Nde1 seems also to be under Cdk1 regulation, but the mechanisms here are less clear. Because this second mechanism appears to be active later in G2, when Cdk1 is inside the nucleus, one possibility is that Cdk1 phosphorylates CENP-F, which signals its exit from inside the nucleus to the NE. Supporting this hypothesis, pharmacological inhibition of Cdk1 in cultured cells blocks CENP-F from leaving the nucleus (Baffet, Hu and Vallee, 2015). Also, CENP-F phosphorylation by Cdk1 was shown to increase its affinity for Nde1, which recruits dynein to the NE in the late apical INM pathway (Wynne and Vallee, 2018), in line with a Cdk1 dependent control of both G2 dynein recruitment mechanisms.

Dynein recruitment to the NE in RGPs during apical INM is important for the proliferation of these cells. Inhibition of apical INM by interfering with dynein or the dynein regulatory pathways arrests nuclei migration

and cell cycle progression (Hu *et al.*, 2013). This causes a decrease in the number of RGPs undergoing mitosis, making the analysis of the role of dynein in mitosis challenging. Nevertheless, studies from cultured cells have shown clear evidence for dynein in mitosis, such as in the spindle formation and metaphase progression (Raaijmakers, Tanenbaum and Medema, 2013; Wynne and Vallee, 2018). Thus, it is likely that dynein has additional roles during the mitosis of RGP cells.

There has been evidence of a contribution of actomyosin in INM, although its relative importance varies between systems (Norden, 2017). In Zebrafish neuroepithelial cells of the retina, actomyosin was suggested to be the main driver of INM, as it was blocked in the presence of blebbistatin, a myosin II inhibitor (Norden *et al.*, 2009). Yet, inhibition of the dynactin subunit p150^{glued}, which is part of the dynein supercomplex also disrupted INM, suggesting that microtubule motors also play a role in retina INM (Del Bene *et al.*, 2008). On the other hand, live imaging of rat embryonic brain slices treated with blebbistatin did not cause a noticeable effect on basal and apical nuclear displacement (Tsai *et al.*, 2010). The disparity in these results has been partially attributed to the length of the pseudostratified epithelia (Norden, 2017), and particularly in the brain, the nuclear distances travelled during INM are several times higher than the diameter of the nucleus itself. Such long movements are highly dependent on microtubule motors.

In contrast to RGPs, the oRG are not in contact with the VS and do not exhibit INM. However, these cells also display nucleokinesis prior to division, as oRG have been found to rapidly move their nucleus, toward the basal process, just prior to mitosis. This behavior was termed mitotic somal translocation (Hansen *et al.*, 2010). In contrast with INM in RGPs, here centrosomes associate with the nucleus throughout its translocation. One study has shown that treatment of brain slices with blebbistatin or an inhibitor of the upstream myosin protein kinase ROCK completely inhibited mitotic somal translocation, suggesting that actin cytoskeleton is required for this behavior (Ostrem *et al.*, 2014). The role of microtubules was also addressed, and treatment of brain slices with nocodazole, which inhibits microtubule polymerization, did not impact nucleokinesis, but inhibited mitosis (Ostrem *et al.*, 2014).

Neurons produced directly from RGP division or indirectly from transient amplifying intermediate progenitors go through a multipolar-to-bipolar transition, where substantial cytoskeleton remodeling occurs (de Anda *et al.*, 2005; Sakakibara *et al.*, 2014a). Dynein has also been shown to participate in this transition, as inhibition of dynein or dynein-associated genes cause a severe arrest in migration, and cells accumulate with a

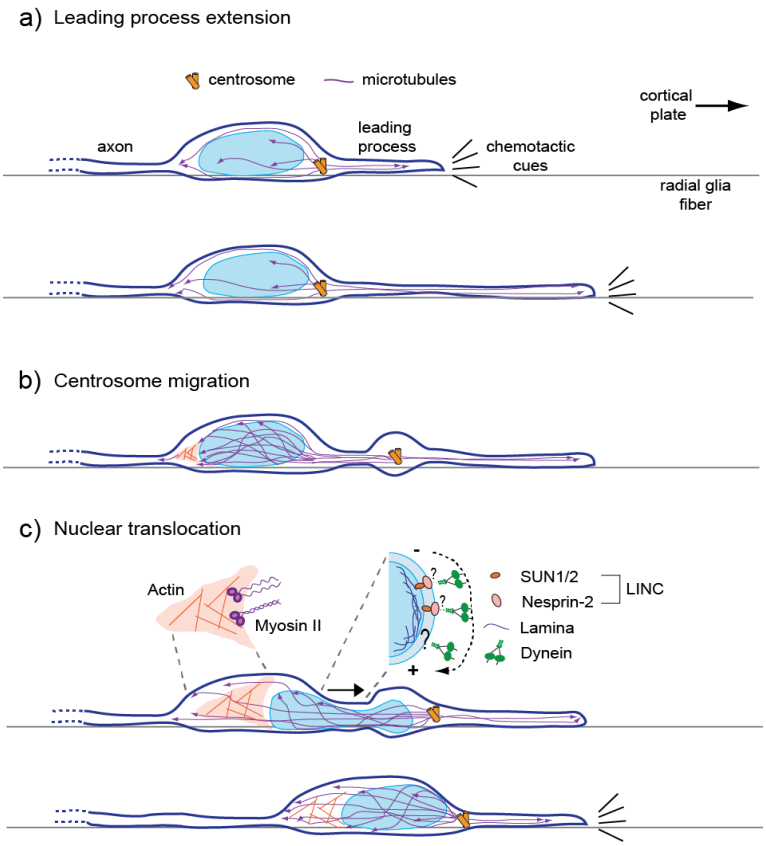

Figure 4: Model for radial post-mitotic neuronal migration. (a) Post-mitotic neurons extend their leading processes and migrate to the CP along the RG fibers. (b) Dynein localizes to cytoplasmic swelling which form in the proximal leading process. It is thought that dynein "pulls" the entire centrosome-associated microtubule cytoskeleton forward. (c) Nuclear translocation is mediated by NE-associated dynein pulling on the surrounding microtubules. Current evidence indicates that the LINC complex serves to recruit dynein to the NE at this stage, though the recruitment mechanisms have not yet been elucidated (question mark). Roles for NPC-mediated dynein recruitment remain possible, but have not been tested. Actomyosin contractility helps the nuclear translocation process from the rear of the nucleus and from the proximal leading process (not shown). Eventually, the nucleus re-acquires its normal shape and the cycle continues with a new round of migratory process extension. Adapted from Bertipaglia et al. 2018.

multipolar morphology (Tsai *et al.*, 2005; Hu *et al.*, 2013; Doobin *et al.*, 2016). This arrest appears to be due to a cell-autonomous effect, in contrast to the other microtubule motor involved in INM, Kif1A. In the latter case, a multipolar arrest was observed upon Kif1A KD, and more interestingly, the surrounding wild-type

neurons were incapable of migrating, thus becoming misplaced mature neurons (Carabalona, Hu and Vallee, 2016). The non-cell autonomous effect was rescued by BDNF treatment of Kif1A KD slices (Carabalona, Hu and Vallee, 2016), suggesting that one component of this migration defect arises from insufficient BDNF secretion to the neighboring cells. Yet, cells depleted for Kif1A remained in the multipolar stage. Despite clear evidence that microtubule motors play a role in the multipolar-to-bipolar transition, the underlying mechanisms are not well understood.

Bipolar neurons in the IZ initiate migration into the CP, and dynein is also required for the following steps of neuronal migration (Figure 4). The first hints that dynein was involved in neuronal migration came from patients with LIS1 mutations, who presented severe defects in gyrification and diminished brain size (Reiner *et al.*, 1993). Further studies using *Lis1*$^{+/-}$ mice have shown severe neocortical layering organization, suggesting that this dynein adaptor and ultimately dynein were important for neuronal migration (Hirotsune *et al.*, 1998; Assadi *et al.*, 2003). Over the years, multiple groups have confirmed the requirement for dynein and dynein-associated proteins in this process, but the mechanisms by which this motor operates in brain development needs to be further elucidated (Bertipaglia, Gonçalves and Vallee, 2018).

First, bipolar neurons in the IZ of the developing neocortex extend a leading process toward the CP. In the proximal region of the leading process a "dilation" is formed and the centrosome migrates into this structure. Then, the nucleus migrates toward the centrosome in a saltatory coordinated fashion (Bellion *et al.*, 2005; Schaar and McConnell, 2005; Tsai, Bremner and Vallee, 2007). Microtubules in migrating neurons are emanated from the centrosome into the leading process and around the nucleus (Tsai, Bremner and Vallee, 2007). Thus, nuclear displacement occurs toward the minus-end and its under dynein control (Shu *et al.*, 2004; Tsai, Bremner and Vallee, 2007). Evidence obtained in cultured migratory neurons has suggested that dynein accumulates around the nucleus, consistent with a role for dynein in nuclear transport, and at the cellular cortex, in particular in the dilations, distally to the centrosome. Thus, dynein likely powers the movement of the centrosome as well (Tsai, Bremner and Vallee, 2007). Additionally, experiments in which DHC and LIS1 are KD in neurons have suggested impaired centrosome transport, further supporting a role for dynein in the movement of the centrosomes (Tsai, Bremner and Vallee, 2007). Nonetheless, more evidence is necessary to support this model.

Actomyosin has been reported to participate in neuronal migration, exerting forces at distinct sites in post-mitotic neurons. Leading process growth in bipolar neurons requires actin at the leading process tip (Jiang

et al., 2015). Additionally, evidence has been obtained that actin accumulates at the rear of the nucleus by immunostaining plated migrating neurons for myosin II light chain (Schaar and McConnell, 2005). In support of an actin role in neuronal migration, myosin II inhibition in the developing brain halts nuclear movement (Bellion *et al.*, 2005; Schaar and McConnell, 2005; Tsai, Bremner and Vallee, 2007). Actin accumulation has also been reported in the proximal region of the leading process and suggested to be involved in the transport of the nucleus and the centrosome (Solecki, 2012; Trivedi *et al.*, 2017). In line with the previous observations, experiments in migratory neurons using traction force microscopy showed that actomyosin produced force at the rear of the nucleus, in the proximal leading process and at the leading process tip (Jiang *et al.*, 2015; Umeshima *et al.*, 2019), confirming a crucial role for this cytoskeleton component in neuronal migration.

Nuclear transport during neuronal migration likely requires the recruitment of dynein to the NE, as it happens with INM (Shu *et al.*, 2004; Tsai, Bremner and Vallee, 2007). However, at this stage dynein recruitment to the NE appears to be dependent on a different additional mechanism. The SUN (Sad1 and UNC-84) proteins in the inner NE and the KASH (Klarsicht, ANC-1, Syne Homology) proteins in the outer NE compose the Linker of Nucleoskeleton and Cytoskeleton (LINC) complex (Chang, Worman and Gundersen, 2015). Evidence from multiple systems has shown that KASH proteins, such as Nesprins, can interact with cytoskeletal elements to regulate nuclear position within the cell, and this is discussed in more detail in the next section. In particular during brain development, the LINC complex is necessary for neuronal migration as judged by the laminary defects in mice depleted for SUN and Nesprin-1/2 proteins, which had disrupted neuronal migration (Zhang *et al.*, 2009). Using *in utero* electroporation, our laboratory has shown that neuronal migration was severely arrested by the expression of the inhibitory KASH domain, which competes with endogenous Nesprins for SUN binding (Hu *et al.*, 2013), further suggesting a role for Nesprins in neuronal migration. Interestingly, work in cultured fibroblasts showed that Nesprin-2 interacts with actin filaments and dynein for correct nuclear position (Gomes, Jani and Gundersen, 2005; Luxton *et al.*, 2010; Kutscheidt *et al.*, 2014; Zhu, Antoku and Gundersen, 2017; Zhu, Liu and Gundersen, 2018). Yet, it is still unclear whether Nesprin-2 recruits dynein and/or actin directly to the NE in migrating neurons.

The literature on the mechanisms for neuronal TST is limited (Nadarajah *et al.*, 2001; Olson and Walsh, 2006; Franco *et al.*, 2011; Sekine *et al.*, 2011; Cooper, 2013; Gil-Sanz *et al.*, 2013). Therefore, the role of the cytoskeleton in this behavior remains unclear, and to our best knowledge no contribution was found for dynein so far.

1.3 Mechanisms of motor protein recruitment to the nuclear envelope in other biological systems.

From a mechanistic perspective, many events during development depend on the interaction of the nucleus with the cytoskeleton (Starr and Fridolfsson, 2010; Bone and Starr, 2016). In fact, across species and cell types, there is a diversity of proteins at the NE that evolved to interact with actin filaments, microtubules and intermediate filaments (Figure 5) (Janota *et al.*, 2017). Due to the complexity of these mechanisms, the current section will be mainly focused on the mechanisms of LINC-dependent microtubule motor recruitment to the NE, which are relevant for this PhD work.

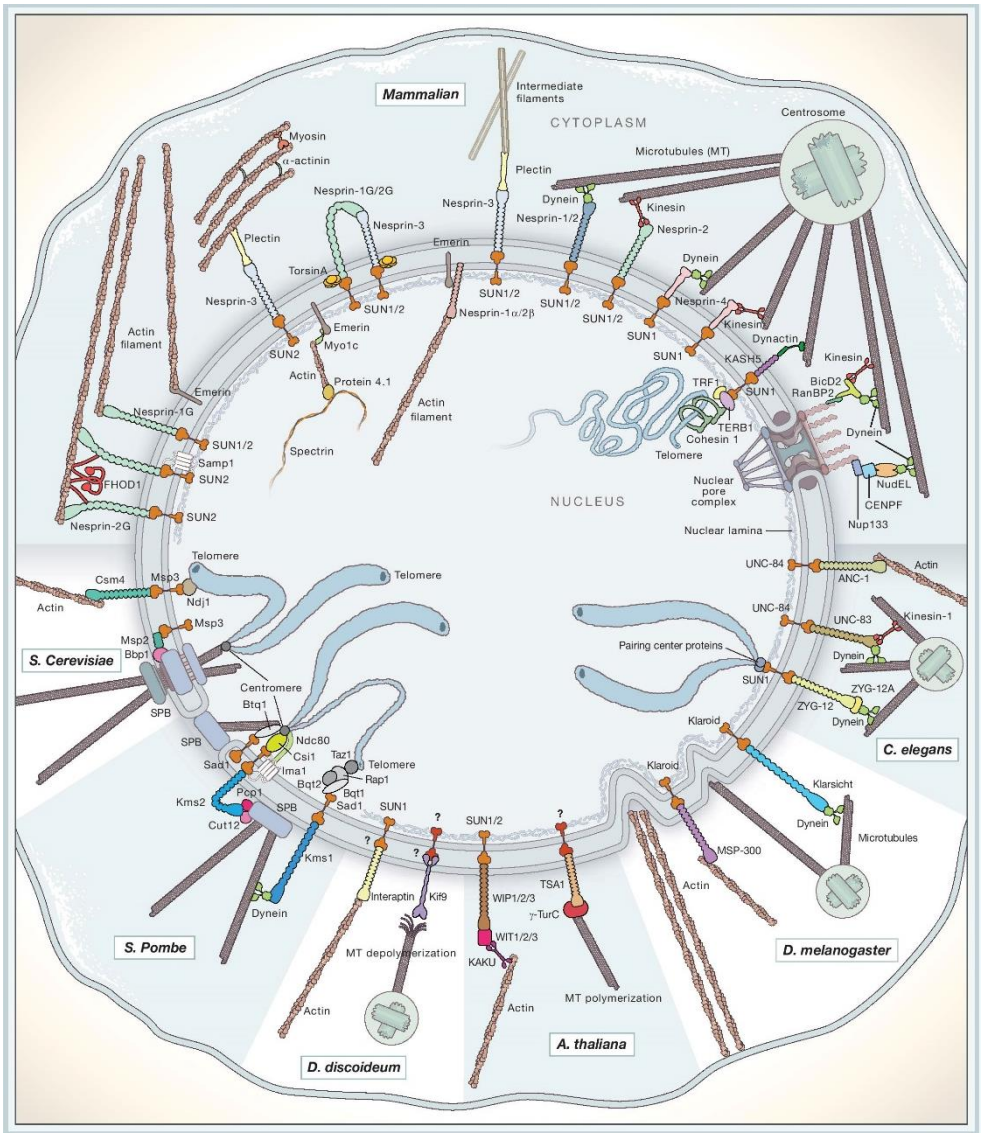

Figure 5: Diagram representing the proteins involved in the connection of the nucleus with the cytoskeleton in several species. Adapted from Janota et. al. 2017.

Studies carried in *C. elegans* embryonic hypodermal cells have helped to understand the importance of microtubule motor recruitment to the NE during nuclear migration *in vivo* (Fridolfsson and Starr, 2010; Fridolfsson *et al.*, 2010; Luxton and Starr, 2014; Lawrence *et al.*, 2016). The KASH protein UNC-83, a Nesprin homologue, was shown to recruit dynein and kinesin-1 to the NE for the displacement of hypodermal cell nuclei. In this system, dynein is anchored to the NE by UNC-83, via two dynein recruitment pathways dependent on BICD-1 and NUD-2, homologues of the mammalian BicD2 and Nde1/L proteins, respectively (Fridolfsson *et al.*, 2010). In wild-type cells, nuclei display bi-directional movement during migration and rolling past roadblocks. Consistent with a function for microtubule motors at the NE in hypodermal cells, disruption of UNC-83 or kinesin-1 arrested nuclear migration (Fridolfsson and Starr, 2010). Dynein, BICD-1 and NUD-2 seemed to play a lesser role in initiating nuclear migration, but rather a more important one in the bi-directional and rolling behaviors of these nuclei. The authors proposed a model in which the nucleus recruits both microtubule motors, and these act cooperatively, so that kinesin-1 is important for nucleus displacement and dynein is necessary for nuclear rotation, which might help the nucleus to navigate through constrictions (Fridolfsson and Starr, 2010).

Also in *C. elegans,* pronuclear migration depends on microtubules and microtubule motors at the NE (Malone *et al.*, 2003). After fertilization, the male and female pronuclei must encounter to fuse and divide. From the male pronucleus, the centrosome emanates microtubules engulfing the female pronucleus. Both nuclei have dynein recruited by the KASH protein ZYG-12 at the NE, which serves to anchor the centrosome to the male pronucleus and to power movement of the female pronucleus toward the centrosome, allowing the nuclear fusion (Malone *et al.*, 2003; Zhou *et al.*, 2009).

Multiple migration events occur during mammalian muscle development, in which myoblasts fuse to create a giant syncytium with hundreds of nuclei that will give rise to the muscle cellular unit, also called myofiber (Metzger *et al.*, 2012; Wilson and Holzbaur, 2012, 2015; Bone and Starr, 2016; Roman and Gomes, 2018). Most of these migration behaviors are microtubule dependent, but an important aspect in muscle development is that microtubules are typically emanated from the several nuclei, which accumulate microtubule nucleating proteins at the NE (Tassin, Maro and Bornens, 1985; Srsen *et al.*, 2009; Roman and Gomes, 2018). After myoblast fusion, first, nuclei migrate to the center of cell, where the other fused nuclei gather. Dynein and dynein-associated genes are recruited to the NE by the PAR protein complex to mediate nuclei migration at this stage (Cadot *et al.*, 2012). Then accumulated nuclei align on a single plane, and the

LINC complex was shown to recruit pericentriolar proteins to the NE, possibly to complete the transition of certain centrosomal proteins from the centrosome to the NE (Gimpel *et al.*, 2017).

Microtubule motors are again important when the nuclei are gathered at the center of the cell and need to spread across the cytoplasm. Here, two models exist to explain this movement that depend on forces exerted by kinesin-1 (Metzger *et al.*, 2012; Wilson and Holzbaur, 2012, 2015). Each nucleus emanates microtubules from the nuclear surface making an array of antiparallel microtubules spread across the cytoplasm. One proposed mechanism for nuclear transport depends on the interaction between kinesin-1 and the Microtubule Associated Protein 7 (MAP-7). These two proteins cross-link the antiparallel microtubules and upon kinesin-1 activation nuclei, are spread apart (Metzger *et al.*, 2012). The other mechanism depends on the recruitment of microtubule motors by the LINC complex to the NE (Wilson and Holzbaur, 2012, 2015). Nesprin-2 recruits kinesin-1, through a conserved domain in its Kinesin Light Chain (KLC). Disruption of the interaction between these two proteins at the NE causes accumulation of nuclei in the cell center. After spreading through the muscle cell, nuclei are anchored at the periphery of the cell, a process thought also to be dependent on KASH proteins (Zhang *et al.*, 2007; Bone and Starr, 2016; Roman and Gomes, 2018).

Cultured fibroblasts have been proven useful for the understanding of the actin- and microtubule-based mechanisms of nuclear position (Starr and Fridolfsson, 2010; Tapley and Starr, 2013; Zhu, Liu and Gundersen, 2018). When fibroblasts polarize, the nucleus moves rearward (Gomes, Jani and Gundersen, 2005) moved by actin cable structures called transmembrane actin-associated nuclear (TAN) lines (Luxton *et al.*, 2010; Kutscheidt *et al.*, 2014). These flow from the leading edge of the cell to the basal side, and contact the nucleus via the calponin homology domain of Nesprin-2, which harnesses the nucleus to the moving cables (Luxton *et al.*, 2010). In parallel, polarizing cells orient the centrosome toward the leading edge in a dynein dependent pathway via PAR3 (Gomes, Jani and Gundersen, 2005; Schmoranzer *et al.*, 2009). Elegant work done with centrifuged cells has shown that nuclear movement toward the centrosome also requires dynein, but not kinesin-1, recruited by the microtubule motor-binding domain of Nesprin-2 to the NE (Zhu, Antoku and Gundersen, 2017). Although the mechanims by which actomyosin moves nuclei rearward are dissected to very detailed level, the mechanisms of Nesprin-2 dependent dynein recruitment need to be fully understood.

As described in the previous section, there are at least three dynein recruitment mechanisms to the NE during brain development (Figure 6). During the G2 phase of the cell cycle, RGPs recruit dynein via RanBP2/BicD2

and Nup133/CENP-F/Nde1 sequential pathways. In neurons dynein is potentially recruited via Nesprin-2. This thesis work sought to answer the question of how dynein is recruited to the NE via these mechanisms.

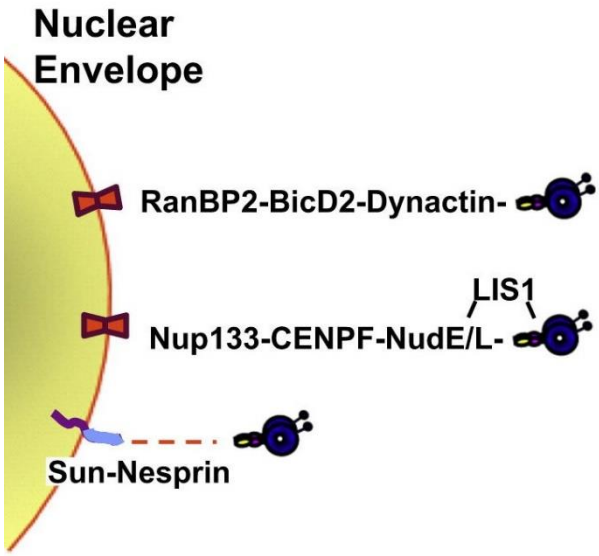

Figure 6: Mechanisms of dynein recruitment to the NE. Diagram representing G2-specific NE dynein recruitment mechanisms via nucleoporins Nup133 and RanBP2. Dynein is also shown linked to the NE by SUN-Nesprin complexes, a mechanism still incompletely understood. Adapted from Hu et al. 2013.

1.4 Dynein motor, the Light Intermediate Chains and dynein adaptors.

In the 1980's, the two major classes of cytoplasmic microtubule motors were found, which elucidated how active transport within cells could occur. Studies using brain purified cytoplasmic microtubules and associated proteins, revealed that the Microtubule Associated Protein 1C (MAP-1C), now known as cytoplasmic dynein-1, co-purified in higher amounts in the presence of ATP, an indication that this protein depended on nucleotide-binding for its activity (Paschal, Shpetner and Vallee, 1987). Further characterization showed that MAP-1C had properties reminiscent of axonemal dyneins (Paschal and Vallee, 1987) that were found years before. This was the first solid evidence for a cytoplasmic retrograde motor. Previously, a microtubule-binding protein with ATPase activity was shown to have translocation properties in the plus-end direction, and was named kinesin (Vale, Reese and Sheetz, 1985). Today, dynein and kinesins are known contributors for many fundamental cellular functions, such as vesicle transport, chromosome separation, nuclear transport, mitotic spindle positioning, and many more.

Cytoplasmic dynein contains diverse accessory subunits, and interacts with many adaptors that mediate or regulate dynein motor and cargo-binding behavior. However, due to the complexity of the molecule a more precise molecular structure of dynein came only after the advances in cryogenic electron microscopy techniques (Carter, Diamant and Urnavicius, 2016). Dynein is a multi-subunit complex composed by two DHCs, two Intermediate Chains (ICs), two dynein Light Intermediate Chains (LICs) and three classes of Light Chains (LCs) each present with two copies (Pfister *et al.*, 2006) (Figure 7). The DHCs dimerize and form the backbone of the molecule. These subunits contain the ATPase domains in the C-terminal region, which are responsible for ATP hydrolysis that power displacement along the microtubules. In the N-terminal portion of the DHCs, also called the tail, ICs and LICs bind to provide stability and cargo binding. The two ICs bind the other class of subunits the LCs. The dynein regulators Nde1/Ndel1 and the dynein regulatory complex dynactin also bind to the ICs. The LICs associate to the DHCs and provide additional cargo-binding capacity to a group of coiled coil dynein adaptors, and these dynein subunits are exclusively present in the cytoplasmic forms of dynein. In contrast with more than 40 kinesins found in mammalian cells, cytoplasmic retrograde transport activity is mainly performed by a single form of dynein (Hirokawa *et al.*, 2009; Vallee, McKenney and Ori-McKenney, 2012). A second type of dynein has been described, cytoplasmic dynein 2, but its functions are exclusively intraflagellar transport in cilia (Grissom, Vaisberg and McIntosh, 2002; Mikami,

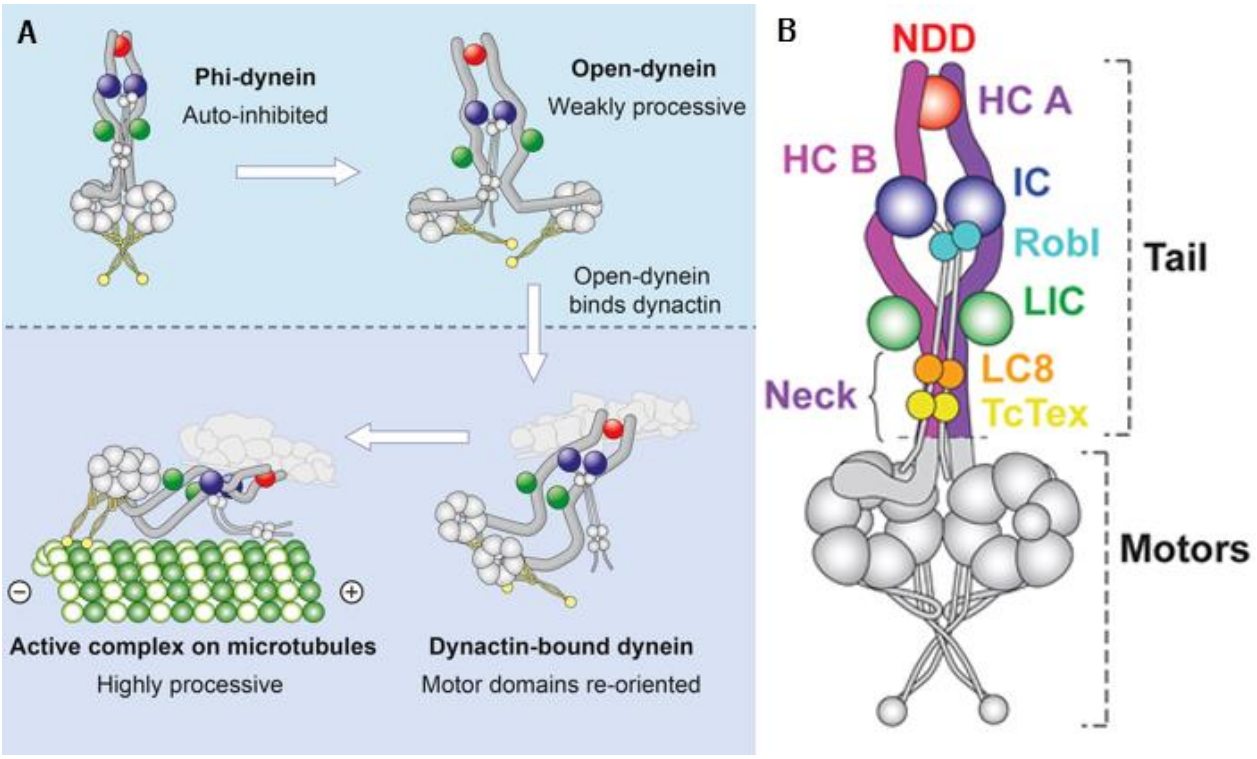

Figure 7: Dynein complex and auto-inhibition mechanism. (A) Diagram of how dynein is an auto-inhibited and non-processive molecule that can be activated by binding to dynactin and to the dynein adaptors. (B) Dynein complex structure and composition. The dynein HC N-terminal dimerization domain (NDD) holds HC A and HC B together. The HCs bind the ICs and the LICs and the LCs (Robl, LC8, and Tctex) bind to the IC N-terminal extended region. Adapted from Zhang et al. 2017.

2002; Taylor *et al.*, 2015), thus it will not be addressed in this thesis. How does dynein carry such a wide array of functions, and the basis for its functional diversity is under intensive investigation.

The dynactin complex binds to the dynein complex to release it from auto-inhibition, but these two complexes associate weakly *in vitro*. An emerging class of dynein adaptors such as BicD2, Spindly, FIP and HOOK proteins have been described to bind and activate the dynein complex. These adaptors recruit dynactin to dynein super-complexes with very high affinity and ensure processive movement (Splinter et al., 2012; McKenney et al., 2014). The N-terminal region of these dynein adaptors binds dynein and dynactin and causes a conformational change in the dynein molecule that aligns both motor domains to allow displacement over long-distances (Zhang *et al.*, 2017) (Figure 7). The C-terminal region of these adaptors binds to membranous vesicles and to the own molecule N-terminal portion, suggesting an auto-inhibitory mechanism.

One possible model for dynein regulation is that cargo to be transported activates the recruitment of dynein adaptors, releasing them from auto-inhibition, which then specifically recruits dynein to ensure processive movement (Carter, Diamant and Urnavicius, 2016; Hoogenraad and Akhmanova, 2016; Reck-Peterson *et al.*, 2018).

One of the contact sites between these important dynein adaptors and the dynein complex is via the LIC subunits (Schroeder *et al.*, 2014). A conserved domain called "CC1-box" within proteins such as BicD2 or Spindly binds to the C-terminal region of the LICs (Gama *et al.*, 2017; Lee *et al.*, 2018). HOOK family proteins, another class of dynein adaptors, appear to use a different domain called the Hook domain within the LIC cargo-binding C-terminal region (Schroeder and Vale, 2016; Lee *et al.*, 2018). A globular Ras-like domain (G-domain) in the N-terminal portion of the LIC molecule binds to the DHC (Schroeder *et al.*, 2014), thus the LICs mediate the binding of the dynein complex to the dynein adaptors.

The LICs are products from two different genes *DYNC1LI1* (LIC1) and *DYNC1LI2* (LIC2) that are present in most vertebrates. Interestingly, in co-immunoprecipitation experiments, LICs form mutually exclusive dynein complexes, meaning that LIC1 cannot immunoprecipitate LIC2 and vice versa. This suggests that LICs define discrete dynein populations within the cell. Both LICs appear to have mostly redundant function in mitosis and organelle transport (Palmer, Hughes and Stephens, 2009; Tan, Scherer and Vallee, 2011; Raaijmakers, Tanenbaum and Medema, 2013; Jones *et al.*, 2014), although discrete functions for each LIC have been reported (Tynan *et al.*, 2000; Palmer, Hughes and Stephens, 2009; Schmoranzer *et al.*, 2009; Tan, 2009; Tan, Scherer and Vallee, 2011). The reason why cells evolved toward having these two genes with apparently redundant functions is unclear, as an understanding of the relative roles for LIC1 and LIC2 *in vivo* has been hampered by lack of an appropriate physiological system to test each of their functions.

AIMS

The main goal of this thesis project is to understand the machinery of dynein recruitment, particularly to the NE, during neocortical development, and gain mechanistic insights concerning dynein regulation and functional diversity overall. The specific aims of this project are to:

i. Dissect the mechanisms of dynein recruitment during neurogenesis and neuronal migration.

ii. Determine the roles of LIC1- vs. LIC2-dynein subpopulations in brain development.

iii. Determine the role of Nesprin-2 in neuronal migration.

REFERENCES

de Anda, F. C. *et al.* (2005) 'Centrosome localization determines neuronal polarity', *Nature*, 436(7051), pp. 704–708. doi: 10.1038/nature03811.

de Anda, F. C. *et al.* (2010) 'Centrosome motility is essential for initial axon formation in the neocortex.', *The Journal of neuroscience : the official journal of the Society for Neuroscience*, 30(31), pp. 10391–406. doi: 10.1523/JNEUROSCI.0381-10.2010.

Assadi, A. H. *et al.* (2003) 'Interaction of reelin signaling and Lis1 in brain development', *Nature Genetics*, 35(3), pp. 270–276. doi: 10.1038/ng1257.

Baffet, A. D., Hu, D. J. and Vallee, R. B. (2015) 'Cdk1 Activates Pre-mitotic Nuclear Envelope Dynein Recruitment and Apical Nuclear Migration in Neural Stem Cells', *Developmental Cell*. Elsevier Inc., 33(6), pp. 703–716. doi: 10.1016/j.devcel.2015.04.022.

Bellion, A. *et al.* (2005) 'Nucleokinesis in tangentially migrating neurons comprises two alternating phases: forward migration of the Golgi/centrosome associated with centrosome splitting and myosin contraction at the rear.', *The Journal of neuroscience : the official journal of the Society for Neuroscience*, 25(24), pp. 5691–9. doi: 10.1523/JNEUROSCI.1030-05.2005.

Del Bene, F. *et al.* (2008) 'Regulation of Neurogenesis by Interkinetic Nuclear Migration through an Apical-Basal Notch Gradient', *Cell*, 134(6), pp. 1055–1065. doi: 10.1016/j.cell.2008.07.017.

Bertipaglia, C., Gonçalves, J. C. and Vallee, R. B. (2018) 'Nuclear migration in mammalian brain development', *Seminars in Cell & Developmental Biology*, 82, pp. 57–66. doi: 10.1016/j.semcdb.2017.11.033.

Bolhy, S. *et al.* (2011) 'A Nup133-dependent NPC-anchored network tethers centrosomes to the nuclear envelope in prophase', *The Journal of Cell Biology*, 192(5), pp. 855–871. doi: 10.1083/jcb.201007118.

Bone, C. R. and Starr, D. A. (2016) 'Nuclear migration events throughout development', *Journal of Cell Science*, 129(10), pp. 1951–1961. doi: 10.1242/jcs.179788.

Cadot, B. *et al.* (2012) 'Nuclear movement during myotube formation is microtubule and dynein dependent and is regulated by Cdc42, Par6 and Par3.', *EMBO reports*, 13(8), pp. 741–9. doi: 10.1038/embor.2012.89.

Carabalona, A., Hu, D. J.-K. and Vallee, R. B. (2016) 'KIF1A inhibition immortalizes brain stem cells but blocks BDNF-mediated neuronal migration', *Nature Neuroscience*, 19(2). doi: 10.1038/nn.4213.

Carter, A. P., Diamant, A. G. and Urnavicius, L. (2016) 'How dynein and dynactin transport cargos: A structural perspective', *Current Opinion in Structural Biology*. Elsevier Ltd, 37, pp. 62–70. doi: 10.1016/j.sbi.2015.12.003.

Chang, W., Worman, H. J. and Gundersen, G. G. (2015) 'Accessorizing and anchoring the LINC complex for multifunctionality', *Journal of Cell Biology*, 208(1), pp. 11–22. doi: 10.1083/jcb.201409047.

Cooper, J. A. (2008) 'A mechanism for inside-out lamination in the neocortex', *Trends in Neurosciences*, 31(3), pp. 113–119. doi: 10.1016/j.tins.2007.12.003.

Cooper, J. A. (2013) 'Mechanisms of cell migration in the nervous system', *The Journal of Cell Biology*, 202(5), pp. 725–734. doi: 10.1083/jcb.201305021.

Cooper, J. A. (2014) 'Molecules and mechanisms that regulate multipolar migration in the intermediate zone.', *Frontiers in cellular neuroscience*, 8(November), p. 386. doi: 10.3389/fncel.2014.00386.

Doetsch, F. (2003) 'The glial identity of neural stem cells.', *Nature neuroscience*, 6(11), pp. 1127–34. doi: 10.1038/nn1144.

Doobin, D. J. *et al.* (2016) 'Severe NDE1-mediated microcephaly results from neural progenitor cell cycle arrests at multiple specific stages', *Nature Communications*. Nature Publishing Group, 7, pp. 1–14. doi: 10.1038/ncomms12551.

Florio, M. and Huttner, W. B. (2014) 'Neural progenitors, neurogenesis and the evolution of the neocortex', *Development*, 141(11), pp. 2182–2194. doi: 10.1242/dev.090571.

Franco, S. J. *et al.* (2011) 'Reelin Regulates Cadherin Function via Dab1/Rap1 to Control Neuronal Migration and Lamination in the Neocortex', *Neuron*, 69(3), pp. 482–497. doi: 10.1016/j.neuron.2011.01.003.

Fridolfsson, H. N. *et al.* (2010) 'UNC-83 coordinates kinesin-1 and dynein activities at the nuclear envelope during nuclear migration', *Developmental Biology*, 338(2), pp. 237–250. doi: 10.1016/j.ydbio.2009.12.004.

Fridolfsson, H. N. and Starr, D. A. (2010) 'Kinesin-1 and dynein at the nuclear envelope mediate the bidirectional migrations of nuclei', *Journal of Cell Biology*, 191(1), pp. 115–128. doi:

10.1083/jcb.201004118.

Gama, J. B. *et al.* (2017) 'Molecular mechanism of dynein recruitment to kinetochores by the Rod-Zw10-Zwilch complex and Spindly', *Journal of Cell Biology*, 216(4), pp. 943–960. doi: 10.1083/jcb.201610108.

Gao, P. *et al.* (2014) 'Deterministic progenitor behavior and unitary production of neurons in the neocortex.', *Cell*. The Authors, 159(4), pp. 775–88. doi: 10.1016/j.cell.2014.10.027.

Gil-Sanz, C. *et al.* (2013) 'Cajal-Retzius cells instruct neuronal migration by coincidence signaling between secreted and contact-dependent guidance cues', *Neuron*, 79(3), pp. 461–477. doi: 10.1016/j.neuron.2013.06.040.

Gimpel, P. *et al.* (2017) 'Nesprin-1α-Dependent Microtubule Nucleation from the Nuclear Envelope via Akap450 Is Necessary for Nuclear Positioning in Muscle Cells', *Current Biology*, 27(19), pp. 2999-3009.e9. doi: 10.1016/j.cub.2017.08.031.

Gomes, E. R., Jani, S. and Gundersen, G. G. (2005) 'Nuclear movement regulated by Cdc42, MRCK, myosin, and actin flow establishes MTOC polarization in migrating cells', *Cell*, 121(3), pp. 451–463. doi: 10.1016/j.cell.2005.02.022.

Govek, E. E., Hatten, M. E. and Van Aelst, L. (2011) 'The role of Rho GTPase proteins in CNS neuronal migration', *Developmental Neurobiology*, 71(6), pp. 528–553. doi: 10.1002/dneu.20850.

Grissom, P. M., Vaisberg, E. A. and McIntosh, J. R. (2002) 'Identification of a Novel Light Intermediate Chain (D2LIC) for Mammalian Cytoplasmic Dynein 2', *Molecular Biology of the Cell*. Edited by D. Drubin, 13(3), pp. 817–829. doi: 10.1091/mbc.01-08-0402.

Hansen, D. V *et al.* (2010) 'Neurogenic radial glia in the outer subventricular zone of human neocortex', *Nature*, 464(7288), pp. 554–561. doi: 10.1038/nature08845.

Haubensak, W. *et al.* (2004) 'Neurons arise in the basal neuroepithelium of the early mammalian telencephalon: a major site of neurogenesis.', *Proceedings of the National Academy of Sciences of the United States of America*, 101(9), pp. 3196–201. doi: 10.1073/pnas.0308600100.

Hirokawa, N. *et al.* (2009) 'Kinesin superfamily motor proteins and intracellular transport', *Nature Reviews Molecular Cell Biology*. Nature Publishing Group, 10(10), pp. 682–696. doi: 10.1038/nrm2774.

Hirotsune, S. *et al.* (1998) 'Graded reduction of Pafah1b1 (Lis1) activity results in neuronal migration defects and early embryonic lethality', *Nature Genetics*, 19(4), pp. 333–339. doi: 10.1038/1221.

Hoogenraad, C. C. and Akhmanova, A. (2016) 'Bicaudal D Family of Motor Adaptors: Linking Dynein Motility to Cargo Binding', *Trends in Cell Biology*. Elsevier Ltd, 26(5), pp. 327–340. doi: 10.1016/j.tcb.2016.01.001.

Hu, D. J.-K. *et al.* (2013) 'Dynein Recruitment to Nuclear Pores Activates Apical Nuclear Migration and Mitotic Entry in Brain Progenitor Cells', *Cell*, 154(6), pp. 1300–1313. doi: 10.1016/j.cell.2013.08.024.

Janota, C. S. *et al.* (2017) 'SnapShot : SnapShot : cytoskeletal Interactions SnapShot : Nucleo- cytoskeletal Interactions', *Cell*. Elsevier, 169(5), pp. 970-970.e1. doi: 10.1016/j.cell.2017.05.014.

Jiang, J. *et al.* (2015) 'Spatiotemporal dynamics of traction forces show three contraction centers in migratory neurons', *Journal of Cell Biology*, 209(5), pp. 759–774. doi: 10.1083/jcb.201410068.

Johnson, M. B. *et al.* (2015) 'Single-cell analysis reveals transcriptional heterogeneity of neural progenitors in human cortex', *Nature Neuroscience*, 18(5), pp. 637–646. doi: 10.1038/nn.3980.

Jones, L. A. *et al.* (2014) 'Dynein light intermediate chains maintain spindle bipolarity by functioning in centriole cohesion', *Journal of Cell Biology*, 207(4), pp. 499–516. doi: 10.1083/jcb.201408025.

Kriegstein, A. and Alvarez-buylla, A. (2009) 'The Glial Nature of Embryonic and Adult Neural Stem Cells', *Annual Reviews of Neuroscience*, pp. 149–184. doi: 10.1146/annurev.neuro.051508.135600.The.

Kutscheidt, S. *et al.* (2014) 'FHOD1 interaction with nesprin-2G mediates TAN line formation and nuclear movement.', *Nature Cell Biology*, 16(7), pp. 708–15. doi: 10.1038/ncb2981.

Lawrence, K. S. *et al.* (2016) 'LINC complexes promote homologous recombination in part through inhibition of nonhomologous end joining', *Journal of Cell Biology*, 215(6), pp. 801–821. doi: 10.1083/jcb.201604112.

Lee, I.-G. *et al.* (2018) 'A conserved interaction of the dynein light intermediate chain with dynein-dynactin effectors necessary for processivity', *Nature Communications*, 9(1), p. 986. doi: 10.1038/s41467-018-03412-8.

Lipka, J. *et al.* (2013) 'Mutations in cytoplasmic dynein and its regulators cause malformations of cortical development and neurodegenerative diseases.', *Biochemical Society transactions*, 41(6), pp. 1605–12. doi: 10.1042/BST20130188.

Lui, J. H., Hansen, D. V. and Kriegstein, A. R. (2011) 'Development and evolution of the human neocortex', *Cell*. Elsevier Inc., 146(1), pp. 18–36. doi: 10.1016/j.cell.2011.06.030.

Luxton, G. G. and Starr, D. A. (2014) 'KASHing up with the nucleus: Novel functional roles of KASH proteins at the cytoplasmic surface of the nucleus', *Current Opinion in Cell Biology*, pp. 69–75. doi: 10.1016/j.ceb.2014.03.002.

Luxton, G. W. G. *et al.* (2010) 'Linear arrays of nuclear envelope proteins harness retrograde actin flow for nuclear movement.', *Science (New York, N.Y.)*, 329(5994), pp. 956–9. doi: 10.1126/science.1189072.

Malone, C. J. *et al.* (2003) 'The C. elegans Hook Protein, ZYG-12, Mediates the Essential Attachment between the Centrosome and Nucleus', *Cell*, 115(7), pp. 825–836. doi: 10.1016/S0092-8674(03)00985-1.

Marín, O. and Müller, U. (2014) 'Lineage origins of GABAergic versus glutamatergic neurons in the neocortex', *Current Opinion in Neurobiology*, 26(Figure 1), pp. 132–141. doi: 10.1016/j.conb.2014.01.015.

McKenney, R. J. *et al.* (2014) 'Activation of cytoplasmic dynein motility by dynactin-cargo adapter complexes.', *Science (New York, N.Y.)*, 345(6194), pp. 337–41. doi: 10.1126/science.1254198.

Merkle, F. T. *et al.* (2004) 'Radial glia give rise to adult neural stem cells in the subventricular zone.', *Proceedings of the National Academy of Sciences of the United States of America*, 101(50), pp. 17528–32. doi: 10.1073/pnas.0407893101.

Metzger, T. *et al.* (2012) 'MAP and kinesin-dependent nuclear positioning is required for skeletal muscle function', *Nature*, 484(7392), pp. 120–124. doi: 10.1038/nature10914.

Mikami, A. (2002) 'Molecular structure of cytoplasmic dynein 2 and its distribution in neuronal and ciliated cells', *Journal of Cell Science*, 115(24), pp. 4801–4808. doi: 10.1242/jcs.00168.

Nadarajah, B. *et al.* (2001) 'Two modes of radial migration in early development of the cerebral cortex.', *Nature neuroscience*, 4(2), pp. 143–150. doi: 10.1038/83967.

Noctor, S. C. *et al.* (2004) 'Cortical neurons arise in symmetric and asymmetric division zones and migrate through specific phases.', *Nature neuroscience*, 7(2), pp. 136–144. doi: 10.1038/nn1172.

Norden, C. *et al.* (2009) 'Actomyosin Is the Main Driver of Interkinetic Nuclear Migration in the Retina', *Cell*. Elsevier Ltd, 138(6), pp. 1195–1208. doi: 10.1016/j.cell.2009.06.032.

Norden, C. (2017) 'Pseudostratified epithelia – cell biology, diversity and roles in organ formation at a glance', *Journal of Cell Science*, 130(11), pp. 1859–1863. doi: 10.1242/jcs.192997.

Nowakowski, T. J. *et al.* (2016) 'Transformation of the Radial Glia Scaffold Demarcates Two Stages of Human Cerebral Cortex Development', *Neuron*. Elsevier Inc., 91(6), pp. 1219–1227. doi: 10.1016/j.neuron.2016.09.005.

Olson, E. C. and Walsh, C. A. (2006) 'Impaired Neuronal Positioning and Dendritogenesis in the Neocortex after Cell-Autonomous Dab1 Suppression', *Journal of Neuroscience*, 26(6), pp. 1767–1775. doi: 10.1523/JNEUROSCI.3000-05.2006.

Ostrem, B. E. L. *et al.* (2014) 'Control of outer radial glial stem cell mitosis in the human brain', *Cell Reports*, 8(3), pp. 656–664. doi: 10.1016/j.celrep.2014.06.058.

Ostrem, B., Di Lullo, E. and Kriegstein, A. (2017) 'oRGs and mitotic somal translocation — a role in development and disease', *Current Opinion in Neurobiology*. Elsevier Ltd, 42, pp. 61–67. doi: 10.1016/j.conb.2016.11.007.

Palmer, K. J., Hughes, H. and Stephens, D. J. (2009) 'Specificity of cytoplasmic dynein subunits in discrete membrane-trafficking steps.', *Molecular biology of the cell*, 20(12), pp. 2885–99. doi: 10.1091/mbc.E08-12-1160.

Paschal, B. M., Shpetner, H. S. and Vallee, R. B. (1987) 'MAP 1C is a microtubule-activated ATPase which translocates microtubules in vitro and has dynein-like properties', *Journal of Cell Biology*, 105(3), pp. 1273–1282. doi: 10.1083/jcb.105.3.1273.

Paschal, B. M. and Vallee, R. B. (1987) 'Retrograde transport by the microtubule-associated protein MAP 1C', *Nature*, 330(6144), pp. 181–183. doi: 10.1038/330181a0.

Pfister, K. K. *et al.* (2006) 'Genetic analysis of the cytoplasmic dynein subunit families', *PLoS Genetics*, 2(1), pp. 11–26. doi: 10.1371/journal.pgen.0020001.

Pinto, L. and Götz, M. (2007) 'Radial glial cell heterogeneity-The source of diverse progeny in the CNS', *Progress in Neurobiology*, 83(1), pp. 2–23. doi: 10.1016/j.pneurobio.2007.02.010.

Poirier, K. *et al.* (2013) 'Mutations in TUBG1, DYNC1H1, KIF5C and KIF2A cause malformations of cortical

development and microcephaly.', *Nature genetics*, 45(6), pp. 639–47. doi: 10.1038/ng.2613.

Pollen, A. A. *et al.* (2015) 'Molecular Identity of Human Outer Radial Glia during Cortical Development', *Cell*. Elsevier Inc., 163(1), pp. 55–67. doi: 10.1016/j.cell.2015.09.004.

Raaijmakers, J. A., Tanenbaum, M. E. and Medema, R. H. (2013) 'Systematic dissection of dynein regulators in mitosis.', *The Journal of cell biology*, 201(2), pp. 201–15. doi: 10.1083/jcb.201208098.

Reck-Peterson, S. L. *et al.* (2018) 'The cytoplasmic dynein transport machinery and its many cargoes', *Nature Reviews Molecular Cell Biology*. Springer US, 19(6), pp. 382–398. doi: 10.1038/s41580-018-0004-3.

Reiner, O. *et al.* (1993) 'Isolation of a Miller-Dieker lissencephaly gene containing G protein beta-subunit-like repeats.', *Nature*. Nature Publishing Group, 364(6439), pp. 717–721. doi: 10.1038/364717a0.

Reiner, O. *et al.* (2016) 'Regulation of neuronal migration, an emerging topic in autism spectrum disorders', *Journal of Neurochemistry*, 136(3), pp. 440–456. doi: 10.1111/jnc.13403.

Roman, W. and Gomes, E. R. (2018) 'Nuclear positioning in skeletal muscle.', *Seminars in cell & developmental biology*. Elsevier Ltd, 82, pp. 51–56. doi: 10.1016/j.semcdb.2017.11.005.

Sakakibara, A. *et al.* (2014) 'Dynamics of centrosome translocation and microtubule organization in neocortical neurons during distinct modes of polarization', *Cerebral Cortex*, 24(5), pp. 1301–1310. doi: 10.1093/cercor/bhs411.

Sauer, F. C. (1935) 'Mitosis in the neural tube', *The Journal of Comparative Neurology*, 62(2), pp. 377–405. doi: 10.1002/cne.900620207.

Sauer, F. C. (1936) 'The interkinetic migration of embryonic epithelial nuclei', *Journal of Morphology*, 60(1), pp. 1–11. doi: 10.1002/jmor.1050600102.

Sauer, M. E. and Walker, B. E. (1959) 'Radioautographic study of interkinetic nuclear migration in the neural tube.', *Proceedings of the Society for Experimental Biology and Medicine. Society for Experimental Biology and Medicine (New York, N.Y.)*, 101(3), pp. 557–60. doi: 10.3181/00379727-101-25014.

Schaar, B. T. and McConnell, S. K. (2005) 'Cytoskeletal coordination during neuronal migration', *Proceedings of the National Academy of Sciences*, 102(38), pp. 13652–13657. doi: 10.1073/pnas.0506008102.

Schmoranzer, J. *et al.* (2009) 'Par3 and Dynein Associate to Regulate Local Microtubule Dynamics and Centrosome Orientation during Migration', *Current Biology*, 19(13), pp. 1065–1074. doi: 10.1016/j.cub.2009.05.065.

Schroeder, C. M. *et al.* (2014) 'A Ras-like domain in the light intermediate chain bridges the dynein motor to a cargo-binding region.', *eLife*, 3, p. e03351. doi: 10.7554/eLife.03351.

Schroeder, C. M. and Vale, R. D. (2016) 'Assembly and Activation of Dynein-Dynactin by the Cargo Adaptor Protein Hook3', *Journal of Cell Biology*, 214(3). doi: 10.1101/047605.

Sekine, K. *et al.* (2011) 'The Outermost Region of the Developing Cortical Plate Is Crucial for Both the Switch of the Radial Migration Mode and the Dab1-Dependent "Inside-Out" Lamination in the Neocortex', *Journal of Neuroscience*, 31(25), pp. 9426–9439. doi: 10.1523/JNEUROSCI.0650-11.2011.

Shu, T. *et al.* (2004) 'Ndel1 operates in a common pathway with LIS1 and cytoplasmic dynein to regulate cortical neuronal positioning', *Neuron*. Cell Press, 44(2), pp. 263–277. doi: 10.1016/j.neuron.2004.09.030.

Sidman, R. L. and Rakic, P. (1973) 'Neuronal migration, with special reference to developing human brain: a review', *Brain Research*, pp. 1–35. doi: 10.1016/0006-8993(73)90617-3.

Solecki, D. J. (2012) 'Sticky situations: Recent advances in control of cell adhesion during neuronal migration', *Current Opinion in Neurobiology*, 22(5), pp. 791–798. doi: 10.1016/j.conb.2012.04.010.

Sousa, A. M. M. *et al.* (2017) 'Evolution of the Human Nervous System Function, Structure, and Development', *Cell*, 170(2), pp. 226–247. doi: 10.1016/J.CELL.2017.06.036.

Splinter, D. *et al.* (2010) 'Bicaudal D2, dynein, and kinesin-1 associate with nuclear pore complexes and regulate centrosome and nuclear positioning during mitotic entry', *PLoS Biology*, 8(4). doi: 10.1371/journal.pbio.1000350.

Splinter, D. *et al.* (2012) 'BICD2, dynactin, and LIS1 cooperate in regulating dynein recruitment to cellular structures', *Molecular Biology of the Cell*, 23(21), pp. 4226–4241. doi: 10.1091/mbc.E12-03-0210.

Srsen, V. *et al.* (2009) 'Centrosome proteins form an insoluble perinuclear matrix during muscle cell differentiation.', *BMC cell biology*, 10, p. 28. doi: 10.1186/1471-2121-10-28.

Starr, D. A. and Fridolfsson, H. N. (2010) 'Interactions between nuclei and the cytoskeleton are mediated by

SUN-KASH nuclear-envelope bridges.', *Annual review of cell and developmental biology*, 26, pp. 421–44. doi: 10.1146/annurev-cellbio-100109-104037.

Tabata, H. and Nakajima, K. (2003) 'Multipolar migration: the third mode of radial neuronal migration in the developing cerebral cortex.', *The Journal of neuroscience : the official journal of the Society for Neuroscience*, 23(31), pp. 9996–10001. Available at: http://www.ncbi.nlm.nih.gov/pubmed/14602813.

Tan, S. C. (2009) 'The Role of Cytoplasmic Dynein Light Intermediate Chains in Dynein-Mediated Transport, Mitosis, and Neural Precursor Migration', *Thesis defence Columbia University*, pp. 1–122.

Tan, S. C., Scherer, J. and Vallee, R. B. (2011) 'Recruitment of dynein to late endosomes and lysosomes through light intermediate chains.', *Molecular biology of the cell*, 22(4), pp. 467–477. doi: 10.1091/mbc.E10-02-0129.

Tapley, E. C. and Starr, D. A. (2013) 'Connecting the nucleus to the cytoskeleton by SUN-KASH bridges across the nuclear envelope', *Current Opinion in Cell Biology*, pp. 1–6. doi: 10.1016/j.ceb.2012.10.014.

Tassin, A. M., Maro, B. and Bornens, M. (1985) 'Fate of microtubule-organizing centers during myogenesis in vitro.', *The Journal of cell biology*, 100(1), pp. 35–46. doi: 10.1083/jcb.100.1.35.

Taylor, S. P. *et al.* (2015) 'Mutations in DYNC2LI1 disrupt cilia function and cause short rib polydactyly syndrome', *Nature Communications*. Nature Publishing Group, 6, p. 7092. doi: 10.1038/ncomms8092.

Trivedi, N. *et al.* (2017) 'Drebrin-mediated microtubule-actomyosin coupling steers cerebellar granule neuron nucleokinesis and migration pathway selection.', *Nature communications*. Nature Publishing Group, 8, p. 14484. doi: 10.1038/ncomms14484.

Tsai, J.-W. *et al.* (2010) 'Kinesin 3 and cytoplasmic dynein mediate interkinetic nuclear migration in neural stem cells.', *Nature neuroscience*. Nature Publishing Group, 13(12), pp. 1463–1471. doi: 10.1038/nn.2665.

Tsai, J.-W., Bremner, K. H. and Vallee, R. B. (2007) 'Dual subcellular roles for LIS1 and dynein in radial neuronal migration in live brain tissue.', *Nature neuroscience*, 10(8), pp. 970–979. doi: 10.1038/nn1934.

Tsai, J. W. *et al.* (2005) 'LIS1 RNA interference blocks neural stem cell division, morphogenesis, and motility at multiple stages', *Journal of Cell Biology*, 170(6), pp. 935–945. doi: 10.1083/jcb.200505166.

Tynan, S. H. *et al.* (2000) 'Light intermediate chain 1 defines a functional subfraction of cytoplasmic dynein which binds to pericentrin', *Journal of Biological Chemistry*, 275(42), pp. 32763–32768. doi: 10.1074/jbc.M001536200.

Umeshima, H. *et al.* (2019) 'Local traction force in the proximal leading process triggers nuclear translocation during neuronal migration.', *Neuroscience research*. Elsevier Ireland Ltd and Japan Neuroscience Society, 142, pp. 38–48. doi: 10.1016/j.neures.2018.04.001.

Vale, R. D., Reese, T. S. and Sheetz, M. P. (1985) 'Identification of a novel force-generating protein, kinesin, involved in microtubule-based motility', *Cell*, 42(1), pp. 39–50. doi: 10.1016/S0092-8674(85)80099-4.

Valiente, M. and Marín, O. (2010) 'Neuronal migration mechanisms in development and disease', *Current Opinion in Neurobiology*, 20(1), pp. 68–78. doi: 10.1016/j.conb.2009.12.003.

Vallee, R. B., McKenney, R. J. and Ori-McKenney, K. M. (2012) 'Multiple modes of cytoplasmic dynein regulation', *Nature Cell Biology*. Nature Publishing Group, 14(3), pp. 224–230. doi: 10.1038/ncb2420.

Vallee, R. B., Rakic, P. and Bhide, P. G. (2008) 'Modes and Mishaps of Neuronal Migration in the', *The Journal of Neuroscience*, 28(46), pp. 11746–11752. doi: 10.1523/JNEUROSCI.3860-08.2008.

Wang, X. *et al.* (2011) 'A new subtype of progenitor cell in the mouse embryonic neocortex.', *Nature neuroscience*. Nature Publishing Group, 14(5), pp. 555–561. doi: 10.1038/nn.2807.

Wilson, M. H. and Holzbaur, E. L. F. (2012) 'Opposing microtubule motors drive robust nuclear dynamics in developing muscle cells', *Journal of Cell Science*, 125(17), pp. 4158–4169. doi: 10.1242/jcs.108688.

Wilson, M. H. and Holzbaur, E. L. F. (2015) 'Nesprins anchor kinesin-1 motors to the nucleus to drive nuclear distribution in muscle cells', *Development*, 142(1), pp. 218–228. doi: 10.1242/dev.114769.

Wonders, C. P. and Anderson, S. A. (2006) 'The origin and specification of cortical interneurons', *Nature Reviews Neuroscience*, 7(9), pp. 687–696. doi: 10.1038/nrn1954.

Wynne, C. L. and Vallee, R. B. (2018) 'Cdk1 phosphorylation of the dynein adapter Nde1 controls cargo binding from G2 to anaphase', *Journal of Cell Biology*, pp. 1–11. doi: 10.1083/jcb.201707081.

Zhang, K. *et al.* (2017) 'Cryo-EM Reveals How Human Cytoplasmic Dynein Is Auto-inhibited and Activated', *Cell*. Elsevier, 169(7), pp. 1303-1314.e18. doi: 10.1016/j.cell.2017.05.025.

Zhang, X. *et al.* (2007) 'Syne-1 and Syne-2 play crucial roles in myonuclear anchorage and motor neuron innervation.', *Development (Cambridge, England)*, 134(5), pp. 901–8. doi: 10.1242/dev.02783.

Zhang, X. *et al.* (2009) 'SUN1/2 and Syne/Nesprin-1/2 Complexes Connect Centrosome to the Nucleus during Neurogenesis and Neuronal Migration in Mice', *Neuron*. Elsevier Ltd, 64(2), pp. 173–187. doi: 10.1016/j.neuron.2009.08.018.

Zhou, K. *et al.* (2009) 'A ZYG-12-dynein interaction at the nuclear envelope defines cytoskeletal architecture in the C. elegans gonad', *Journal of Cell Biology*, 186(2), pp. 229–241. doi: 10.1083/jcb.200902101.

Zhu, R., Antoku, S. and Gundersen, G. G. (2017) 'Centrifugal Displacement of Nuclei Reveals Multiple LINC Complex Mechanisms for Homeostatic Nuclear Positioning', *Current Biology*. Elsevier Ltd., pp. 1–14. doi: 10.1016/j.cub.2017.08.073.

Zhu, R., Liu, C. and Gundersen, G. G. (2018) 'Nuclear positioning in migrating fibroblasts', *Seminars in Cell & Developmental Biology*. Elsevier Ltd, 82, pp. 41–50. doi: 10.1016/j.semcdb.2017.11.006.

CHAPTER 2 – EXPERIMENTAL WORK

CHAPTER 2.1

Distinct roles for dynein light intermediate chains in neurogenesis, migration, and terminal somal translocation

João Carlos Gonçalves, Tiago J. Dantas, Richard B. Vallee

The Journal of Cell Biology, volume. 218, number 3, pages 808-819

DOI: 10.1083/jcb.201806112

TITLE: Distinct roles for dynein light intermediate chains in neurogenesis, migration, and terminal somal translocation

RUNNING TITLE: Dynein LIC1 and LIC2 in neocortical development.

AUTHORS AND AFFILIATIONS

João Carlos Gonçalves[1, 2, 3], Tiago J. Dantas[1, 4, 5], Richard B. Vallee[1*]

1 - Department of Pathology and Cell Biology, Columbia University Medical Center, New York, NY, USA.

2 - Life and Health Sciences Research Institute (ICVS), School of Medicine, University of Minho, Campus Gualtar, Braga, Portugal.

3 - ICVS/3B's - PT Government Associate Laboratory, Braga/Guimarães, Portugal.

4 - i3S - Instituto de Investigação e Inovação em Saúde, University of Porto, Porto, Portugal.

5 - IBMC – Instituto de Biologia Molecular e Celular, University of Porto, Porto, Portugal.

*Corresponding author: Richard B. Vallee (rv2025@columbia.edu)

KEYWORDS

Dynein light intermediate chains, BicD2, neocortical development, terminal somal translocation, interkinetic nuclear migration, radial glial progenitors.

Abbreviations used in this Chapter: LIC, Dynein light intermediate chain; G-domain, GTPase-like domain; A-domain, Adaptor domain; HC, dynein heavy chain; RGP, Radial glial progenitor; INM, Interkinetic nuclear migration; TST, Terminal somal translocation; VS, Ventricular surface; VZ, Ventricular zone; SVZ, Subventricular zone; IZ, Intermediate zone; CP, Cortical plate; MZ, Marginal zone; KD, Knockdown.

SUMMARY

The retrograde microtubule motor cytoplasmic dynein is fundamental for mammalian brain development. Gonçalves et al. identify distinct roles for dynein cargo-binding subunits, the light intermediate chains, in neocortical development and uncover a novel function for dynein in terminal somal translocation of neurons.

ABSTRACT

Cytoplasmic dynein participates in multiple aspects of neocortical development. These include neural progenitor proliferation, morphogenesis, and neuronal migration. The cytoplasmic dynein light intermediate chains (LICs) 1 and 2 are cargo-binding subunits, though their relative roles are not well understood. Here, we used *in utero* electroporation of shRNAs or LIC functional domains to determine the relative contributions of the two LICs in the developing rat brain. We find that LIC1, through BicD2, is required for apical nuclear migration in neural progenitors. In newborn neurons, we observe specific roles for LIC1 in the multipolar-to-bipolar transition and glial-guided neuronal migration. In contrast, LIC2 contributes to a novel dynein role in the little-studied mode of migration, terminal somal translocation. Together, our results provide novel insight into the LICs' unique functions during brain development and dynein regulation over all.

INTRODUCTION

Cytoplasmic dynein 1 (hereafter "dynein") carries out a very extensive range of functions in the cell. A number of dynein dependent mechanisms are required for vertebrate brain development (Bertipaglia, Gonçalves and Vallee, 2018), and impaired dynein function has been associated with multiple neurodevelopmental diseases (Reiner *et al.*, 1993; Lipka *et al.*, 2013; Poirier *et al.*, 2013; Fiorillo *et al.*, 2014; Jamuar *et al.*, 2014). Dynein is essential for the proliferation of embryonic neural stem cells, known as radial glial progenitors (RGPs) (Tsai *et al.*, 2005, 2010), which give rise to most neurons and glia in the cerebral cortex (Kriegstein and Alvarez-buylla, 2009). RGPs have a unique morphology, with an apical process that contacts the surface of the inner cerebral ventricle and a basal process that spans the entire neocortex to contact the pial surface. RGP nuclei oscillate in synchrony with cell cycle progression, a behavior termed interkinetic nuclear migration (INM). During INM the RGP nuclei migrate away from the ventricular surface (VS) throughout G1 (basal migration), and return to the VS during G2 (apical migration). Apical INM in RGPs is driven by nuclear envelope-associated dynein and mitotic entry occurs only when the RGP nucleus has reached the VS (Hu *et al.*, 2013; Baffet, Hu and Vallee, 2015; Doobin *et al.*, 2016).

Neurons originating from RGP divisions migrate out of the inner neocortical proliferative region, the ventricular zone (VZ) to the subventricular and intermediate zones (SVZ/IZ), where they first adopt a multipolar morphology. Multipolar cells require dynein for transition into bipolar neurons, and for their subsequent glial-guided migration to the cortical plate (CP) along the basal processes of the RGPs (Shu *et al.*, 2004; Tsai *et al.*, 2005; Tsai, Bremner and Vallee, 2007). In the outermost region of the CP, neurons engage in a final form of non-glial guided migration called terminal somal translocation (TST) (Nadarajah *et al.*, 2001; Franco *et al.*, 2011; Sekine *et al.*, 2011). Whether dynein also contributes to this final stage of neuronal migration is unknown.

How a single form of dynein may carry out a wide range of functions has been a central question in the field. Dynein has a number of subunits, which contribute to cargo binding and motor regulation. The function of one class of cytoplasmic-specific dynein subunits, the light intermediate chains (LICs), remains poorly understood. In vertebrates, two highly similar genes *DYNC1LI1* and *DYNC1LI2* (Pfister *et al.*, 2006) encode LIC1 and LIC2 respectively, which integrate the dynein complex. The divergent LIC3 (*DYNC2LI*) associates exclusively to ciliary cytoplasmic dynein-2 to mediate intraflagellar transport (Grissom, Vaisberg and McIntosh, 2002; Mikami, 2002; Taylor *et al.*, 2015). Recently, LIC1 and LIC2 have been shown to link dynein to an

emerging class of dynein cargo adaptor proteins, which include the BicD and Hook proteins, RILP, and Spindly (Fig. 1 A and B) (Scherer, Yi and Vallee, 2014; Schroeder *et al.*, 2014; Schroeder and Vale, 2016; Gama *et al.*, 2017; Lee *et al.*, 2018). These adaptors serve specifically to recruit supercomplexes of dynein and its regulators to diverse forms of subcellular cargo (reviewed in (Reck-Peterson *et al.*, 2018)). Some studies have addressed LIC1 *vs.* LIC2-dynein roles in cultured cells and mainly suggested overlapping functions (Palmer, Hughes and Stephens, 2009; Tan, Scherer and Vallee, 2011; Raaijmakers, Tanenbaum and Medema, 2013; Jones *et al.*, 2014). To determine LIC1 and LIC2 relative roles *in vivo* we have examined their requirement during neocortical development. We find that LIC1 and LIC2 play essential, but only partially overlapping roles in neurogenesis and neuronal migration, and we identify a novel role for dynein and LIC2 in the little-explored mechanism of TST.

RESULTS AND DISCUSSION

Effects of LIC1 and LIC2 depletion in RGP apical nuclear migration

To investigate whether the LIC proteins have distinct or overlapping roles in RGP INM, we delivered shRNAs against *Dync1li1* (LIC1) and/or *Dync1li2* (LIC2) into the lateral ventricles of embryonic day 16 (E16) rat embryos, using *in utero* electroporation. Analysis of the VZ in electroporated brain slices was performed 4 days after electroporation, at E20. RNAi efficiency was determined by qRT-PCR and immunoblotting (Supp. Fig 1 A, B), which confirmed successful reduction in protein levels. LIC1 knockdown (KD) caused a pronounced shift in the distribution of RGP nuclei away from the VS (Fig. 1 C, D), consistent with inhibition of apical INM. We also observed a marked decrease in mitotic index (Fig. 1F), consistent with the inability of the nuclei to reach the VS and enter mitosis. To test LIC1 function in apical INM more directly, we performed live imaging of LIC1-depleted RGPs in brain slices. LIC1 KD severely inhibited RGP apical nuclear migration, arresting nuclei before they could reach the VS (Fig. 1 G, Supp. video 1, 2). Previous work from our lab (Hu *et al.*, 2013) revealed that RGP nuclei may arrest far from (>30μm) or near to (<10μm) the VS following expression of shRNAs against genes that mediate early G2 *vs.* late G2 nuclear envelope dynein recruitment. We found that LIC1 KD arrested RGP nuclei at similar distances to those found upon depletion of early G2-dynein recruitment proteins (Fig. 1E), such as BicD2 (Hu *et al.*, 2013), a LIC interactor protein (Schroeder *et al.*, 2014; Lee *et al.*, 2018).

Increasing dynein recruitment to the nuclear envelope by BicD2 overexpression overcomes knockdown of genes in the late G2-dynein-recruitment pathway (Hu *et al.*, 2013; Doobin *et al.*, 2016). To examine the functional relationship between BicD2 and LIC1 in our system we tested whether BicD2 expression could rescue the effects of LIC1 KD. BicD2 overexpression in a LIC1 KD background failed to restore normal nuclear distribution (Fig. 1 H, I). This result is consistent with a common role for BicD2 and LIC1 in apical INM.

In contrast to our LIC1 KD results, LIC2 KD had no detectable effect on RGP apical nuclear migration or mitosis (Fig. 1 C-G, Supp. video 3). To address whether depletion of both subunits would cause more severe effects on RGP nuclear distribution, we co-expressed shRNAs for LIC1 and LIC2. Reduced levels of both subunits phenocopied LIC1 KD alone (Fig. 1 C-F), supporting a predominant role for LIC1 in apical INM. To test whether these results might reflect differences in LIC1 *vs.* LIC2 protein levels, we measured the relative amounts of dynein subunits in brain lysates during late embryogenesis and adulthood (Supp. Fig. 1 C, D).

The ratio of LIC1 to LIC2 protein levels was unaltered across developmental stages. In addition, staining of E20 brain slices with LIC1- or LIC2- specific antibodies showed cytoplasmic expression throughout the several layers of the developing neocortex for both subunits (Supp. Fig. 1 E-H). Therefore, the effects of LIC1 *vs.* LIC2 KD are likely to result from differential LIC physiological roles.

Mechanistic insight from the LIC functional domains

To test the relative cargo-binding role of the LICs more directly, we generated cDNAs encoding individual LIC functional domains, the N-terminal GTPase-like domain (G-domain) and the C-terminal Adaptor domain (A-domain) (Fig.1 B). The G-domain of each LIC co-immunoprecipitated the dynein heavy chain (HC) and the intermediate chain (IC), but not the endogenous LICs (Supp. Fig. 2 A and B). This suggests that expression of the G-domain competes with the endogenous LICs for a common HC binding site. The C-terminal A-domain binds directly to BicD2 and other dynein adaptor proteins, but does not co-immunoprecipitate the dynein complex (Schroeder *et al.*, 2014; Gama *et al.*, 2017; Lee *et al.*, 2018).

To understand further the functional roles of the LICs we electroporated the full-length, G-domain and A-domain versions of each LIC. Expression of the LIC1 or LIC2 A-domains had no detectable effect in RGP nuclear distribution or mitotic index (Supp. Fig. 2 C-E). Interestingly, expression of full-length LIC1 caused a moderate shift in the RGP nuclei toward the VS (Fig. 2 A, B), consistent with enhanced dynein activity in apical nuclear migration. We observed no such effect for LIC2 (Fig.2 A, B). In contrast, expression of the LIC1 G-domain caused a marked displacement of RGP nuclei away from the VS, at distances similar to those seen with LIC1 KD (>30μm). LIC1 G-domain also caused a strong reduction in mitotic index (Fig. 2 A-D). Surprisingly, despite a common LIC binding site within the HC (Tynan, Gee and Vallee, 2000), the LIC2 G-domain had no apparent effect on the RGP nuclear position or mitotic index (Fig.2 A-D). Together, these results confirm a more important cargo-binding role for LIC1 in INM, consistent with the LIC1 and LIC2 KD effects.

LIC1 and LIC2 share high sequence similarity within both dynein- and cargo-binding domains (Tynan *et al.*, 2000; Pfister *et al.*, 2006). Thus, despite the differences in LIC1 *vs.* LIC2 KD effects, we asked whether LIC2 could compensate LIC1 depletion. To test this possibility we co-expressed LIC1 shRNA with a control vector, RNAi insensitive LIC1 or LIC2 cDNAs. Electroporation of LIC1 cDNA on a LIC1 KD background rescued RGP nuclear position and mitotic index (Fig. 2 E-H). Remarkably, expression of LIC2 cDNA on a LIC1 KD

background was able to rescue RGP nuclei position and mitotic index to control GFP levels (Fig. 2 E-H). However, when compared to LIC1 self-rescue, LIC2 rescue of LIC1 KD showed RGP nuclei slightly, but significantly, shifted away from the VS (Fig. 2 E, F). This again suggests that apical INM is preferentially mediated by LIC1, but increased amounts of LIC2 can overcome LIC1 depletion and restore apical INM.

Our results show that LIC1 is essential for BicD2-mediated apical INM. However, the ability of LIC2 to rescue LIC1 KD RGP nuclear distribution and mitotic index suggests that the two LICs are both capable of binding to BicD2. To address this possibility, we incubated embryonic brain lysate with bacterially purified BicD2 N-terminal region, which binds dynein and its regulatory complex dynactin (Splinter *et al.*, 2012; McKenney *et al.*, 2014). Immunoblotting revealed that BicD2 bound both LICs, though LIC1 was significantly more enriched compared to LIC2 (Fig. 2 I, J). Therefore, although BicD2 can interact with either LIC, BicD2 preferentially recruits LIC1-dynein complexes. These results likely account for the predominant role of LIC1 in apical INM and the ability of LIC2 to rescue apical INM when LIC1 is depleted.

LIC1 and LIC2 have distinct roles in post-mitotic neurons

We previously found that dynein is required for post-mitotic neuronal morphogenesis and subsequent migration into the CP, their final destination (Tsai *et al.*, 2005; Tsai, Bremner and Vallee, 2007). Therefore, we analyzed the distribution of electroporated cells in each of the neocortical layers upon depletion of each LIC. LIC1 KD caused a striking reduction in the number of neurons in the CP (Fig. 3 A, C), with most electroporated cells retained in the SVZ/IZ. In contrast, LIC2 KD had little effect in the progression of post-mitotic neurons to the CP (Fig. 3 A, C). Double LIC KD gave results similar to those effects for LIC1 KD alone (Fig. 3 A, C). Thus, we find that LIC1 is essential for both INM and neuronal migration to the CP, whereas LIC2 is dispensable for these cell behaviors.

Next, we tested the effects of expressing the full-length LICs and their G-domains on neocortical cellular distribution. Expression of LIC1 or LIC2 full-length cDNA had no noticeable effect on proportion of cells in the SVZ/IZ and CP (Fig. 3 B, D). Expression of LIC2 G-domain had no detectable effect on the proportion of cells in these regions either (Fig. 3 B, D), consistent with our LIC2 KD results. We note that there was a mild decrease in the number of cells in the VZ with LIC2 G-domain expression, but the basis for this is unclear. In contrast to these conditions, expression of the LIC1 G-domain caused severe accumulation of electroporated

neurons in the SVZ/IZ and a marked reduction within the CP (Fig. 3 B, D), consistent with the effects of LIC1 KD.

As neurons migrate out of the IZ into the CP, they transition from a multipolar-to-bipolar migratory morphology. LIC1 KD caused a robust increase in the number of multipolar cells at the expense of bipolar cells (Fig. 3 E). In contrast, expression of the LIC1 G-domain had no effect on the proportion of multipolar and bipolar neurons (Fig. 3 E), presumably reflecting a lesser degree of dynein inhibition. Once becoming bipolar in the SVZ/IZ, neurons initiate migration toward the CP using the glial (RGP) fibers as scaffolds, a mechanism known to require dynein (Tsai et al. 2007). Our results suggested that SVZ/IZ neurons expressing the LIC1 G-domain were able to become bipolar, but were unable to migrate toward the CP. To test this hypothesis and determine whether LICs participate in glial-guided migration, we performed live imaging of the upper IZ/lower CP region and followed the migration of neurons transfected with control vector, LIC1 G-domain and LIC2 G-domain. In contrast to control, neuronal cell bodies expressing LIC1 G-domain remained mostly immotile throughout the imaging period (Fig. 3F Supp. video 4 and 5). Expression of the LIC2 G-domain had no significant effect, as cell bodies were able to migrate distances similar to those for control cells (Fig. 3F Supp. video 6). Together, these results support fundamental roles for LIC1, but not LIC2, in the multipolar-to-bipolar transition and in glial-guided neuronal migration.

Novel role for dynein in terminal somal translocation

Despite the minimal role we found for LIC2 in INM, in the multipolar-to-bipolar transition and in glial-guided migration, LIC2 KD and LIC2 G-domain expression caused a striking decrease in the number of cells reaching the uppermost layers of the CP (Fig. 4 A, B; Supp. Fig 3 A, B). The arrested cells also had elongated processes contacting the outer marginal zone (MZ), but their cell bodies were located in deeper neocortical layers compared to control (Fig. 4 C). This suggested an impairment of the last stage of neuronal migration, known as terminal somal translocation (TST). This behavior involves MZ contact and subsequent shortening of the leading process of the migrating neuron, as the soma continuously move toward the pial surface of the brain (Nadarajah *et al.*, 2001; Franco *et al.*, 2011; Sekine *et al.*, 2011). Unlike the preceding glial-guided neuronal migration along the RGP basal processes, TST does not utilize glial scaffolding, and the role of motor proteins is elusive (Cooper, 2013).

To test LIC2 function in TST more directly, we performed live imaging of LIC2 G-domain and LIC2 shRNA electroporated neurons in the upper CP. In control cells, the leading process contacted the MZ, and cell bodies migrated appropriately toward the pial surface as their leading process shortened (Fig. 4 D, Supp. Video 7). Processes of neurons expressing the LIC2 G-domain or a LIC2 shRNA still contacted the MZ, but the cell bodies remained immotile throughout the imaging period (Fig. 4 D, Supp. Video 8; Supp. Fig. 3 C, Supp. Video 9), further confirming a key role for LIC2 in TST. To our knowledge, these results are the first to show a role for motor proteins in TST and identify a novel function for dynein during brain development.

LICs are required for neuronal migration in the post-natal rat brain

To determine the extent to which depleting LICs delays or permanently blocks neuronal migration, we introduced LIC1 or LIC2 shRNAs into E16 rat brain and analyzed them two weeks later, at post-natal day7 (P7) (Fig. 5 A, B). LIC1 KD caused a marked accumulation of cell bodies in the white matter with a reduction in the number of neurons in the post-natal neocortex, a striking outcome not observed in controls or in LIC2 depleted brains. In contrast, LIC2 KD neurons bypassed the white matter, though they were unable to migrate to the upper neocortical layers. These data are consistent with our results in the embryonic brain and further support our findings of fundamental, but distinct, roles for LIC1 and LIC2 *in vivo*.

Molecular Roles of LICs in Brain Development

Notoriously, we find differences in LIC1 *vs.* LIC2 phenotypes at multiple stages of neocortical development (Fig. 5 C). Expression of LIC1 shRNA or LIC1 G-domain potently interfered with the dynein-driven apical INM. Similar analysis for LIC2 had no detectable effect. Nonetheless, LIC2 overexpression completely rescued the LIC1 KD phenotype, indicating that abundant LIC2 is capable of serving in this function. Seeking to explain this surprising result we found differences in LIC1 *vs.* LIC2 binding to BicD2, the dynein adaptor in apical INM. We do note that other molecules interact differentially with the two LICs, most notably pericentrin and PAR3 (Purohit *et al.*, 1999; Tynan *et al.*, 2000; Schmoranzer *et al.*, 2009; Mahale *et al.*, 2016). Conceivably these interactions might also contribute to the phenotypic differences between the LICs that we observe.

Analysis of each LIC in post-mitotic neuronal migration, revealed further differential roles. We found that LIC1 inhibition impedes newborn neurons from reaching the CP by disrupting at least two distinct mechanisms: the multipolar-to-bipolar transition, and glial-guided migration. These results mimicked those for the dynein heavy chain KD (Tsai et al. 2005; Tsai et al. 2007), which would disrupt overall dynein motor activity. LIC2

had no noticeable function at these stages. Interestingly, BicD2 KD was reported to cause a multipolar accumulation at the expense of bipolar neurons (Hu et al. 2013), comparable to our results with LIC1 KD. This is consistent with a stronger role for LIC1 to mediate BicD2 dependent functions, as seen in RGPs. Thus we hypothesize that the BicD2 - LIC1 interaction might be also active during multipolar-to-bipolar transition.

The minor role for LIC2 in earlier stages of brain development allowed us to uncover a novel role for dynein in neuronal TST. Neurons expressing LIC2 shRNA or LIC2 G-domain reached the CP, but there was a marked accumulation of cell bodies abnormally far from the pial surface. We found that the processes of these cells were still able to contact the MZ, suggesting that LIC2 is not required for process extension, but is essential for somal translocation. Using live imaging, we confirmed this specific arrest in neuronal cell body movement. Although our results reveal a clear role for LIC2 in TST, we cannot determine whether LIC1 also has a role at this stage. This is because the effects of LIC1 inhibition severely inhibit neuronal migration prior to this last step. We believe these results are the first evidence of a dynein role in TST. Thus, altogether, our data reveals a succession of dynein functions throughout neocortical development, which depends on differential roles of LICs at several stages.

The differential functionality of LICs in brain development, primarily non-overlapping, is consistent with earlier evidence that these dynein subunits exist in distinct LIC1- and LIC2-containing dynein fractions as judged by co-Immunoprecipitation studies (Tynan *et al.*, 2000). Our current study provides further insight into the mechanisms underlying differential LIC function. In particular, we find that expression of the LIC G-domains strongly interferes with dynein function *in vivo*, as determined by the effects on neurogenesis and neuronal migration in the developing rat brain. A reasonable explanation for the inhibitory effect of the G-domain expression would be the competition with endogenous LICs for the LIC binding site located within the tail region of the dynein HC. In this case, the prediction would be a similar phenotype from the expression of either LIC G-domain. Surprisingly, however, the phenotypes are clearly distinct. For this reason, we speculate that each LIC might associate preferentially with dynein complexes of specific composition and/or post-translational modifications. Interestingly, a recent dynein interactome analysis detected an enrichment for different dynein light chain subunits in LIC1- *vs.* LIC2-containing dynein (Redwine *et al.*, 2017), suggesting that LIC integration into the dynein complex may depend on or dictate a specific dynein subunit composition. How each LIC integrates the dynein complex likely contributes to the differential LIC1 and LIC2 functions *in vivo,* but the mechanisms for this remain to be determined.

FIGURES AND FIGURE LEGENDS

Figure 1

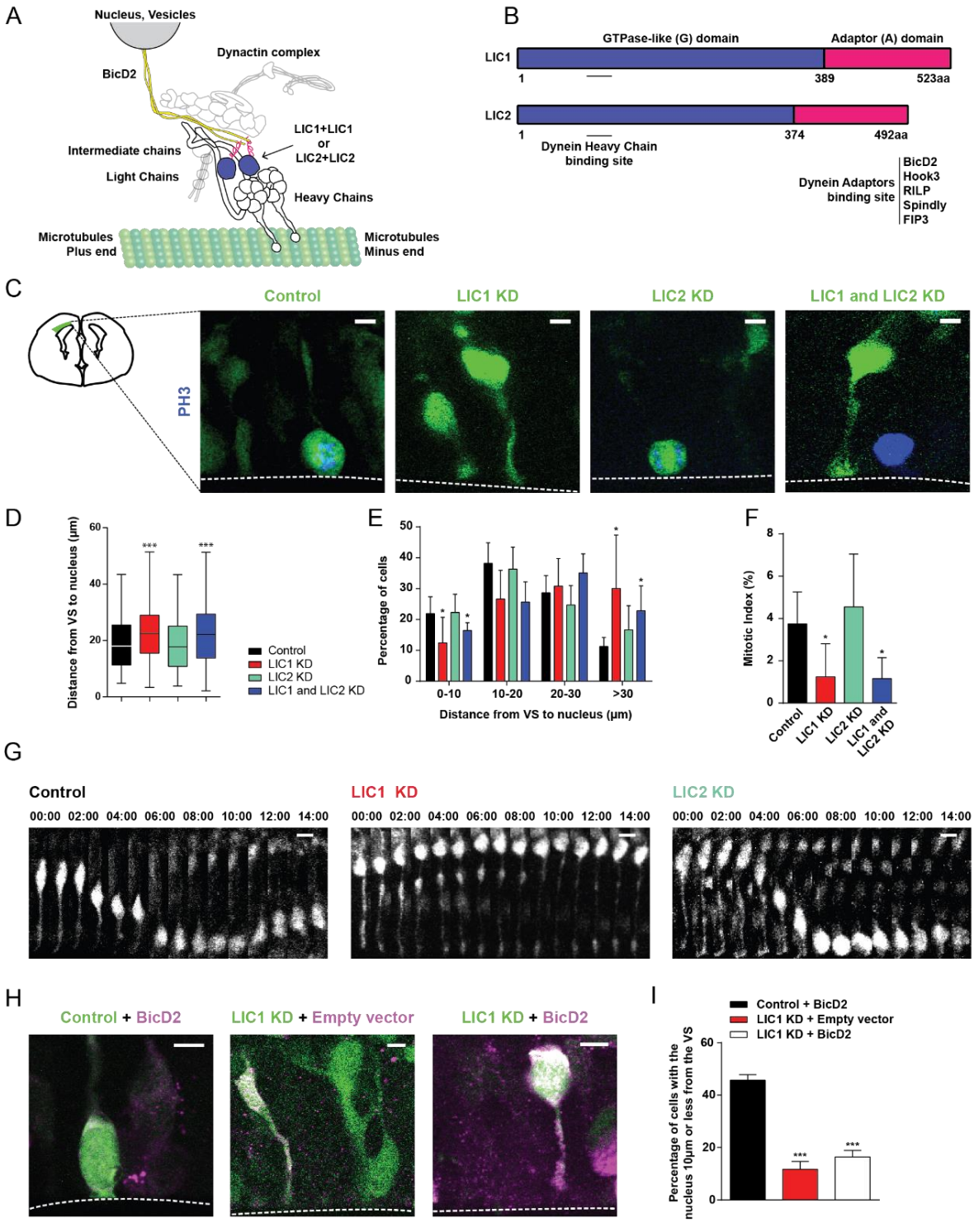

Figure 1

Distinct roles for the LICs in apical INM. (A, B) Diagrammatic representation of the **(A)** dynein-dynactin-BicD2 complex (modified from (Carter, Diamant and Urnavicius, 2016)). LIC1 or LIC2 composition defines distinct dynein subfractions (Tynan *et al.*, 2000). **(B)** LIC functional domains and interactors. **(C-G)** Embryonic day 16 (E16) rat brains were *in utero* electroporated with control vector or shRNAs for LIC1 and/or LIC2 and subsequently imaged live or fixed 4 days post injection (d.p.i), at E20. **(C)** Fixed images of the VZ from electroporated brains stained for the mitotic marker phosphohistone-H3 (PH3). Dashed line represents the VS. **(D, E, I)** Quantification of distance between the RGP nuclei and the VS across conditions **(F)** Effect of LIC1 and/or LIC2 KD on RGP cell mitotic index. **(G)** Time-lapse images for control, LIC1 KD or LIC2 KD in RGPs (Supplementary Movies 1–3). Images are shown with 60min intervals (hh:mm). **(H, I)** E16 brains were *in utero* electroporated with BicD2 on a wild type or LIC1 KD background or LIC1 KD alone. Analysis was done 4 d.p.i. (**H**) Representative images from electroporated RGPs at the VZ. Data presented as Box-and-Whiskers plot in **D**; and data shown as mean±s.d. in **E**, **F** and **I.** Unpaired T-test was used in **D, E, F** and **I** (*P<0.05; **P<0.01;***P<0.001). Data in **D, E** and **F** includes at least 337 RGPs from at least 5 embryos and data in **I** includes at least 165 RGPs from at least 4 embryos. **C** and **H** scale bars, 5μm. **G** scale bar, 10μm.

Figure 2

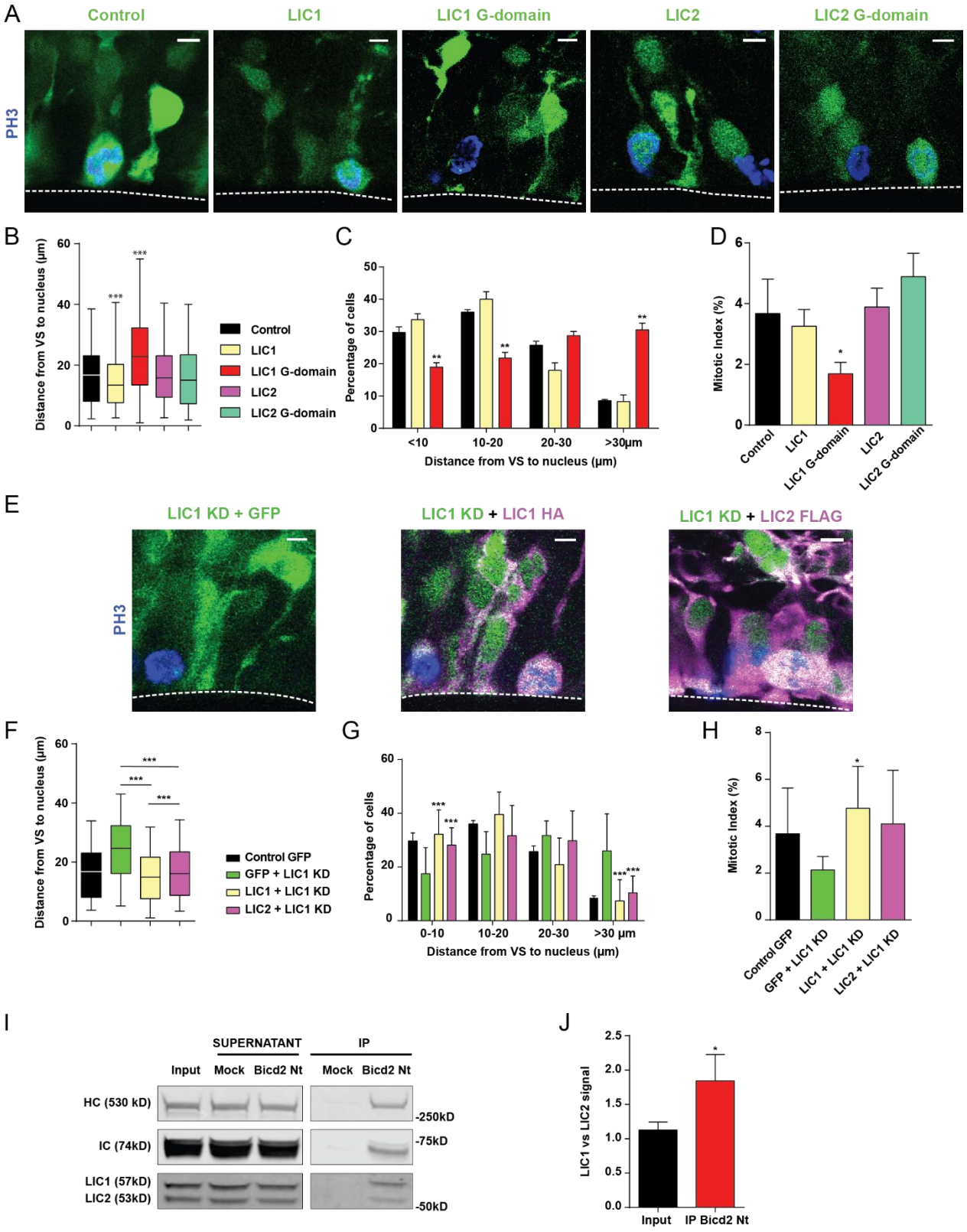
A
Control
LIC1
LIC1 G-domain
LIC2
LIC2 G-domain
PH3
B
Distance from VS to nucleus (μm)
Control
LIC1
LIC1 G-domain
LIC2
LIC2 G-domain
C
Percentage of cells
<10
10-20
20-30
>30μm
Distance from VS to nucleus (μm)
D
Mitotic Index (%)
Control
LIC1
LIC1 G-domain
LIC2
LIC2 G-domain
E
LIC1 KD + GFP
LIC1 KD + LIC1 HA
LIC1 KD + LIC2 FLAG
PH3
F
Distance from VS to nucleus (μm)
Control GFP
GFP + LIC1 KD
LIC1 + LIC1 KD
LIC2 + LIC1 KD
G
Percentage of cells
0-10
10-20
20-30
>30 μm
Distance from VS to nucleus (μm)
H
Mitotic Index (%)
Control GFP
GFP + LIC1 KD
LIC1 + LIC1 KD
LIC2 + LIC1 KD
I
SUPERNATANT
IP
Input
Mock
Bicd2 Nt
Mock
Bicd2 Nt
HC (530 kD)
IC (74kD)
LIC1 (57kD)
LIC2 (53kD)
-250kD
-75kD
-50kD
J
LIC1 vs LIC2 signal
Input
IP Bicd2 Nt

Figure 2

Mechanisms contributing to the differential LIC roles in apical INM (A-D) E16 brains were *in utero* electroporated with control vector, the full-length or G-domain of either LIC. Analysis was performed at 4 d.p.i. **(A)** Fixed images of the VZ from electroporated brains stained for PH3 **(B, C)** Quantification of the distance between RGP nuclei and the VS across the various conditions. **(D)** Effect of the various cDNAs expression on RGP mitotic index. **(E-H)** shRNA for LIC1 was injected into the embryonic brain at E16 together with GFP alone, HA-tagged LIC1 RNAi resistant, or FLAG-tagged standard LIC2 cDNA and analyzed 4 d.p.i. **(E)** Fixed images of the VZ from electroporated brains stained for PH3 and epitope tag. **(F, G)** Quantifications of the distance between RGP nuclei and the VS across the various conditions. **(H)** Mitotic index for the LIC1 rescue and LIC2 cross-rescue. Although statistically non-significant (p=0.06), LIC2 partially reestablishes mitotic index. **(I, J)** BicD2 pull-down from embryonic rat brain lysate was evaluated for co-immunoprecipitation with dynein heavy chain (HC), intermediate chain (IC), and LIC subunits. **(J)** Quantification of the signal intensity of LIC1 *vs.* LIC2 in the input lane and the IP lane. Data presented as Box-and-Whiskers plot in **B** and **F**; and data shown as mean±s.d. in **C**, **D**, **G**, **H** and **J**. Unpaired T-test was used in **B, C, D, F, G, H** and **J** (*P<0.05; **P<0.01; ***P<0.001). Data in **B, C** and **D** includes at least 343 RGPs from at least 3 embryos and data in **F**, **G** and **H** includes at least 1574 RGPs from at least 6 embryos. Data in **J** includes 4 different pull-downs. **A** and **E** scale bars, 5μm.

Figure 3

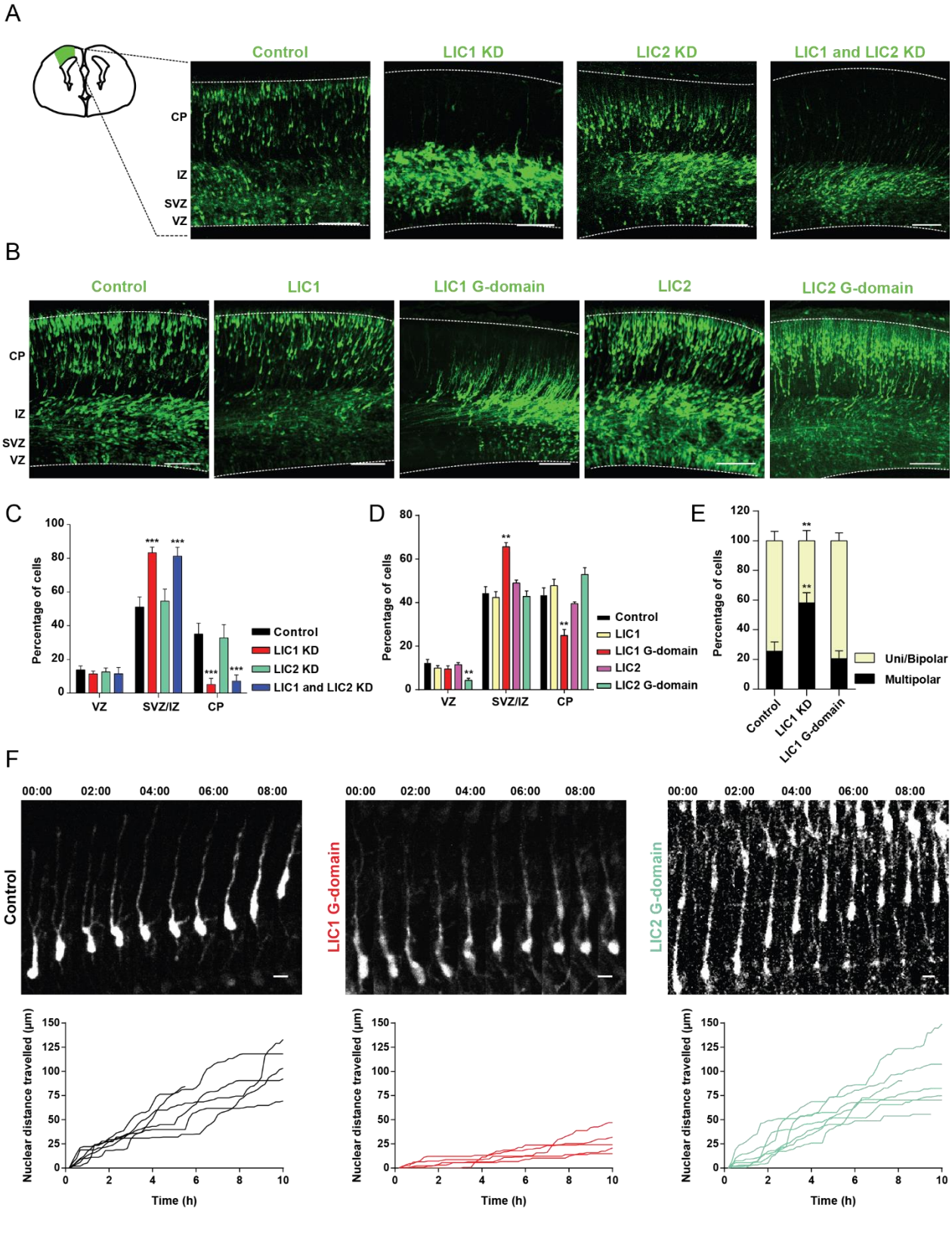
A
Control
LIC1 KD
LIC2 KD
LIC1 and LIC2 KD
CP
IZ
SVZ
VZ
B
Control
LIC1
LIC1 G-domain
LIC2
LIC2 G-domain
CP
IZ
SVZ
VZ
C
Percentage of cells
Control
LIC1 KD
LIC2 KD
LIC1 and LIC2 KD
VZ
SVZ/IZ
CP
D
Percentage of cells
Control
LIC1
LIC1 G-domain
LIC2
LIC2 G-domain
VZ
SVZ/IZ
CP
E
Percentage of cells
Uni/Bipolar
Multipolar
Control
LIC1 KD
LIC1 G-domain
F
Control
LIC1 G-domain
LIC2 G-domain
00:00
02:00
04:00
06:00
08:00
Nuclear distance travelled (µm)
Time (h)

Figure 3

Distinct roles for the LICs in post-mitotic neurons. (A-E) E16 rat embryonic brains were *in utero* electroporated with shRNAs for LIC1 and/or LIC2, or functional domains from of each LIC. Analysis was performed 4 d.p.i. Images of the neocortex injected with **(A)** control vector or shRNAs for LIC1 and/or LIC2 and **(B)** full-length or G-domain versions of LIC1 or LIC2. **(C, D)** Quantification of the proportion of transfected cells in each layer of the neocortex across conditions. **(E)** Quantification of the number of multipolar versus uni/bipolar E20 neurons in the neocortex. **(F)** Time-lapse images for control, LIC1 G-domain or LIC2 G-domain in migrating neurons (Supplementary Movies 4–6). Images are shown at 60min intervals (hh:mm). Representative tracings are shown at the bottom. Data presented as mean±s.d. Unpaired T-test was used in **C**, **D** and **E** (***P<0.001, **P<0.01). Data in **C** includes at least 2130 cells from at least 6 embryos, data in **D** includes at least 1856 cells from at least 3 embryos and data in **E** includes at least 335 cells from at least 5 embryos. **A** and **B** scale bars, 100μm. **F** scale bar, 10μm.

Figure 4

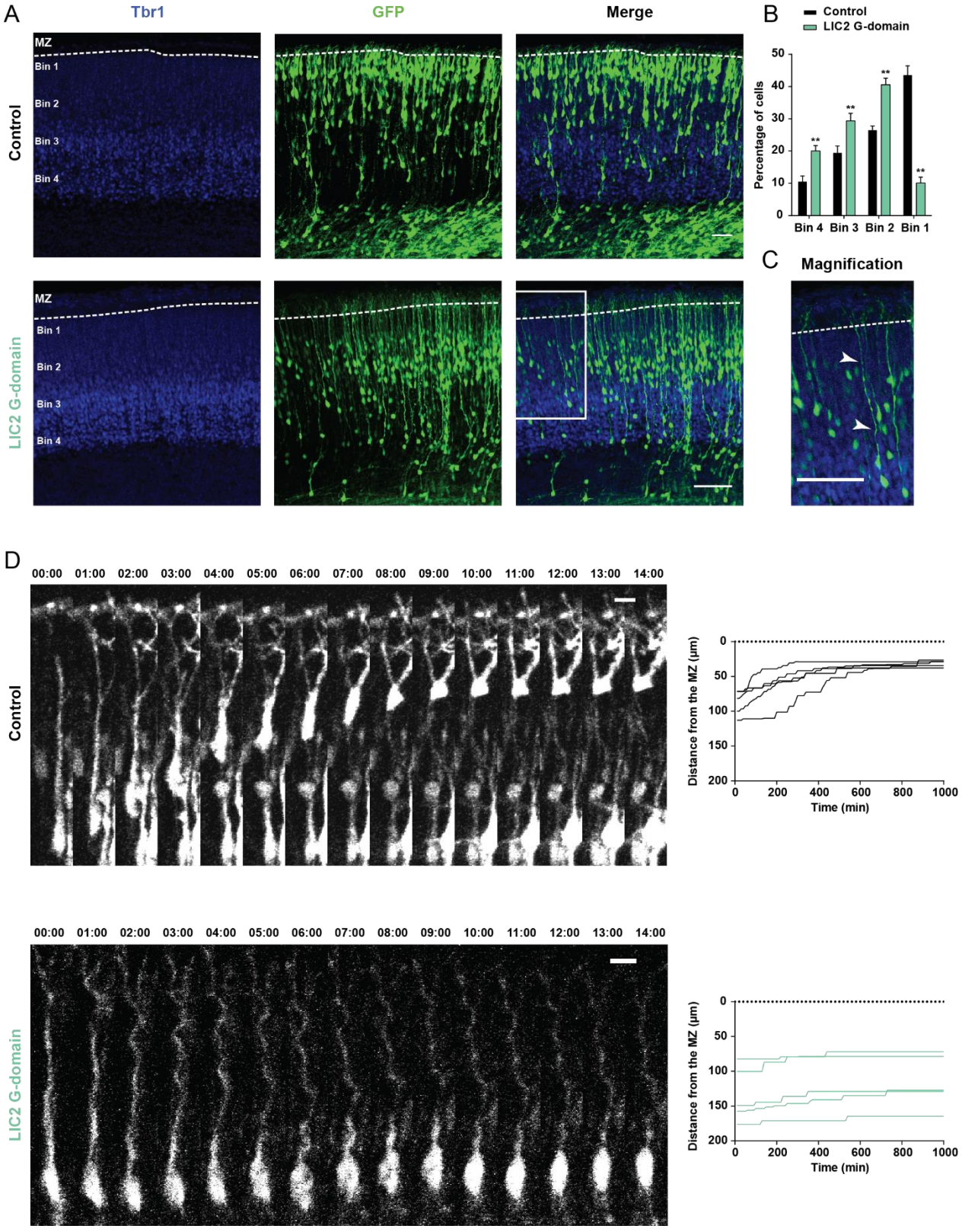
A
Tbr1
GFP
Merge
Control
LIC2 G-domain
MZ
Bin 1
Bin 2
Bin 3
Bin 4
B
Control
LIC2 G-domain
Percentage of cells
Bin 4
Bin 3
Bin 2
Bin 1
C
Magnification
D
00:00
01:00
02:00
03:00
04:00
05:00
06:00
07:00
08:00
09:00
10:00
11:00
12:00
13:00
14:00
Distance from the MZ (μm)
Time (min)

Figure 4

Dynein is required for terminal somal translocation of migrating neurons. (A-D) E16 brains were *in utero* electroporated with control vector or LIC2 G-domain, and were analyzed by fixed and live imaging 4 d.p.i. Brain slices were stained for the post-mitotic neuronal marker, Tbr1. The CP was equally divided in bins for quantifications purposes. **(A)** Images of the CP for each condition. **(B)** Quantification of the proportion of electroporated cells in each bin of the CP. **(C)** Magnification of the delimited region in bottom right panel in A. Arrowheads mark the elongated migrating process. **(D)** Time-lapse images for control and LIC2 G-domain in migrating neurons. Images are shown at 60min intervals (hh:mm). Respective representative tracings, from multiple migratory neurons for each condition, are shown at right (Supplementary Movies 7–8). Data are presented as mean±s.d. in **B**, and Unpaired T-test was used (** $P < 0.01$). Data in **B** includes at least 3035 cells from at least 6 embryos. **A** and **C** scale bars, 40μm. **D** scale bar, 10μm.

Figure 5

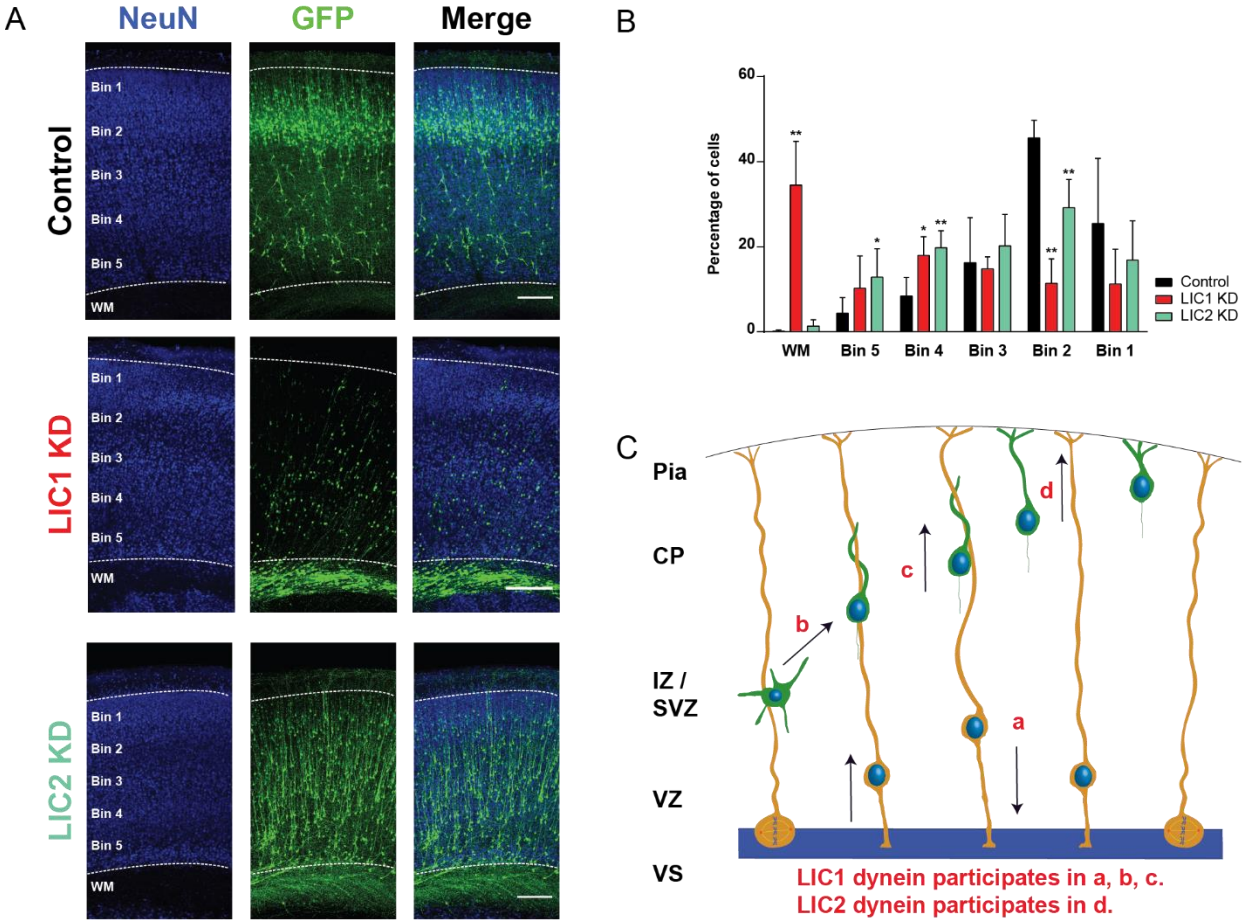
A
NeuN
GFP
Merge
Control
LIC1 KD
LIC2 KD
Bin 1
Bin 2
Bin 3
Bin 4
Bin 5
WM
B
Percentage of cells
60
40
20
0
WM
Bin 5
Bin 4
Bin 3
Bin 2
Bin 1
Control
LIC1 KD
LIC2 KD
C
Pia
CP
IZ / SVZ
VZ
VS
a
b
c
d
LIC1 dynein participates in a, b, c.
LIC2 dynein participates in d.

Figure 5

LIC inhibition severely impairs neuronal migration at post-natal stages. (A, B) E16 rat brains were *in utero* electroporated with control vector or shRNAs for LIC1 or LIC2. Analysis was done two weeks post injection, at P7. Brain slices were stained for the mature neuronal marker, NeuN. The CP was equally divided in bins for quantifications purposes. **(A)** Images of the post-natal neocortex across conditions. **(B)** Quantification the distribution of cells through the White matter (WM) and the CP. Data are presented as mean±s.d. in **B**, and Unpaired T-test was used (* P<0.05, ** P< 0.01). Data in **B** includes at least 1215 cells from at least 4 pups, per condition. **A** scale bar 200µm. **(C)** Schematic illustration showing LIC roles in neocortical development. In yellow, RGPs undergoing INM. In green, multipolar post-mitotic neurons become bipolar and migrate to the CP. LIC1 participates in the apical nuclear migration of RGPs **(a),** the multipolar-to-bipolar transition **(b)** and glial-guided migration **(c)**. LIC2 had no significant function in the previous behaviors, but plays an essential role in TST of neurons **(d)**.

METHODS

Ethics statement

All the experiments were done in accordance with the animal welfare guidelines and the guidance of the Institutional Animal Care and Use Committee (IACUC) at Columbia University.

In utero electroporation

Plasmids encoding for shRNAs or cDNA were injected into the developing brain at embryonic day 16 (E16) and electroporated as described (Baffet *et al.*, 2016). In more detail, timed pregnant Sprague Dawley E16 rats were anaesthetized with a ketamine xylazine cocktail administered intraperitoneally, and toe pinch was performed to ensure deep anesthesia. To avoid excessive heating loss during the surgical procedure, an external heating source was provided. For pain management buprenorphine and bupivacaine were administered subcutaneously, before the surgery. Abdominal cavity was opened and uterine horns exposed and trans-illuminated for clear identification of the brain ventricles. For easy visualization of the DNA in the brain ventricular space, a non-toxic dye (Sigma, F7252) was added to the DNA before surgery and injected with a sharpened glass needle. After injection, embryos were subjected to five electric impulses (50V, 50ms each, separated by 1s intervals) delivered by an electroporator (Harvard Apparatus ECM 830), to target the DNA to RGPs in the lateral neocortex. The embryos were returned to the abdominal cavity and the wound was closed. Rats were monitored every day post-surgery and buprenorphine was administered every 12h for the first 48h, for post-operative pain control.

Immunohistochemistry and live imaging

For embryonic brain harvesting, pregnant rats were re-anesthetized and the surgical wound was reopened 4 d.p.i (at E20) to expose the uterus.

For fixed imaging, embryonic (E20) or post-natal (P7) rat brains were harvested and immersed in PBS with 4% PFA overnight. They were then embedded in 4% of agarose (Sigma, A9539) and sliced in a vibratome (Leica, VT 1200S) in 100µm slices for embryonic brains or 200 µm for P7 brains. After blocking in 5% normal donkey serum (Sigma, D9663) in PBS-Triton 0.5% for 1 hour, slices were incubated with primary antibodies diluted in the blocking solution, overnight on a shaker, at 4°C. Secondary antibodies (1:500) and DAPI (4',6-

diamidino-2-phenylindole, Thermo Scientific, 62248, 1:10.000 dilution) were diluted in PBS and incubated for 2 h at room temperature. Slices were mounted with Aqua-Poly mounting media (Polysciences, 18606).

For live imaging, the dissected rat brains were embedded in 4% low melting agarose (IBI Scientific, IB70057) diluted in artificial cerebrospinal fluid (Baffet *et al.*, 2016) and sliced into 300µm coronal sections. The slices were placed on porous filters (EMB Millipore, PICMORG50) in cortical culture medium containing 25% Hanks balanced salt solution (Life Technologies, 24020-117), 47% basal MEM (Life Technologies, 21010-046), 25% normal horse serum (Life Technologies, 26050-088), 1% penicillin/ streptomycin/glutamine (Life Technologies, 10378-016), and 2% of 30% glucose (Sigma, G5767) in a 50mm glass-bottom dish (MatTek Corporation, P50G-0-14-F) and imaged on an IX80 laser scanning confocal microscope (Olympus FV1000 Spectral Confocal System) at intervals of 10 min for up to 24 h.

RNAi and Constructs

shRNA expressing constructs were designed to target internal gene sequences unique to *Dync1li1* (LIC1) or *Dync1li2 (*LIC2), in a pRetro-U6G vector (Cellogenetics, MD, USA), which also expressed soluble GFP to label transfected cells. The target sequence for *Dync1li1* (LIC1) used was 5'- GTTGATTAGAGACTTCCAA-3' and the target sequence for *Dync1li2* (LIC2) was 5'-GCCAGAAGATGCATATGAA-3'. Empty vector of pEGFP-C1 was used a control (Clontech). LIC1 and LIC2 rat cDNA constructs were taken from pCMV beta (Tynan *et al.*, 2000) and cloned into pCAGIG vector (Addgene plasmid #11159)(Matsuda and Cepko, 2004) using NotI sites. Full-length and functional domain constructs of LIC1 and LIC2 were HA (YPYPVPDYA) and FLAG (DYKDDDDK) tagged, respectively (Tynan *et al.*, 2000). pCAGIG empty-vector was used as control for the experiments with LIC1 and LIC2 full-length and functional domains. For better process visualization in the quantifications of Fig 3.E and P7 experiments, shRNAs were co-injected with pCAGIG empty vector. Silent point mutations were made in LIC1 cDNA for RNAi resistance and functional domains were amplified by PCR amplification using KOD Hot Start DNA Polymerase (Millipore, 71086). pIRES2 DsRed-Express2 BicD2 (Clontech) was described previously (Hu *et al.*, 2013) and pDsRed-Express2-C1 (Clontech) was used as control. Soluble DsRed signal was enhanced using anti-mCherry antibody (described below). BicD2 N-terminal 25-400aa with an N-terminal strepII-SNAPf cassette (McKenney *et al.*, 2014) was a kind gift from Dr. Richard McKenney (UC Davis, California, USA).

Western Blot and Co-IP

shRNAs and LIC functional domains were transfected in rat C6 brain glioma cells cultured in DMEM supplemented with 10% FBS, 1% penicillin/streptomycin and maintained at 37°C with 5% CO_2. Transfection with shRNAs for LIC1 or LIC2 and LIC1 and LIC2 G-domains was performed using a Lonza Nucleofector kit V and an Amaxa Nucleofector according to the manufacturer's instructions. Cells transfected with shRNAs and LIC functional domains were collected 72h (for shRNAs) or 30h (G-domains) after transfection.

For brain samples, pregnant E16, E18, or E20 rats were anesthetized as described above. Embryonic brains were harvested and the brains of the pregnant rats were used as the adult samples.

Cells transfected with shRNAs and brain samples were lysed on ice in Lysis Buffer (pH = 7.2, 50mM Tris-HCL, 150mM NaCl, 1%Triton X-100 and 0.5% deoxycholic acid buffer) containing 1mM DTT and a protease inhibitor cocktail (Sigma, P8340). Purified lysates were loaded on a polyacrylamide gel and transferred to a polyvinylidene difluoride membrane. The membrane was blocked in PBS with 0.5% powdered milk, incubated with primary antibodies diluted in PBS with 0.1% of powder milk, washed and incubated with secondary LI-COR antibodies in PBS. Imaging of the blots was carried out using an Odyssey system (LI-COR).

For the co-immunoprecipitation experiments in Supp. Fig. 2 A, B, LIC G-domain transfected C6 cells were lysed with RIPA buffer (pH = 7.4, 50mM Tris-HCL, 100mM NaCl, 1mM EGTA, 0.5% NP-40) containing 1mM DTT and a protease inhibitor cocktail on ice. Anti-HA (Abcam, ab137838) or anti-FLAG (Abcam, ab1162) antibodies were incubated with magnetic beads (Invitrogen, 10002D) for 1h and then with cell lysates for 2h. Blotting was performed has described above. For better separation of LIC1 (57kD), LIC2 (53kD) and antibody heavy chain (50kD) bands gel running was done for longer periods.

For the co-immunoprecipitation experiments in Fig. 2 I,J, embryonic brains (E20) were lysed with Brain buffer (pH= 7.2, 50mM Pipes, 50mM Hepes, 2mM MgCl2, 1mM EDTA) containing DTT and a protease inhibitor cocktail and subjected to mechanical lysis in a dounce homogenizer on ice. SNAP-BicD2 was purified as described (McKenney *et al.*, 2014) and incubated Streptactin Sepharose beads (GE life sciences 28-9355-99) for 1h and then with brain lysates for 3h. Blotting was performed has described above.

Antibodies

Antibodies used for Immunofluorescence include anti-pH3 (Abcam, ab14955, 1:1000), anti-Tbr1 (Abcam, ab31940, 1:300), anti-mCherry (Abcam, ab167453, 1:1000), anti-NeuN (Millipore, MAB377, 1:300), anti-HA (Sigma-Aldrich, H6908, 1:2000), anti-FLAG (Abcam, ab1162, 1:2000), anti-LIC1 ((Tan, Scherer and

Vallee, 2011), 1:300) and anti-LIC2 ((Tynan *et al.*, 2000), 1:300). Donkey fluorophore-conjugated secondary antibodies (Jackson Labs, 1:500 dilution) were used.

Antibodies used for western blotting include anti-p150^{Glued} (BD, 610474,1:1000), anti-dynein intermediate chain clone 74.1 (University of Virginia, 1:1000), anti-LICs ((Tynan *et al.*, 2000), 1:500), anti-LIC1 ((Tan, Scherer and Vallee, 2011), 1:500), anti-LIC2 ((Tynan *et al.*, 2000), 1:1000), anti–dynein heavy chain (Suzuki *et al.*, 2007), 1:1000) and anti-GAPDH (Abcam, ab8245, 1:1000). To develop in a LI-COR system, fluorescent secondary antibodies (1:10,000) were acquired from Invitrogen and Rockland.

Reverse Transcription-PCR analysis

C6 cells were cultured and transfected with shRNAs for LIC1 and LIC2 using an Amaxa Nucleofector as described for western blot. mRNA extraction, cDNA synthesis and quantitative PCR were performed using the Power SYBR Green Cells-to-Ct Kit (Ambion/Thermofisher). cDNAs were analyzed by quantitative PCR using an ABI 7900 HT machine. Primers were designed to have melting temperatures of about 60 degrees and to generate amplicons of 70 to 200 base pairs, separated by at least one intron. Target cDNA levels were analyzed by the comparative cycle (Ct) method and values were normalized against b-actin and GAPDH expression levels. The primers used in this study were: GAPDH FW: 5'-CAACTCCCTCAAGATTGTCAGCAA-3'; GAPDH RV: 5'-GGCATGGACTGTGGTCATGA-3'; *Dync1li1* (LIC1) FW: 5'-GGGAAAACAAGCCTCATAAGAAG-3'; *Dync1li1* (LIC1) RV: 5'- AACTTGAGTAGCCCTTTGTGGTA-3'; *Dync1li2* (LIC2) FW: 5'-GACCCTGGTCATTTTTGTTGC -3'; *Dync1li2* (LIC2) RV: 5'- CCCGTAAAACACTAGCCCAT-3'.

Imaging and statistical analysis.

All images were collected with an IX80 laser scanning confocal microscope (Olympus FV100 Spectral Confocal System). Brain sections were imaged using a 60x 1.42 N.A. oil objective or a 10x 0.40 N.A. air objective. All images were analyzed using ImageJ software (NIH, Bethesda, MD, USA).

All statistical analysis was performed using Prism (GraphPad Software, La Jolla, CA, USA). Unpaired T-test (two-tailed) was used to determine significance between two groups. Statistical significance for LIC1 *vs.* LIC2 signal (Supp. Fig. 1 D) was performed with one-way ANOVA followed by Tukey's test. Data distribution was assumed to be normal, but this was not formally tested. Definition of statistical significance was $P < 0.05$.

For each experiment, embryos were collected from at least 3 different mothers, for each condition. Mitotic index was measured as the percentage of electroporated RGP cells positive for PH3. The bars in the data presented as Box-and-Whiskers represent 1-99 percentile range.

Online supplemental material

Fig. S1 shows the RNAi knockdown efficiency and the LIC1 and LIC2 relative protein expression across development. Fig. S2 shows the effects of the G-domains expression in the dynein complex and the effects of the A-domains expression in RGP behavior. Fig. S3 shows the effects of LIC2 shRNA expression in neuronal TST. Videos 1, 2 and 3 show the effects of LIC inhibition in apical INM. Videos 4, 5 and 6 show the effect of LIC inhibition in glial-guided migration. Videos 7, 8, 9 show the effects of LIC2 inhibition in neuronal TST.

ACKNOWLEDGEMENTS

We thank Drs. Aditi Falnikar, Chiara Bertipaglia and David Doobin for the critical reading of the manuscript and the members of the Vallee lab for technical expertise and productive discussions. We thank Dr. Caitlin L. Wynne for the SNAP-BicD2 purified protein. This project was supported by NIH HD40182 and GM105536 to R.B.V., and the Fundação para a Ciência e a Tecnologia MD/PhD Scholarship PD/BD/113766/2015 to J.C.G.

The authors declare no competing financial interests.

REFERENCES

Baffet, A. D. *et al.* (2016) 'Cellular and subcellular imaging of motor protein-based behavior in embryonic rat brain', *Methods in Cell Biology*, 131, pp. 349–363. doi: 10.1016/bs.mcb.2015.06.013.

Baffet, A. D., Hu, D. J. and Vallee, R. B. (2015) 'Cdk1 Activates Pre-mitotic Nuclear Envelope Dynein Recruitment and Apical Nuclear Migration in Neural Stem Cells', *Developmental Cell*. Elsevier Inc., 33(6), pp. 703–716. doi: 10.1016/j.devcel.2015.04.022.

Bertipaglia, C., Gonçalves, J. C. and Vallee, R. B. (2018) 'Nuclear migration in mammalian brain development', *Seminars in Cell & Developmental Biology*, 82, pp. 57–66. doi: 10.1016/j.semcdb.2017.11.033.

Carter, A. P., Diamant, A. G. and Urnavicius, L. (2016) 'How dynein and dynactin transport cargos: A structural perspective', *Current Opinion in Structural Biology*. Elsevier Ltd, 37, pp. 62–70. doi: 10.1016/j.sbi.2015.12.003.

Cooper, J. A. (2013) 'Mechanisms of cell migration in the nervous system', *The Journal of Cell Biology*, 202(5), pp. 725–734. doi: 10.1083/jcb.201305021.

Doobin, D. J. *et al.* (2016) 'Severe NDE1-mediated microcephaly results from neural progenitor cell cycle arrests at multiple specific stages', *Nature Communications*. Nature Publishing Group, 7, pp. 1–14. doi: 10.1038/ncomms12551.

Fiorillo, C. *et al.* (2014) 'Novel dynein DYNC1H1 neck and motor domain mutations link distal spinal muscular atrophy and abnormal cortical development', *Human Mutation*, 35(3), pp. 298–302. doi: 10.1002/humu.22491.

Franco, S. J. *et al.* (2011) 'Reelin Regulates Cadherin Function via Dab1/Rap1 to Control Neuronal Migration and Lamination in the Neocortex', *Neuron*, 69(3), pp. 482–497. doi: 10.1016/j.neuron.2011.01.003.

Gama, J. B. *et al.* (2017) 'Molecular mechanism of dynein recruitment to kinetochores by the Rod-Zw10-Zwilch complex and Spindly', *Journal of Cell Biology*, 216(4), pp. 943–960. doi: 10.1083/jcb.201610108.

Grissom, P. M., Vaisberg, E. A. and McIntosh, J. R. (2002) 'Identification of a Novel Light Intermediate Chain (D2LIC) for Mammalian Cytoplasmic Dynein 2', *Molecular Biology of the Cell*. Edited by D. Drubin, 13(3), pp.

817–829. doi: 10.1091/mbc.01-08-0402.

Hu, D. J.-K. *et al.* (2013) 'Dynein Recruitment to Nuclear Pores Activates Apical Nuclear Migration and Mitotic Entry in Brain Progenitor Cells', *Cell*, 154(6), pp. 1300–1313. doi: 10.1016/j.cell.2013.08.024.

Jamuar, S. S. *et al.* (2014) 'Somatic Mutations in Cerebral Cortical Malformations', *New England Journal of Medicine*, 371(8), pp. 733–743. doi: 10.1056/NEJMoa1314432.

Jones, L. A. *et al.* (2014) 'Dynein light intermediate chains maintain spindle bipolarity by functioning in centriole cohesion', *Journal of Cell Biology*, 207(4), pp. 499–516. doi: 10.1083/jcb.201408025.

Kriegstein, A. and Alvarez-buylla, A. (2009) 'The Glial Nature of Embryonic and Adult Neural Stem Cells', *Annual Reviews of Neuroscience*, pp. 149–184. doi: 10.1146/annurev.neuro.051508.135600.The.

Lee, I.-G. *et al.* (2018) 'A conserved interaction of the dynein light intermediate chain with dynein-dynactin effectors necessary for processivity', *Nature Communications*, 9(1), p. 986. doi: 10.1038/s41467-018-03412-8.

Lipka, J. *et al.* (2013) 'Mutations in cytoplasmic dynein and its regulators cause malformations of cortical development and neurodegenerative diseases.', *Biochemical Society transactions*, 41(6), pp. 1605–12. doi: 10.1042/BST20130188.

Mahale, S. *et al.* (2016) 'The light intermediate chain 2 subpopulation of dynein regulates mitotic spindle orientation', *Scientific Reports*, 6(1), pp. 1–16. doi: 10.1038/s41598-016-0030-3.

Matsuda, T. and Cepko, C. L. (2004) 'Electroporation and RNA interference in the rodent retina in vivo and in vitro', *Proceedings of the National Academy of Sciences*, 101(1), pp. 16–22. doi: 10.1073/pnas.2235688100.

McKenney, R. J. *et al.* (2014) 'Activation of cytoplasmic dynein motility by dynactin-cargo adapter complexes.', *Science (New York, N.Y.)*, 345(6194), pp. 337–41. doi: 10.1126/science.1254198.

Mikami, A. (2002) 'Molecular structure of cytoplasmic dynein 2 and its distribution in neuronal and ciliated cells', *Journal of Cell Science*, 115(24), pp. 4801–4808. doi: 10.1242/jcs.00168.

Nadarajah, B. *et al.* (2001) 'Two modes of radial migration in early development of the cerebral cortex.', *Nature neuroscience*, 4(2), pp. 143–150. doi: 10.1038/83967.

Palmer, K. J., Hughes, H. and Stephens, D. J. (2009) 'Specificity of cytoplasmic dynein subunits in discrete membrane-trafficking steps.', *Molecular biology of the cell*, 20(12), pp. 2885–99. doi: 10.1091/mbc.E08-12-1160.

Pfister, K. K. *et al.* (2006) 'Genetic analysis of the cytoplasmic dynein subunit families', *PLoS Genetics*, 2(1), pp. 11–26. doi: 10.1371/journal.pgen.0020001.

Poirier, K. *et al.* (2013) 'Mutations in TUBG1, DYNC1H1, KIF5C and KIF2A cause malformations of cortical development and microcephaly.', *Nature genetics*, 45(6), pp. 639–47. doi: 10.1038/ng.2613.

Purohit, A. *et al.* (1999) 'Direct interaction of pericentrin with cytoplasmic dynein light intermediate chain contributes to mitotic spindle organization', *Journal of Cell Biology*, 147(3), pp. 481–491. doi: 10.1083/jcb.147.3.481.

Raaijmakers, J. A., Tanenbaum, M. E. and Medema, R. H. (2013) 'Systematic dissection of dynein regulators in mitosis.', *The Journal of cell biology*, 201(2), pp. 201–15. doi: 10.1083/jcb.201208098.

Reck-Peterson, S. L. *et al.* (2018) 'The cytoplasmic dynein transport machinery and its many cargoes', *Nature Reviews Molecular Cell Biology*. Springer US, 19(6), pp. 382–398. doi: 10.1038/s41580-018-0004-3.

Redwine, W. B. *et al.* (2017) 'The human cytoplasmic dynein interactome reveals novel activators of motility', *eLife*, 6, pp. 1–27. doi: 10.7554/eLife.28257.

Reiner, O. *et al.* (1993) 'Isolation of a Miller-Dieker lissencephaly gene containing G protein beta-subunit-like repeats.', *Nature*. Nature Publishing Group, 364(6439), pp. 717–721. doi: 10.1038/364717a0.

Scherer, J., Yi, J. and Vallee, R. B. (2014) 'PKA-dependent dynein switching from lysosomes to adenovirus: A novel form of host-virus competition', *Journal of Cell Biology*, 205(2), pp. 163–177. doi: 10.1083/jcb.201307116.

Schmoranzer, J. *et al.* (2009) 'Par3 and Dynein Associate to Regulate Local Microtubule Dynamics and Centrosome Orientation during Migration', *Current Biology*, 19(13), pp. 1065–1074. doi: 10.1016/j.cub.2009.05.065.

Schroeder, C. M. *et al.* (2014) 'A Ras-like domain in the light intermediate chain bridges the dynein motor to a cargo-binding region.', *eLife*, 3, p. e03351. doi: 10.7554/eLife.03351.

Schroeder, C. M. and Vale, R. D. (2016) 'Assembly and Activation of Dynein-Dynactin by the Cargo Adaptor Protein Hook3', *Journal of Cell Biology*, 214(3). doi: 10.1101/047605.

Sekine, K. *et al.* (2011) 'The Outermost Region of the Developing Cortical Plate Is Crucial for Both the Switch of the Radial Migration Mode and the Dab1-Dependent "Inside-Out" Lamination in the Neocortex', *Journal of Neuroscience*, 31(25), pp. 9426–9439. doi: 10.1523/JNEUROSCI.0650-11.2011.

Shu, T. *et al.* (2004) 'Ndel1 operates in a common pathway with LIS1 and cytoplasmic dynein to regulate cortical neuronal positioning', *Neuron*. Cell Press, 44(2), pp. 263–277. doi: 10.1016/j.neuron.2004.09.030.

Splinter, D. *et al.* (2012) 'BICD2, dynactin, and LIS1 cooperate in regulating dynein recruitment to cellular structures', *Molecular Biology of the Cell*, 23(21), pp. 4226–4241. doi: 10.1091/mbc.E12-03-0210.

Suzuki, S. O. *et al.* (2007) 'Expression patterns of LIS1, dynein and their interaction partners dynactin, NudE, NudEL and NudC in human gliomas suggest roles in invasion and proliferation', *Acta Neuropathologica*, 113(5), pp. 591–599. doi: 10.1007/s00401-006-0180-7.

Tan, S. C., Scherer, J. and Vallee, R. B. (2011) 'Recruitment of dynein to late endosomes and lysosomes through light intermediate chains.', *Molecular biology of the cell*, 22(4), pp. 467–477. doi: 10.1091/mbc.E10-02-0129.

Taylor, S. P. *et al.* (2015) 'Mutations in DYNC2LI1 disrupt cilia function and cause short rib polydactyly syndrome', *Nature Communications*. Nature Publishing Group, 6, p. 7092. doi: 10.1038/ncomms8092.

Tsai, J.-W. *et al.* (2010) 'Kinesin 3 and cytoplasmic dynein mediate interkinetic nuclear migration in neural stem cells.', *Nature neuroscience*. Nature Publishing Group, 13(12), pp. 1463–1471. doi: 10.1038/nn.2665.

Tsai, J.-W., Bremner, K. H. and Vallee, R. B. (2007) 'Dual subcellular roles for LIS1 and dynein in radial neuronal migration in live brain tissue.', *Nature neuroscience*, 10(8), pp. 970–979. doi: 10.1038/nn1934.

Tsai, J. W. *et al.* (2005) 'LIS1 RNA interference blocks neural stem cell division, morphogenesis, and motility at multiple stages', *Journal of Cell Biology*, 170(6), pp. 935–945. doi: 10.1083/jcb.200505166.

Tynan, S. H. *et al.* (2000) 'Light intermediate chain 1 defines a functional subfraction of cytoplasmic dynein which binds to pericentrin', *Journal of Biological Chemistry*, 275(42), pp. 32763–32768. doi:

10.1074/jbc.M001536200.

Tynan, S. H., Gee, M. A. and Vallee, R. B. (2000) 'Distinct but overlapping sites within the cytoplasmic dynein heavy chain for dimerization and for intermediate chain and light intermediate chain binding', *Journal of Biological Chemistry*, 275(42), pp. 32769–32774. doi: 10.1074/jbc.M001537200.

CHAPTER 2.1 – Supplementary material

Distinct roles for dynein light intermediate chains in neurogenesis, migration, and terminal somal translocation

João Carlos Gonçalves, Tiago J. Dantas, Richard B. Vallee

The Journal of Cell Biology, volume. 218, number 3, pages 808-819

DOI: 10.1083/jcb.201806112

Supplemental figure 1

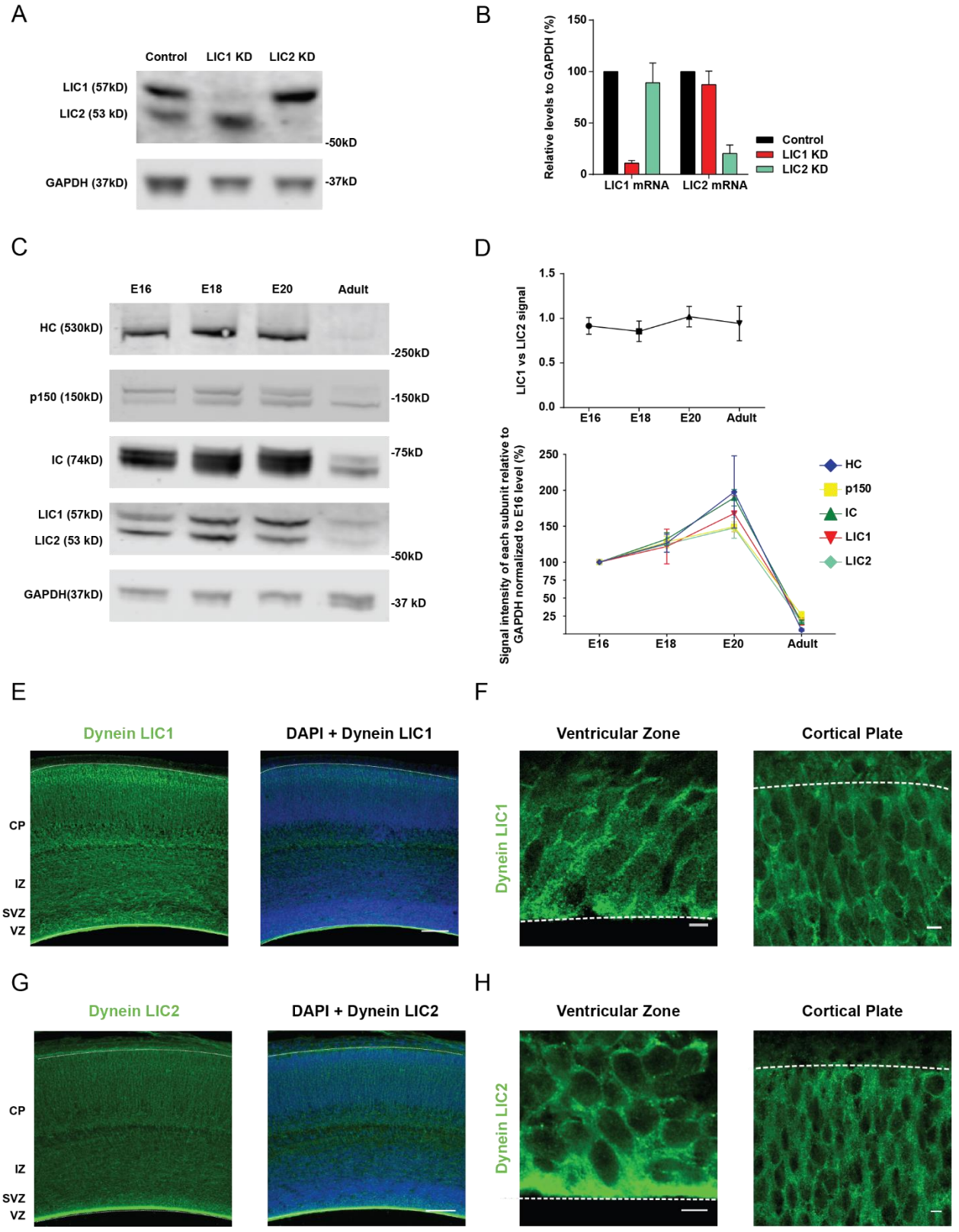

Supplementary figure 1

Knockdown efficiency and relative expression of the LICs across development. (A, B) C6 rat glioma cells were transfected with control vector or shRNAs for LIC1 or LIC2 for 72 hours. **(A)** Western blot analysis confirms successful protein KD. **(B)** qRT-PCR analysis confirms reduction in LIC1 and LIC2 mRNA levels, which were reduced to 10.9% and 20.3%, respectively (n=2). **(C)** Relative expression of LICs in rat brain tissue. Levels of dynein heavy chain (HC), dynactin p150^{Glued}, intermediate chain (IC), and LIC subunits were accessed at different late embryonic stages and adulthood, with GAPDH as control (n=4). **(D)** Quantification of the relative signal from each band reveals that LIC1/LIC2 ratio remains constant throughout the considered developmental stages. There was a strong decrease in the expression of dynein related genes in the adult. **(E-H)** E20 brains were stained with LIC1 and LIC2 specific antibodies (Tan, Scherer and Vallee, 2011). **(E-G)** Each LIC is detected throughout the neocortical layers. **(F-H)** High magnification images of the VZ and CP show diffuse cytoplasmic distribution of each LIC. **E** and **G** scale bars, 100µm. **F** and **H** scale bar, 5µm. Error bars = SD.

Supplemental figure 2

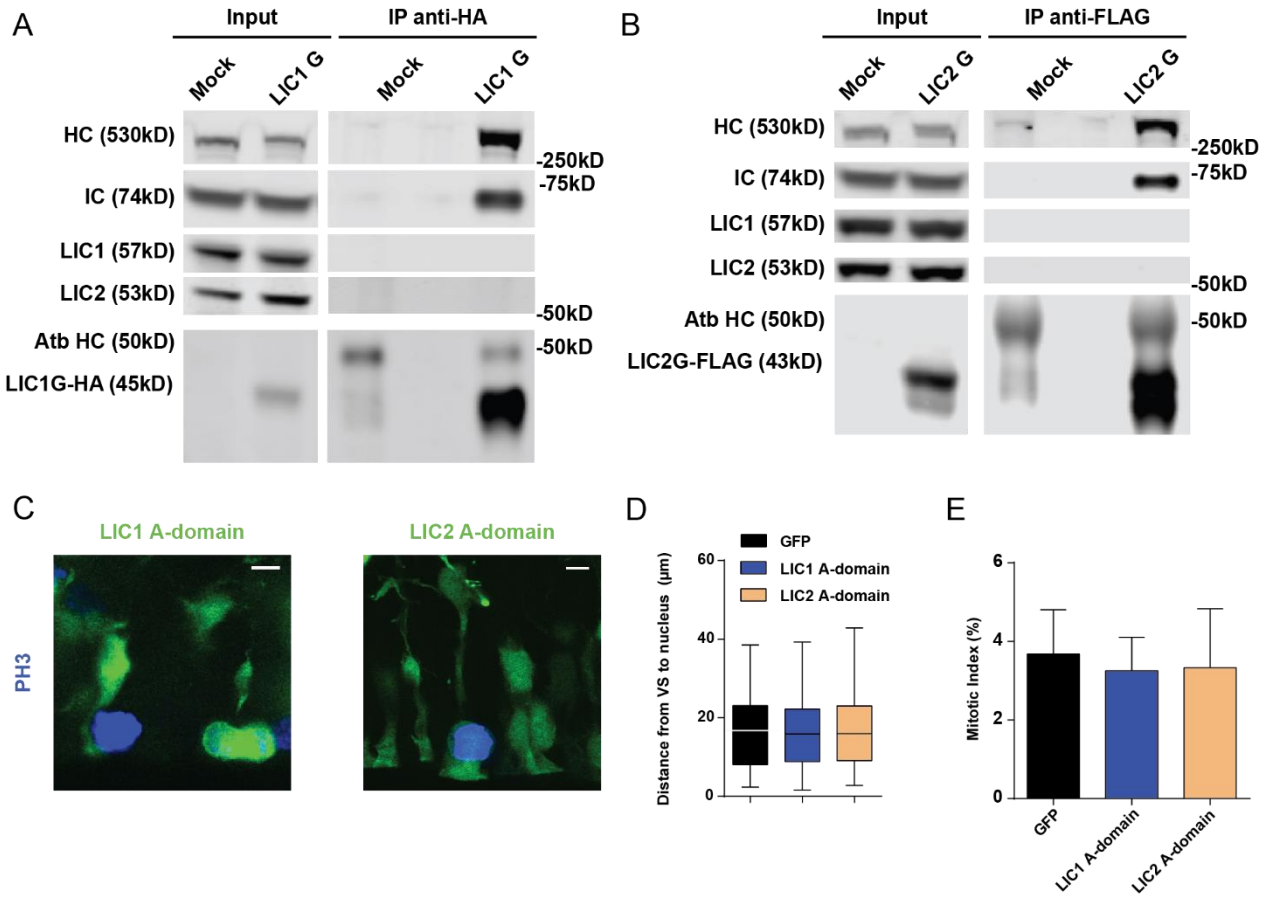

Supplementary figure 2

LIC G-domain interactors within the dynein complex and effects of expressing LIC A-domains on apical INM. **(A, B)** Immunoprecipitation from lysates of C6 glioma cells overexpressing **(A)** HA-LIC1 G-domain or **(B)** Flag-LIC2 G-domain with a mAb against HA or Flag, respectively. Antibodies against HC, IC, LIC1 and LIC2 were used to detect these proteins in the lysate input and pellet samples. The G-domain was able to co-immunoprecipitate HC and IC, but not the LICs suggesting that LIC G-domains are incorporated into the dynein complex and compete with the endogenous LIC, for HC binding (n=3). **(C-E)** E16 brains were injected with GFP alone, LIC1 A domain or LIC2 A-domain. **(C)** Representative images from the VZ. **(D)** Quantitative data showing no differences between nuclear distribution of RGPs transfected with GFP, LIC1 A-domain or LIC2 G-domain. **(E)** Mitotic index for each condition. Expression of the LIC1 A-domain or LIC2 A-domain has no effect on mitotic index. Data presented as Box-and-Whiskers plot in **D**; and shown as mean±s.d. in **E**. Unpaired t-test was used in **D** and **E.** Data in **D** and **E** includes at least 678 RGPs from at least 3 embryos from different mothers, per condition. **C** scale bar, 5μm.

Supplemental figure 3

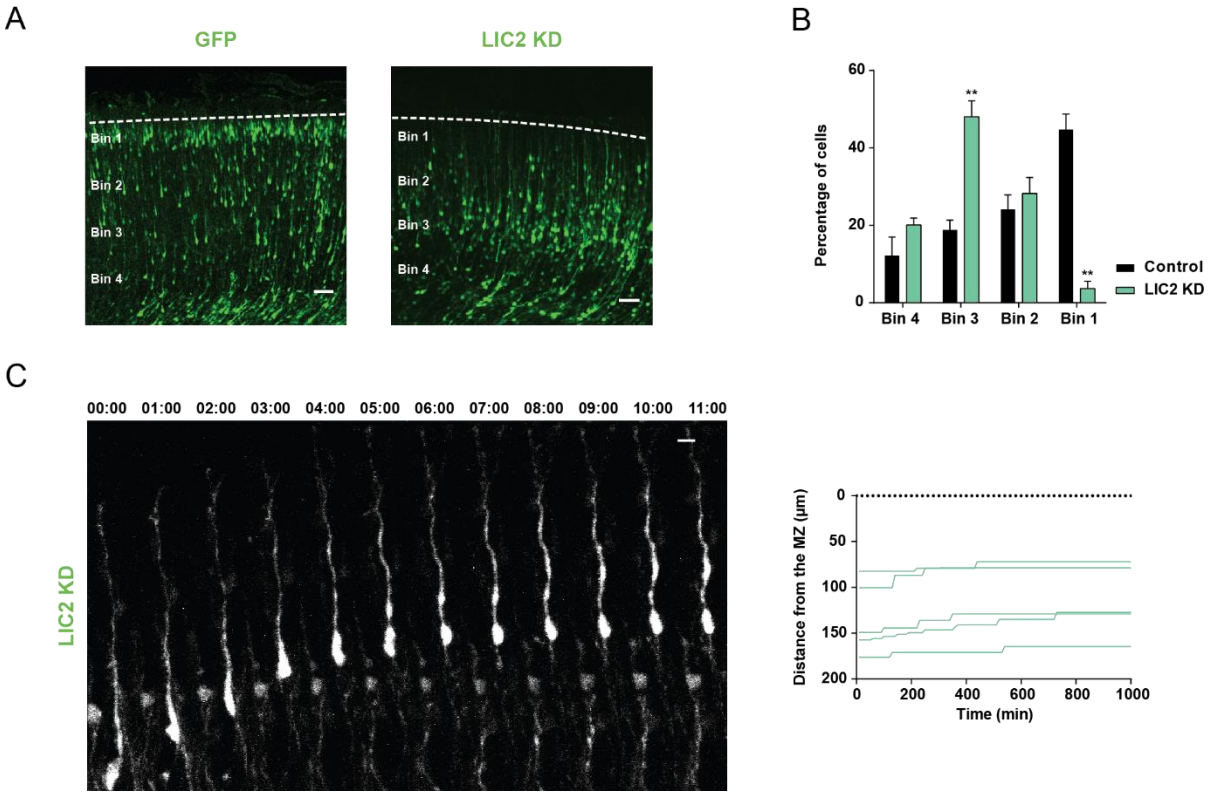

Supplementary figure 3

LIC2 knockdown effect on the cellular distribution in the CP. E16 brains were electroporated with control vector or LIC2 KD, and were analyzed by fixed imaging at E20. **(A)** Representative images of the CP for each condition, divided in 4 equal bins for quantification purposes. **(B)** Quantification of the proportion of transfected cells in each layer of the CP. LIC2 KD caused a substantial decrease in the number of cell bodies that reach the uppermost region of the CP (Bin 1), compared to control. **(C)** Time-lapse images for LIC2 KD in migrating neurons. Images are shown at 60min intervals (hh:mm). Respective representative tracings, from multiple migratory neurons, are shown at right (Supplementary Movie 9). Data are presented as mean±s.d. and Unpaired T-test was used (** $P< 0.01$) in **B.** Data in **B** includes at least 742 cells from at least 5 embryos from different mothers, per condition. **A** scale bar, 40μm. **C** scale bar, 10μm.

Supplementary Movie 1

Live imaging example of E20 embryonic rat brain electroporated with GFP control vector at E16. Transfected RGPs were continuously imaged in the VZ for 13hr20min at 10 min intervals. Scale bar 10μm.

Supplementary Movie 2

Live imaging example of E20 embryonic rat brain electroporated with LIC1 shRNA at E16. Transfected RGPs were continuously imaged in the VZ for 16hr50min at 10 min intervals. Scale bar 10μm.

Supplementary Movie 3

Live imaging example of E20 embryonic rat brain electroporated with LIC2 shRNA at E16. Transfected RGPs were continuously imaged in the VZ for 15hrs at 10 min intervals. Scale bar, 10μm.

Supplementary Movie 4

Live imaging example of E20 embryonic rat brain electroporated with GFP control vector at E16. Migrating neurons were continuously imaged in the upper IZ/CP for 26hr20min at 10 min intervals. Scale bar, 10μm.

Supplementary Movie 5

Live imaging example of E20 embryonic rat brain electroporated with LIC1 G-domain at E16. Migrating neurons were continuously imaged in the upper IZ/CP for 19hr20min at 10 min intervals. Scale bar, 10μm

Supplementary Movie 6

Live imaging example of E20 embryonic rat brain electroporated with LIC2 G-domain at E16. Migrating neurons were continuously imaged in the upper IZ/CP for 18hr50min at 10 min intervals. Scale bar, 10μm.

Supplementary Movie 7

Live imaging example of E20 embryonic rat brain electroporated with GFP control vector at E16. Migrating neurons were continuously imaged in the upper CP at for 18hr10min at 10 min intervals. Scale bar, 10μm.

Supplementary Movie 8

Live imaging example of E20 embryonic rat brain electroporated with LIC2 G-domain at E16. Migrating neurons were continuously imaged in the upper CP for 17hr50min at 10 min intervals. Scale bar, 10μm.

Supplementary Movie 9

Live imaging example of E20 embryonic rat brain electroporated with LIC2 shRNA at E16. Migrating neurons were continuously imaged in the upper CP for 16hr10min at 10 min intervals. Scale bar, 10μm.

REFERENCES

Tan, S. C., Scherer, J. and Vallee, R. B. (2011) 'Recruitment of dynein to late endosomes and lysosomes through light intermediate chains.', *Molecular biology of the cell*, 22(4), pp. 467–477. doi: 10.1091/mbc.E10-02-0129.

CHAPTER 2.2

Nesprin-2 recruits dynein via its adaptor BicD2 for nuclear transport during neuronal migration.

João Carlos Gonçalves, Sebastian Quintremil, Julie Yi, Richard B. Vallee

(Manuscript to be submitted)

TITLE: Nesprin-2 recruits dynein via its adaptor BicD2 for nuclear transport during neuronal migration.

AUTHORS AND AFFILIATIONS

João Carlos Gonçalves[1, 2, 3], Sebastian Quintremil[1], Julie Yi[1], Richard B. Vallee[1*]

1 - Department of Pathology and Cell Biology, Columbia University Medical Center, New York, NY, USA.

2 - Life and Health Sciences Research Institute (ICVS), School of Medicine, University of Minho, Campus Gualtar, Braga, Portugal.

3 - ICVS/3B's - PT Government Associate Laboratory, Braga/Guimarães, Portugal.

*Corresponding author: Richard B. Vallee (rv2025@columbia.edu)

KEYWORDS

Nesprin-2, BicD2, cytoplasmic dynein-1, brain development, neuronal migration, nucleus-centrosome coupling, nuclear transport

Abbreviations used in this Chapter: N-C, Nucleus-Centrosome; NE, Nuclear envelope; VZ, Ventricular Zone; IZ, intermediate zone; CP, Cortical plate; RGP, Radial glial progenitor; INM, interkinetic nuclear migration; LINC, Linker of Nucleoskeleton and Cytoskeleton; KASH, Klarsicht, ANC-1, and Syne homology; SR, spectrin repeat; SUN, Sad1 and UNC-84; Nesprin-2 isoform (N2G)

SUMMARY

Microtubule motor proteins play fundamental roles in neuronal migration, but the underlying mechanisms remain far from understood. Here, Gonçalves et al. find that the nuclear envelope protein Nesprin-2 recruits cytoplasmic dynein, via the dynein adaptor BicD2 in neuronal and non-neuronal cells. Inhibition of the Nesprin-2/BicD2 interaction severely disrupts neuronal migration by nucleus-centrosome uncoupling.

ABSTRACT

Microtubule motors are fundamental for neuronal migration. Cytoplasmic dynein, in particular, transports both the nucleus and the centrosome in migratory neurons. Nesprin-2 has been implicated in neuronal migration, and has been found to recruit dynein to the nuclear envelope in G0-phase non-neuronal cells. However, the mechanism for Nesprin-2-mediated dynein recruitment during neuronal migration and more generally remains largely unexplored. To address this question, we expressed chimeric KASH domain-containing fragments of Nesprin-2 in E16 rat brain using *in utero* electroporation. We found that expression of the Nesprin-2 fragment containing the KASH domain and the actin filament-binding domain, but lacking the recently identified dynein-binding region causes a severe reduction in neuronal migration to the CP. Although nuclear movement was severely inhibited, centrosome advance appeared normal, resulting in a very striking increase in nucleus-centrosome separation, often to more than 100μm. These results reveal a specific role for Nesprin-2-associated dynein in nuclear, but not centrosome, transport. By immunofluorescence analysis in cultured cells and co-immunoprecipitation studies, we found the dynein adaptor BicD2 to co-localize at the nuclear envelope and interact directly with Nesprin-2. Inhibition of BicD2 function in migrating neurons caused marked inhibition of neuronal migration with the striking increase in nucleus-centrosome spacing, as we observed for the dynein binding-deficient Nesprin fragment. Finally, we tested the role of kinesin-1, which can also be recruited by Nesprin-2 to the nucleus, during neuronal migration. We found that inhibition of this motor caused an increase in migration velocity. Overall, our data identify Nesprin-2 as a potential BicD2 "cargo", and has important findings for understanding the fundamental mechanisms of neuronal migration.

INTRODUCTION

Proper cell migration is critical to the formation and functioning of diverse tissues and organs. In the Ventricular Zone (VZ) of the developing brain, neurons are initially generated from radial glial progenitor cells (RGPs)(Noctor *et al.*, 2004), which undergo cell cycle-dependent nuclear oscillations, called interkinetic nuclear migration (INM). Following mitosis at the ventricular surface (VS), committed neurons migrate toward the cortical plate (CP), where they establish the laminar arrangement characteristic of the cerebral cortex. On the way to the CP, post-mitotic neurons undergo successive aspects of polarization. In the intermediate zone (IZ) of the embryonic neocortex, the neurons generate a trailing axon and a thicker leading migratory process, which extends into the CP. Then, the centrosome advances into the migratory process followed by forward nuclear movement, each in a coordinated saltatory fashion.

Work over the past several years has revealed important roles for cytoskeletal motor proteins in brain development (Cooper, 2013; Bertipaglia, Gonçalves and Vallee, 2018), and human mutations in these genes can lead to severe neurodevelopmental pathologies, such as lissencephaly and microcephaly (Reiner *et al.*, 1993; Poirier *et al.*, 2013; Jamuar *et al.*, 2014). In the VZ of the developing brain, the recruitment of cytoplasmic dynein-1 (hereafter "dynein") to the RGP nuclear envelope (NE) is crucial for their proliferation (Hu *et al.*, 2013). During G2 phase of the cell cycle, dynein is recruited by two successive RanBP2/BicD2- and Nup133/CENP-F/Nde1-dependent mechanisms that are each under control of Cdk1, to mediate apical INM in RGP cells (Hu *et al.*, 2013; Baffet, Hu and Vallee, 2015). Later, in post-mitotic neurons dynein is required for the multipolar-to-bipolar transition in the IZ and subsequent directed neuronal migration to the CP (Shu *et al.*, 2004; Tsai *et al.*, 2005; Gonçalves, Dantas and Vallee, 2019), where nuclear transport in migratory neurons requires both myosin IIb and dynein (Tanaka *et al.*, 2004; Bellion *et al.*, 2005; Schaar and McConnell, 2005; Tsai, Bremner and Vallee, 2007; Solecki *et al.*, 2009). Evidence has been obtained that dynein, and possibly kinesin-1, are required at the NE during neuronal migration, but the mechanisms of dynein recruitment in this case are less clear (Tsai, Bremner and Vallee, 2007; Zhang *et al.*, 2009; Wu *et al.*, 2018).

The SUN (for Sad1 and UNC-84) proteins in the inner NE and the KASH (for Klarsicht, ANC-1, Syne Homology) proteins, such as Nesprins, in the outer NE comprise the Linker of Nucleoskeleton and Cytoskeleton (LINC) complex (reviewed in Chang et al. 2015). Nesprins can interact with cytoskeletal elements to regulate nuclear position within the cell. Work in cultured fibroblasts showed that Nesprin-2 interacts with actin filaments and

dynein for correct nuclear positioning (Gomes, Jani and Gundersen, 2005; Luxton *et al.*, 2010; Zhu, Antoku and Gundersen, 2017). During brain development, the LINC complex was found to be required for neuronal migration as judged by the lamination defects observed in KO mice for SUN and Nesprin-1/2 proteins, which showed disrupted radial migration (Zhang *et al.*, 2009). Further implicating nesprins in neuronal migration, expression of the inhibitory KASH domain by *in utero* electroporation in post-mitotic rat cortical neurons severely arrested their movement (Hu *et al.*, 2013). Yet, the precise mechanisms by which Nesprin-2 recruits motors to the NE in neurons and in general has remained unclear.

We have now introduced mutant forms of Nesprin-2 into the embryonic rat brain that allowed us to dissect the precise roles of this protein on neuronal migration. We found that Nesprin-2 recruits dynein to the NE of post-mitotic neurons and in non-neuronal cells, via a novel Nesprin-BicD2 interaction. Notably, Kinesin-1 inhibition increased minus-end directed nuclear movement in migrating neurons, identifying cooperative roles for both microtubule motor proteins in this fundamental behavior.

RESULTS

Roles for Nesprin-2 functional domains in neuronal migration.

To determine whether Nesprin-2 is present at the NE of neuronal cells in the rat brain, we stained for the endogenous protein with a specific antibody (Luxton *et al.*, 2010). We found strong peri-nuclear decoration in the cells throughout the different layers of the neocortex (Fig. 1A and Supp. Fig. 1 A).

The "giant" Nesprin-2 isoform (N2G) contains several discrete structural and functional domains, with a molecular weight around 800kDa. To address the roles of the cytoskeleton-interacting domains in neuronal migration, we used 3 chimeric cDNA constructs previously generated by and tested in cultured fibroblasts, in the laboratory of Dr. Gundersen (Luxton *et al.*, 2010; Zhu, Antoku and Gundersen, 2017) (Fig. 1 B). The "Mini N2G SR" construct contains a calponin homology domain for actin binding, and the spectrin repeats (SR) 52-56, which contain a microtubule motor-binding domain; the "Mini N2G" region encoding the calponin homology domain; and the "N2G SR" region encoding SR 52-56. All three constructs contain the conserved KASH domain, which targets the overexpressed protein to the NE by competing with endogenous KASH proteins for the binding to SUN proteins (Luxton *et al.*, 2010). We used *in utero* electroporation to deliver our constructs, which are HA-tagged and co-express soluble GFP, into embryonic day 16 (E16) rat brain. Successful expression and NE targeting were confirmed in electroporated brain slices (Supp. Fig. 1 B).

Nesprin-2 is required for neuronal migration (Zhang *et al.*, 2009; Hu *et al.*, 2013), but whether this is via actin and/or microtubule cytoskeleton is uncertain. To test the involvement of the Nesprin-2 functional domains in the migration of post-mitotic neurons, we electroporated the Nesprin-2 constructs into E16 rat brain and analyzed the proportion of cells reaching the CP, by E20. Expression of the Mini N2G construct caused a marked decrease the number of cells reaching the CP, strikingly different from the empty vector control (Fig. 1 C, D). The neuronal cell bodies were arrested in the upper IZ, and extended highly elongated processes into the CP (Fig. 1 E, F). In contrast, Mini N2G SR expressing cells were able to reach the CP in higher numbers when compared to the Mini N2G, although in lesser amounts than GFP alone (Fig. 1 C, D). This is consistent with a role for Nesprin-2 in neuronal migration and suggests that binding of Nesprin-2 to microtubule motors is required for nuclear transport at this stage. Furthermore, the number of Mini N2G SR expressing cells that reached the CP was similar to that for N2G SR, suggesting that the Nesprin-2 calponin homology domain by itself does not contribute for neuronal migration.

Role for Nesprin-2 functional domains in nucleus-centrosome coupling.

During migration, neurons extend a leading process and in its proximal region one or more dilations, also called swellings, form, toward which the centrosome moves, followed by the nucleus (Bellion *et al.*, 2005; Schaar and McConnell, 2005; Tsai, Bremner and Vallee, 2007). The LINC complex is well established as an N-C connector (Zhang *et al.*, 2009; Chang, Worman and Gundersen, 2015) and we wanted to test the importance of the Nesprin-2 functional domains in centrosome *vs.* nucleus behavior in migrating neurons. For that we expressed the Nesprin-2 chimeric constructs together with the PACT domain (pericentrin-AKAP450 centrosomal targeting) tagged with DsRed to mark centrosomes (Gillingham and Munro, 2000; Konno *et al.*, 2008; Baudoin *et al.*, 2012), in the E16 brain, and analyzed N-C distance by fixed imaging at E20. Expression of Mini N2G increased the N-C median distance by more than 50-fold when compared to GFP alone, and to more than 7-fold when compared to Mini N2G SR (Fig. 2 A, B). Removal of the Nesprin 2 calponin homology domain had no effect on N-C distance, as expression of the N2G SR construct caused an effect similar to Mini N2G SR (Fig. 2 A, B). This suggests that the microtubule motor-binding domain, but not the calponin homology domain, is necessary for nuclear migration and coupling nuclear movement to that of the centrosome. We note that expression of Mini N2G SR caused a substantial increase in N-C spacing when compared to the GFP control (Fig. 2 A, B). Overall, these results are consistent with, and likely explain, the observed decrease in the number of cells reaching the CP, when Nesprin-2 is incapable of binding to microtubule motors.

To test the roles of Nesprin-2 functional domains in nuclear and centrosome migration more directly, we performed live imaging analysis of embryonic brain slices from rat *in utero* electroporated to express GFP alone, Mini N2G, or N2G SR. As expected, the nuclei of GFP- transfected neurons migrated toward the centrosome as the latter advanced. However, in neurons transfected with Mini N2G, the nucleus remained immobile (Fig. 2 C, Supp. Video 1-3). The centrosome and the dilations in these cells displayed oscillatory excursions within the leading process (Fig. 2 C, Supp. Video 3), suggesting that centrosome transport machinery remained intact, although without net forward movement. Conversely, expression of the N2G SR caused only a slight increase in the N-C distance, with clear nuclear movement toward the centrosome (Fig. 2 C, Supp. Video 2), consistent with our fixed imaging results. Together our results demonstrate a fundamental role for the microtubule motor-binding domain of Nesprin-2 in nuclear, but not centrosome, migration.

Nesprin-2 recruits dynein via its adaptor BicD2

Previous work from our lab revealed that knockdown of the dynein heavy chain, which contains the motor domain, or of the dynein regulator LIS1, each causes delays of both nuclear and centrosome movement in migrating post-mitotic neurons in rat brain (Tsai, Bremner and Vallee, 2007). Our current data indicate that Nesprin-2 contributes only to nuclear transport in these cells. We have found two distinct and successive nucleoporin-mediated mechanisms for dynein recruitment to the RGP NE during the G2 phase of the cell cycle. Nesprins might take over this function in neurons, though whether they recruit dynein directly or with the help of specific dynein regulators, and which ones, emerge as important questions. The *C. elegans* KASH protein, UNC-83, was reported to interact with homologues of the dynein regulators BicD and Nde1. Therefore, we tested whether these might interact with Nesprin-2 in mammals and mediate dynein recruitment to the NE. For this purpose, we first used cultured non-neuronal HeLaM cells, which have been proven useful in detecting dynein and its cofactors at the G2 NE (Splinter *et al.*, 2010; Hu *et al.*, 2013; Baffet, Hu and Vallee, 2015)(Supp. Fig. 2 A). HeLaM cells were transfected with GFP-Mini N2G or GFP-Mini N2G SR and stained for endogenous BicD proteins. In GFP-Mini N2G expressing cells, BicD2 could be readily detected at the NE during G2. Interestingly, GFP-Mini N2G SR showed clear NE co-localization with endogenous BicD2 in G2 and non-G2 phase of the cell cycle cells (Supp. Fig. 2 A-E). We also observed this behavior for BicD1, a closely related BicD2 protein, with likely fewer contributions for brain development (Hu *et al.*, 2013) (Supp. Fig. 2 F, G). We also stained Mini N2G SR-expressing cells for Nde1/Ndel1, but we failed to see clear NE decoration in non-G2 cells (Supp. Fig. 2 A, H, I). These results suggest that the microtubule motor-binding domain of Nesprin-2 recruits BicD2, but not Nde1/Ndel1 proteins, to the HeLaM NEs.

To confirm cell cycle independent co-localization of the dynein adaptor BicD2 with Nesprin-2 at the NE, we transfected cultured NIH3T3 fibroblasts with GFP-Mini N2G or GFP-N2G SR, and then we synchronized the cells in G0 by serum starvation (Zhu, Antoku and Gundersen, 2017). Cells were fixed and stained for endogenous dynein and BicD2 proteins. Consistent with published data(Zhu, Antoku and Gundersen, 2017), cells expressing GFP-N2G SR, but not GFP-Mini N2G, showed clear dynein decoration at the NE (Fig. 3 A). Notably with regard to the current study, GFP-N2G SR-transfected cells also exhibited a strong BicD2 signal at the NE, which we did not observe in cells expressing GFP-Mini N2G (Fig. 3 B). These results strongly suggest that Nesprin-2 recruits dynein via its adaptor BicD2.

To test whether Nesprin-2 interacts physically with BicD2, we performed pull-downs from embryonic rat brain lysates with bacterially purified GST *vs.* GST-N2G SR, and blotted our membranes for BicD2. Pull-down of GST-N2G SR revealed a strong reactive for BicD2 (Fig. 3 C) supporting a BicD2-Nesprin-2 interaction through the previously identified microtubule motor-binding domain.

BicD2 consists of an N-terminal coiled-coil that binds to the dynein complex and a C-terminal coiled-coil region that binds to cellular dynein cargoes, as Rab6 and RanBP2 (Matanis *et al.*, 2002; Splinter *et al.*, 2010). To test whether Nesprin-2 might interact with the BicD2 C-terminal region we performed pull downs with bacterially purified GST-BicD2 C-terminus (BicD2 CT) from HeLaM cell lysates transfected with GFP-Mini N2G or N2G SR, and immunoblotted our membranes for GFP. Consistent with our hypothesis, GST-BicD2 CT was able to pull down GFP-N2G SR, but not GFP-Mini N2G (Fig. 3 D). This observation further supports a Nesprin-2 interaction with BicD2 *via* its C-terminal cargo-binding region.

Finally, we wondered whether the interaction of Nesprin-2 with BicD2 was direct or involved an intermediate protein. To address this question we incubated bacterially purified His-BicD2 CT with GST or GST-N2G SR and we pulled down the formed complexes with GST capturing beads. Using a BicD2 C-terminal specific antibody against our membranes, we saw a clear BicD2 band with GST-N2G SR, but not GST alone (Fig. 3 E). This is consistent with our previous findings and confirms a direct interaction between the C-terminal region of BicD2 and its novel cargo Nesprin-2.

BicD2 participates in neuronal migration in a cell-autonomous fashion

BicD2 roles in brain development include dynein recruitment to the NE in apical INM and the multipolar-to-bipolar transition of newborn neurons (Hu *et al.*, 2013). Data from BicD2 KO mice has suggested a contribution of this protein for the migration of cerebellar neurons in a non-cell autonomous fashion (Hu *et al.*, 2013; Jaarsma *et al.*, 2014). Our observation that Nesprin-2 interacts with BicD2 and recruits this protein to the NE lead us to think whether BicD2 is also required for nuclear transport in migration neurons. To test this, we electroporated E16 brains with a conditional construct that expresses BicD2 CT under a NeuroD1 promoter, which specifically allows for protein expression after the multipolar stage and bypasses the requirement for BicD2 in earlier stages of brain development (Guerrier *et al.*, 2009; Carabalona, Hu and Vallee, 2016). We analyzed the number of cells in the IZ and the CP of the embryonic neocortex, by E20. Expression of BicD2 CT in post mitotic neurons caused a strong accumulation of cells in the IZ, at the expense

of the number of cells that reached the CP (Fig. 4 A, B). This is consistent with a new cell autonomous role for BicD2 in neuronal migration.

We reasoned that the BicD2 CT domain might cause these results by competing for Nesprin binding, with the endogenous BicD proteins. This effect would in turn, interfere with neuronal migration by hampering nuclear transport. To test this, we electroporated E16 brains with BicD2 CT construct, and we analyzed N-C behavior by fixed and live imaging, at E20. Expression of the truncated version of BicD2 caused a marked increase in the N-C distance (Fig. 4 C, D). Live monitoring of neurons expressing BicD2 CT showed a clear inhibition in nuclear movement, while the centrosome was separated by abnormally large distances (Fig. 4 E). We also note the dynamics of the centrosome, which was constantly oscillating within the leading process, without net forward movement comparable to what we had observed with expression of Mini N2G (Supp. Video 4). This, data confirms the requirement for BicD2 in nuclear, but not centrosome transport, during neuronal migration.

Our prior work revealed that the nucleoporin RanBP2 recruited BicD2 to the RGP NE during G2-specific apical INM. Nonetheless, we tested whether this mechanism might have a role in migratory neurons, as well. For this purpose, we expressed both RanBP2 and BicD2 shRNAs, and analyzed N-C separation in post-mitotic migrating neurons. Although BicD2 RNAi caused a significant increase in N-C spacing, we saw no effect from RanBP2 RNAi (Supp. Fig. 3 A, B). These results support a major or unique requirement for our Nesprin-2-dependent BicD2/dynein recruitment mechanism.

Effects of Kinesin-1 inhibition in neuronal migration

KASH proteins, including Nesprin-2, can recruit both dynein and kinesin-1 to the NE (Fridolfsson and Starr, 2010; Schneider *et al.*, 2011; Wilson and Holzbaur, 2012; Wu *et al.*, 2018). There is evidence that kinesin-1 recruitment to the NE via Nesprin-2 contributes for nuclear positioning in the developing muscle (Wilson and Holzbaur, 2012, 2015) and possibly in migrating cerebellar neurons (Wu *et al.*, 2018). Yet, the relative contribution of kinesin-1 in nuclear transport during neuronal migration remains uncertain.

Kinesin-1 family consists of 3 kinesin heavy chain (KIF5A, B and C) and 4 Kinesin Light Chain (KLC1 to 4) coding genes. The KIF5A, B and C molecules contain the ATPase domain and can form homo and heterodimers. Cargo binding to kinesin-1 can occur through the kinesin heavy chain or the KLCs, which associate with the heavy chain dimers. In the case of Nesprin-2 a direct interaction with KLC was shown to

occur via the KLC tetratricopeptide repeat (TPR) domain that targets kinesin-1 to the NE (Schneider *et al.*, 2011; Wilson and Holzbaur, 2015). In addition, BicD2 was also reported to recruit kinesin-1 (Grigoriev *et al.*, 2007; Splinter *et al.*, 2010), suggesting that this microtubule motor could be recruited to the NE by at least two mechanisms. Thus, to determine the specific contribution of kinesin-1 during neuronal migration we first produced HA-tagged constructs encoding the Kif5B tail domain and the TPR domain of the KLC1, each of which were reported to inhibit kinesin-1 function (Wilson and Holzbaur, 2015; Wu *et al.*, 2018). Then, we electroporated the truncated kinesin-1 subunits, and analyzed the effects in rat brain slices at E20 by fixed and live imaging. Surprisingly, expression of the Kif5B tail or the KLC TPR domains substantially increased the number of electroporated cells reaching the CP (Fig. 5 A, B). Remarkably, by live imaging analysis we observed an increase in the average velocity in neurons electroporated with the KLC TPR (Fig. 5 C, D). These results suggest that kinesin-1 acts to restrain overall neuronal displacement. We also wanted to determine the extent of kinesin-1 contribution to N-C coupling. For that, we *in utero* electroporated E16 brains with control, Kif5B tail or KLC TPR domains, and analyzed N-C distance, by E20. The N-C spacing in Kif5B tail or KLC TPR expressing neurons was similar to control (Supp. Fig. 5 A, B). These data indicate that Nesprin-2-dependent nuclear transport during neuronal migration majorly depends on the recruitment of dynein via BicD2, while kinesin-1 function appears to be residual, if not inhibitory.

The KLC TPR domain has been shown to interact through a conserved LEWD motif in the microtubule motor-binding domain region of Nesprin-2 (Wilson and Holzbaur, 2015). To more specifically address the relative kinesin-1 contribution via Nesprin-2 in our system, we mutated the LEWD motif in our N2G SR construct and replaced it with two alanines (N2G SR LEAA), which were shown to abolish kinesin-1 binding to Nesprin-2 (Wilson and Holzbaur, 2015), but not to the dynein regulatory complex dynactin (Zhu, Antoku and Gundersen, 2017). We first tested whether the N2G SR LEAA construct could bind to BicD2. To address this, we performed pull downs with GST-BicD2 CT from HeLaM cell lysates expressing GFP-Mini N2G, GFP-N2G SR or GFP-N2G SR LEAA. Importantly, while GST-BicD2 CT could bind to GFP-N2G SR, we observed a striking decrease in the signal of GFP-N2G LEAA, similar to the GFP-Mini N2G (Supp. Fig. 4 A). These results suggest that the LEAA mutation reduces the binding of BicD2 to Nesprin-2, likely interfering with the recruitment of both dynein and kinesin microtubule motors.

The finding that the LEAA mutation in Nesprin-2 interferes with BicD2 binding, allowed us to test the contribution of the Nesprin-2/BicD2 mechanism during neuronal migration further. To evaluate the effects of

the LEAA mutation *in vivo* we *in utero* electroporated E16 brains with N2G SR or N2G SR LEAA and analyzed soma distribution in the neocortex, by E20. The number of N2G SR LEAA transfected cells reaching the CP was significantly reduced when compared to N2G SR (Supp. Fig. 4 B, C). To test whether this effect was due to impaired nuclear migration we *in utero* electroporated E16 brains with N2G SR or N2G SR LEAA, and analyzed N-C distance, by E20. We found that expression of N2G SR LEAA caused an increase in N-C spacing when compared to the N2G SR (Supp. Fig. 4 D, E). These provide additional evidence in support of our model that Nesprin-2 recruitment of BicD2/dynein is required for neuronal migration, specifically in nuclear transport.

DISCUSSION

Our results identify Nesprin-2 as new and critically important interactor for BicD2, the already multivalent dynein cargo-adaptor protein capable of binding both Rab6 and RanBP2 (Matanis *et al.*, 2002; Splinter *et al.*, 2010). We find that Nesprin-2 inhibition completely and strikingly uncouples centrosomal from nuclear movement. We determined Nesprin-2 function during nuclear movement to its ability to recruit dynein to the NE, which we found to be mediated by BicD2. Together, these results lead a novel and unifying mechanism for the basic, but incompletely understood process of neuronal migration (Fig. 5 H).

LINC complexes are involved in multiple modes of nuclear migration (reviewed in Bone and Starr, 2016). One of these mechanisms depends on the recruitment of dynein and/or kinesin-1 by Nesprin-2 to the NE to adjust nuclear position (Wilson and Holzbaur, 2012, 2015; Zhu, Antoku and Gundersen, 2017; Wu *et al.*, 2018). In particular, during neocortical development it has been suggested that Nesprin-2 mediates N-C connection in migrating neurons (Zhang *et al.*, 2009). Here, by replacing endogenous Nesprins with discrete functional domains of Nesprin-2, we found that the recruitment of microtubule motors to the NE via Nesprin-2 to be essential for nuclear migration in post-mitotic neurons. Although the expression of the Mini N2G SR construct did not fully mimic the endogenous Nesprins, conceivably due to the truncation of relevant, but still uncharacterized domains, we observed, however, that by introducing the relatively small region of the microtubule motor-binding domain together with the KASH domain (N2G SR), neuronal migration occurred in substantial amounts. Interestingly, by expressing the Mini N2G construct, we were able to completely uncouple the arrested nucleus from the centrosome, as the latter progressed into the leading process. In this case, the leading process extension was conserved, dilations were formed, and the centrosome was in some cases more than 100µm distant from the nucleus. These findings support the current model in which the centrosome has its own transport machinery and moves independently in front of the nucleus, which in turn responds to the centrosome advance by migrating into to the space in-between. Notoriously, judging by our live imaging analysis, the dilations and centrosome do not move toward the CP efficiently when they are very distant from the nucleus. We think that upon N-C separation by very high non-physiological distances, centrosome transport machinery might become impaired.

The actin cytoskeleton plays a pivotal role in neuronal migration (Bellion *et al.*, 2005; Schaar and McConnell, 2005; Tsai, Bremner and Vallee, 2007; Solecki *et al.*, 2009; He *et al.*, 2010; Martini and Valdeolmillos, 2010; Jiang *et al.*, 2015). It has been suggested that the activity of the non-muscle myosin II is necessary for nuclear

advance in migrating neurons by contracting actin filaments at the rear of the nucleus (Bellion *et al.*, 2005; Schaar and McConnell, 2005; Martini and Valdeolmillos, 2010). Accumulation and activity of actin filaments in the proximal region of the leading process was also observed. It has been proposed that actin pulls the centrosome and the nucleus (Solecki *et al.*, 2009; He *et al.*, 2010; Jiang *et al.*, 2015), perhaps by interacting with the microtubule cytoskeleton to regulate neuronal migration (Trivedi *et al.*, 2017). In fibroblasts, actin filaments were shown to interact directly with the nucleus via the calponin homology domain of Nesprin-2 to move the nucleus (Luxton *et al.*, 2010). Here, we find this domain by itself to be dispensable for nuclear movement, suggesting that actin does not require contact with Nesprin-2 at the nucleus to displace it.

Looking to determine whether kinesin-1 contributes for N-C coupling in our system, we found that kinesin-1 inhibition increased the number of cells that could reach the CP, and this was explained by the faster migration of these neurons. In addition, we did not find an involvement of this motor in N-C coupling in migration neurons. The literature on the role of kinesin-1 in neuronal migration is scarce. One recent study has shown that kinesin-1 inhibition, by expressing the Kif5B tail domain, disrupts cerebellar granular neuron migration *in vivo* (Wu *et al.*, 2018), and whether the discrepancy with our results is due to different systems is uncertain (Umeshima, Hirano and Kengaku, 2007). Importantly, in another study with a different kinesin, kinesin-5, in a model of neocortical development comparable to ours has shown that kinesin-5 inhibition causes an increase in the migrating of cells to the CP and augments the velocity of migrating neurons. The authors argued that kinesin-5 inhibition might increase the sliding of antiparallel microtubules, and this could enhance migration (Falnikar, Tole and Baas, 2011; Rao *et al.*, 2016). The mechanisms by which kinesin-1 can determine muscle position has been studied in muscle cells. Two models exist to explain kinesin-1 dependent nuclei positioning, one that results from the sliding of antiparallel microtubules by this motor and another that depends on a Nesprin-dependent recruitment of kinesins to the nuclear envelope (Metzger *et al.*, 2012; Wilson and Holzbaur, 2015). In line with a role of kinesins in nuclear position acting at the nuclear surface, expression of Nesprin-4, which recruits kinesin-1 to the NE, induces movement of the nuclei away from the centrosome (Roux *et al.*, 2009) and in G2 cells dynein inhibition by injection of an inhibitory antibody causes nucleus separation from the centrosome (Splinter *et al.*, 2010). Altogether, there is convincing evidence that kinesin-1 can affect nuclear position, but the precise mechanisms by which kinesin-1 contributes for brain development are unclear. Nonetheless, we think that kinesin-1 inhibition could release dynein, thus favoring minus-end net displacement (Shubeita *et al.*, 2008). This could explain the enhancing effect in neuronal migration upon kinesin-1 inhibition, as nuclear transport depends majorly on dynein motor.

Dynein is the major retrograde motor in the cell and this single motor performs a wide array of cellular activities. Cargo adaptor proteins, such as BicD2, are under intensive investigation, as these adaptors specifically recruit dynein to membranous organelles to ensure processive movement. Here, we find Nesprin-2 as another nuclear cargo for BicD2. Using co-immunoprecipitation and immunofluorescence approaches, we found that the microtubule motor-binding domain of Nesprin-2 is necessary and sufficient to recruit this protein to the NE. This interaction, which we found to be direct, adds up to the already described BicD2 cargos, such as Rab6-containing vesicles (Matanis *et al.*, 2002) and the nucleoporin RanBP2 during G2 (Splinter *et al.*, 2010). Previous work from our lab and others has shown that during G2 phase of the cell cycle, Cdk1 phosphorylates RanBP2, which causes the displacement of BicD2 from Rab6 vesicles, and potentially other cytoplasmic cargoes, toward the nucleus (Baffet, Hu and Vallee, 2015; Noell *et al.*, 2018). This shift in BicD2 localization and function is important in neural stem cells for apical INM and progression through mitosis. In migrating neurons, however, this Cdk1 mechanism is most likely not relevant during neuronal migration, as the neurons are post-mitotic and we do not find a substantial role for RanBP2 in this behavior. Notoriously, neurons use Nesprin-2/BicD2 mechanism to recruit dynein to the NE during neuronal migration. Thus, understanding the regulatory mechanisms of BicD2 sub-cellular localization will clarify how this protein is recruited to the NE during neuronal migration and this will ultimately be important to understand dynein functional diversity.

FIGURES AND FIGURE LEGENDS

Figure 1

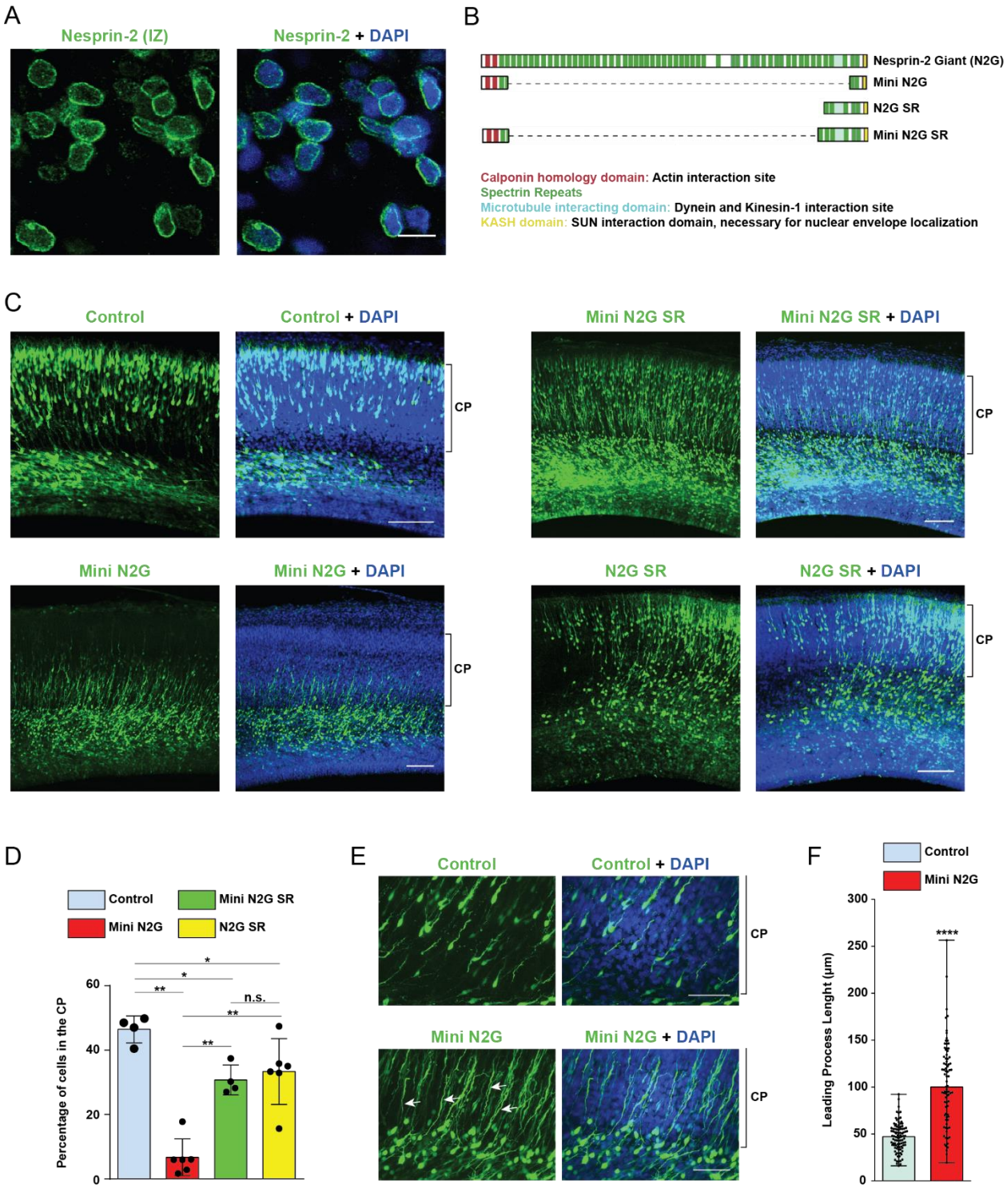

Figure 1

Roles of Nesprin-2 functional domains in neuronal migration. (A) Embryonic day 20 (E20) rat brain slices were stained with DAPI and for endogenous Nesprin-2, and a representative image from the Intermediate Zone (IZ) where pre-migratory neurons reside is depicted. **(B)** Diagrammatic representation of the Nesprin-2 Giant (N2G) isoform and the known functional domains used in this work (adapted from (Zhu, Antoku and Gundersen, 2017). **(C-F)** E16 rat brain was *in utero* electroporated with control empty vector, Mini N2G SR, Mini N2G or N2G SR constructs, and subsequently imaged 4 days post injection, at E20. **(C)** Representative images of the neocortex with electroporated cells in green and stained with DAPI. Brackets show the Cortical Plate (CP) margins. **(D)** Quantification of the proportion of cells reaching the CP across conditions. **(E)** Magnified images of the upper IZ and lower CP of Control and Mini N2G electroporated brains. Mini N2G expressing cells have over-elongated and bulky leading processes (arrows). **(F)** Quantification of the leading process length in electroporated neurons. Data presented as scatter dot plot with bar representing mean±s.d. in **D**, and as scatter dot plot with bar representing median with range in **F**. Mann Whitney test for non-parametric distributions was used in **D** unpaired T-Test with Welch's correction in **F** (*P<0.05; **P<0.01; ****P<0.0001; n.s. non-significant). Data in **D** includes at least 967 electroporated cells from at least 4 embryos, per condition. Data in **F** includes at least 83 neurons from at least 3 embryos, per condition. **A** scale bar, 10μm. **C** scale bar, 100μm. **E** scale bar, 50μm.

Figure 2

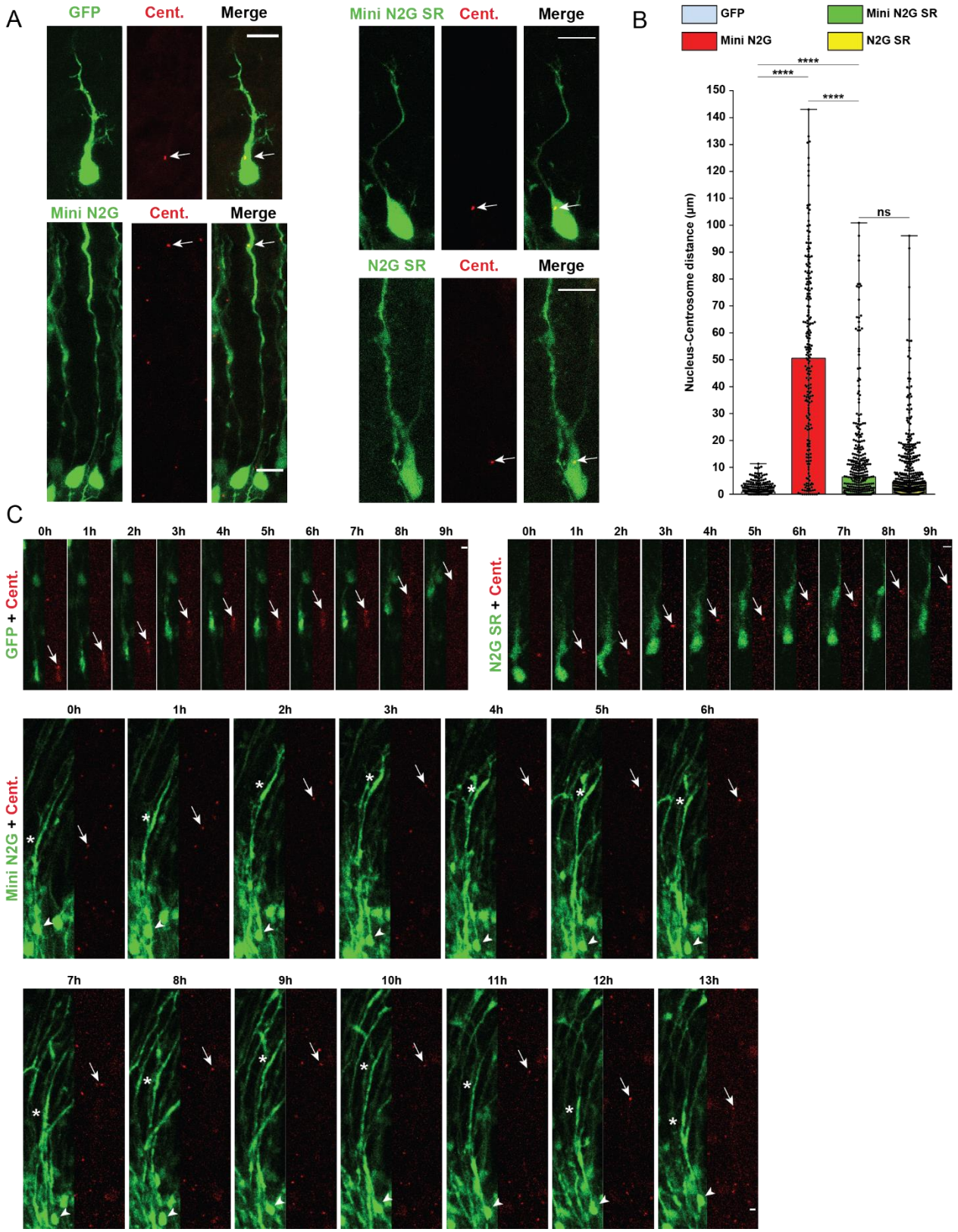
A
GFP
Cent.
Merge
Mini N2G SR
Cent.
Merge
Mini N2G
Cent.
Merge
N2G SR
Cent.
Merge
B
GFP
Mini N2G SR
Mini N2G
N2G SR
****
****
****
ns
Nucleus-Centrosome distance (µm)
150
140
130
120
110
100
90
80
70
60
50
40
30
20
10
0
C
GFP + Cent.
N2G SR + Cent.
Mini N2G + Cent.
0h
1h
2h
3h
4h
5h
6h
7h
8h
9h
10h
11h
12h
13h

Figure 2

Roles of Nesprin-2 functional domains in Nucleus-Centrosome coupling. (A-C) E16 rat brain was *in utero* electroporated with control vector or Nesprin-2 functional domains together with PACT-DsRed, and subsequently imaged fixed or live by E20. **(A)** Fixed images of electroporated neurons in the CP showing the centrosome (Cent.) position (arrows) relative to the soma. **(B)** Quantification of the N-C distance across conditions. **(C)** Time-lapse images for electroporated migrating neurons (Supplementary Movies 1–3). Images are shown at 1h intervals (hh). Arrows, arrowheads and asterisks indicate centrosomes, cell bodies and leading process dilations respectively. Data presented as scatter dot plot with bar representing median with range in **B**. Mann Whitney test for non-parametric distributions was used in **B** (****P<0.0001; n.s. non-significant). Data in **B** includes at least 217 electroporated neurons from at least 3 embryos, per condition. **A** scale bar, 10μm. **C** scale bar, 5μm.

Figure 3

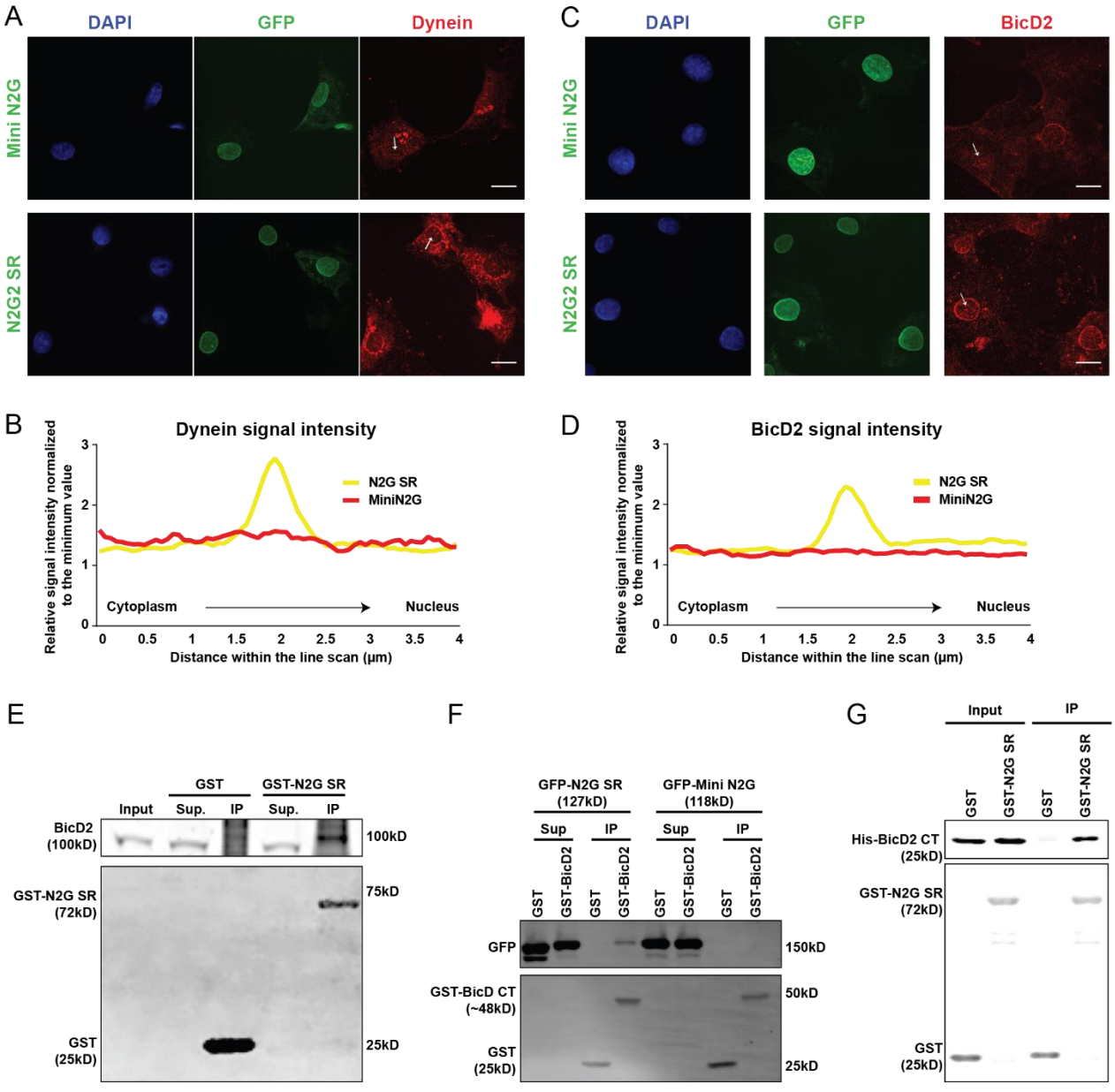
A
DAPI
GFP
Dynein
Mini N2G
N2G2 SR
C
DAPI
GFP
BicD2
Mini N2G
N2G2 SR
B
Dynein signal intensity
Relative signal intensity normalized to the minimum value
N2G SR
MiniN2G
Cytoplasm
Nucleus
Distance within the line scan (μm)
D
BicD2 signal intensity
Relative signal intensity normalized to the minimum value
N2G SR
MiniN2G
Cytoplasm
Nucleus
Distance within the line scan (μm)
E
GST
GST-N2G SR
Input
Sup.
IP
Sup.
IP
BicD2 (100kD)
100kD
GST-N2G SR (72kD)
75kD
GST (25kD)
25kD
F
GFP-N2G SR (127kD)
GFP-Mini N2G (118kD)
Sup
IP
Sup
IP
GST
GST-BicD2
GST
GST-BicD2
GST
GST-BicD2
GST
GST-BicD2
GFP
150kD
GST-BicD CT (~48kD)
50kD
GST (25kD)
25kD
G
Input
IP
GST
GST-N2G SR
GST
GST-N2G SR
His-BicD2 CT (25kD)
GST-N2G SR (72kD)
GST (25kD)

Figure 3

BicD2 co-localization and interaction with Nesprin-2. (A-D) Cultured NIH 3T3 fibroblasts were transfected with GFP-Mini N2G or GFP-N2G SR and stained with DAPI and for endogenous dynein or BicD2. Arrows indicate the line scan position done for quantifications purposes. **(A, C)** Representative fixed images and **(B, D)** line scan quantifications are shown. **(E)** GST-N2G SR pull down from embryonic rat brain lysate was evaluated for BicD2 co-immunoprecipitation. **(F)** GST-BicD2 CT pull downs from HeLaM cell lysates expressing GFP-Mini N2G or GFP-N2G SR were evaluated for GFP co-immunoprecipitation. **(G)** GST-N2G SR pull down from BicD2 CT protein concentrate was evaluated for BicD2 CT co-immunoprecipitation. Data are presented as superimposed symbols at mean with a connecting line in **B** and **D**. Data in **B** and **D** includes line scan analysis from at least 6 and 12 cells, respectively. **A** and **C** scale bar, 10μm.

Figure 4

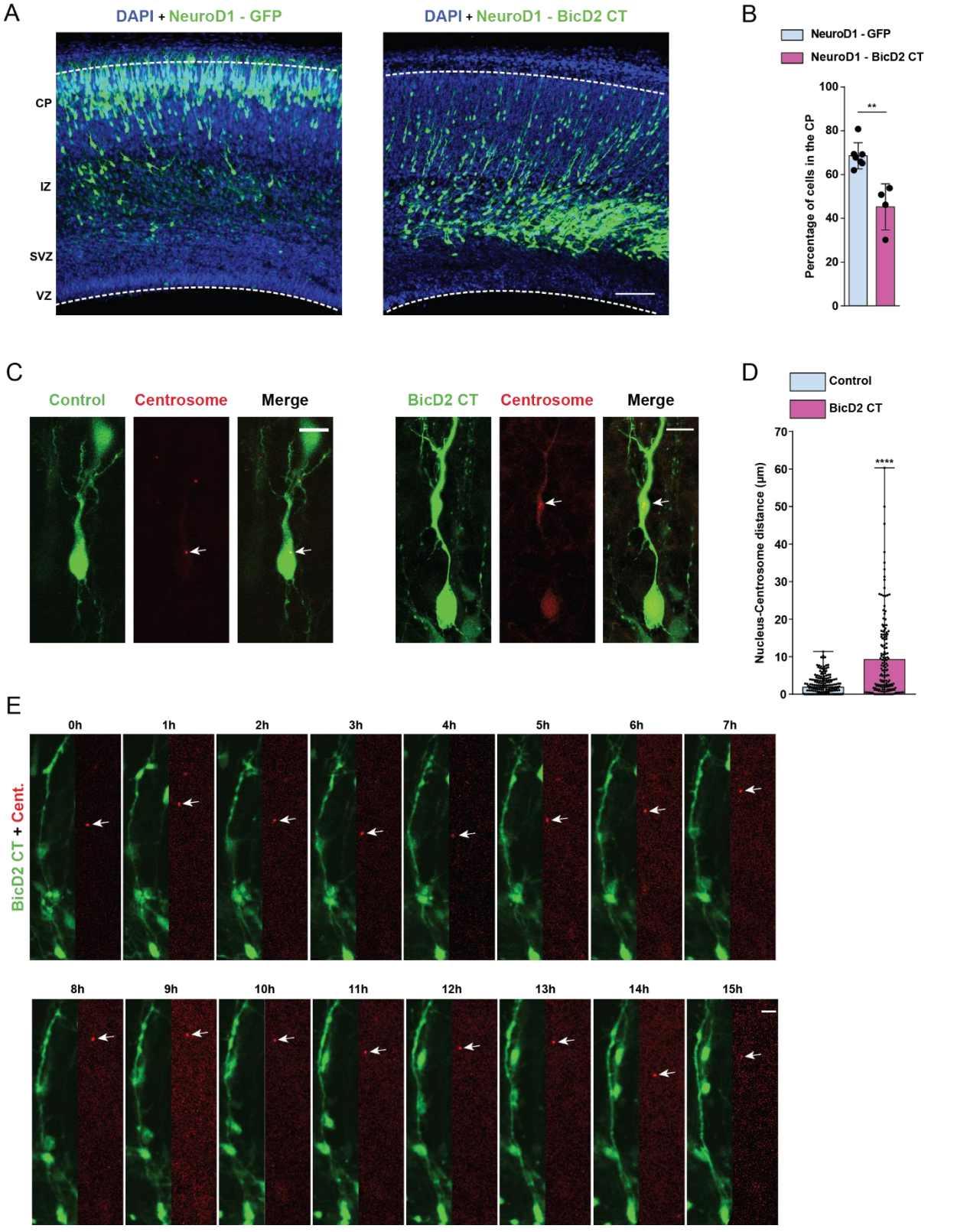
A
DAPI + NeuroD1 - GFP
DAPI + NeuroD1 - BicD2 CT
CP
IZ
SVZ
VZ
B
NeuroD1 - GFP
NeuroD1 - BicD2 CT
Percentage of cells in the CP
**
C
Control
Centrosome
Merge
BicD2 CT
Centrosome
Merge
D
Control
BicD2 CT
Nucleus-Centrosome distance (µm)
****
E
BicD2 CT + Cent.
0h
1h
2h
3h
4h
5h
6h
7h
8h
9h
10h
11h
12h
13h
14h
15h

Figure 4

Effects of BicD2 inhibition in neuronal migration. (A, B) E16 rat brain was *in utero* electroporated with control or conditional BicD2 CT expressing vector, under NeuroD1 promoter regulation. Brains were imaged and analyzed at E20. **(A)** Representative images of the neocortex with electroporated cells in green and stained with DAPI. **(B)** Quantification of the proportion of cells that reach the CP. **(C-E)** E16 rat brain was *in utero* electroporated with control or BicD2 CT expressing vectors together with PACT-DsRed, and subsequently imaged fixed or live by E20. **(C)** Fixed images of electroporated neurons in the CP showing the centrosome position (arrows) relative to the soma. **(D)** Quantification of the N-C distance across conditions. **(E)** Time-lapse images for electroporated migrating neurons (Supplementary Movies 4). Images are shown at 1h intervals (hh). Arrows indicate centrosomes. Data presented as mean±s.d. in **B** and as scatter dot plot with bar representing median with range in **D**. Mann Whitney test for non-parametric distributions was used in **B** and **D** (**P<0.01; ****P<0.0001). Data in **B** includes at least 3235 electroporated cells from at least 4 embryos from different mothers, per condition. Data in **D** includes at least 169 electroporated cells from at least 4 embryos from different mothers, per condition. **A** scale bar, 100μm. **C** and **E** scale bars, 10μm.

Figure 5

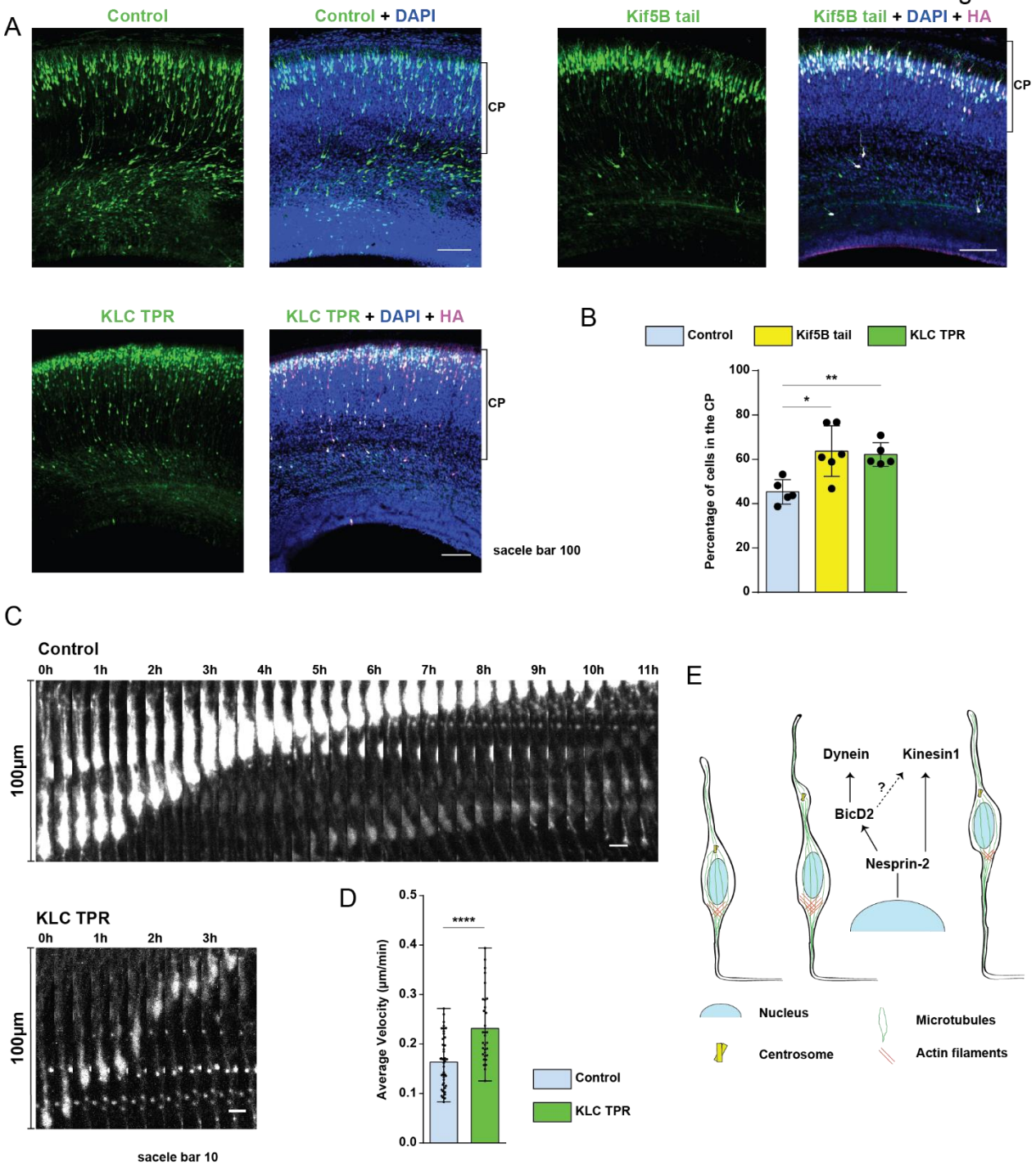
A
Control
Control + DAPI
Kif5B tail
Kif5B tail + DAPI + HA
CP
KLC TPR
KLC TPR + DAPI + HA
sacele bar 100
B
Control
Kif5B tail
KLC TPR
Percentage of cells in the CP
C
Control
0h 1h 2h 3h 4h 5h 6h 7h 8h 9h 10h 11h
100μm
KLC TPR
0h 1h 2h 3h
sacele bar 10
D
Average Velocity (μm/min)
****
E
Dynein
Kinesin1
BicD2
Nesprin-2
Nucleus
Centrosome
Microtubules
Actin filaments

Figure 5

Roles for Kinesin-1 in neuronal migration. (A-D) E16 rat brain was *in utero* electroporated with control, Kif5B tail or KLC TPR expressing constructs, and subsequently imaged by fixed and live imaging at E20. **(A)** Fixed images of the neocortex with electroporated cells in green, stained with DAPI and for HA. Brackets show CP margins. **(B)** Quantification of the proportion of cells reaching the CP. **(C)** Time-lapse images for control and KLC TPR expressing neurons (Supplementary Movies 5, 6) during the time to complete 100µm displacement. Images are shown at 20min intervals. **(D)** Quantification neuronal migration velocity in control *vs.* KLC TPR. Data presented as scatter dot plot with bar representing mean±s.d. in **B**, and as scatter dot plot with bar representing mean with range in **D**. Mann Whitney test for non-parametric distributions was used in **B** (*P<0.05; **P<0.01). Unpaired T-Test with Welch's correction was used in **D** (**P<0.01; ****P<0.0001). Data in **B** includes at least 967 electroporated cells from at least 4 embryos, per condition. Data in **D** includes 45 and 57 migrating neurons for control and KLC TPR, respectively. **A** scale bar, 100µm. **C** scale bar, 10µm. **(E)** Diagrammatic representation of the microtubule motors recruitment mechanisms to the NE during neuronal migration. After leading process extension, the centrosome migrates into the leading process. This is followed by forward nuclear movement dependent on dynein and BicD2 recruitment to the NE by Nesprin-2. It is possible that Kinesin1 is recruited either directly via Nesprin-2 or indirectly via BicD2, and this might oppose dynein dependent movement.

METHODS

Ethics statement

All the experiments were done in accordance with the animal welfare guidelines and the guidance of the Institutional Animal Care and Use Committee (IACUC) at Columbia University.

In utero electroporation

Plasmids encoding for shRNAs or cDNA were injected into the developing brain at embryonic day 16 (E16) and electroporated as described (Baffet *et al.*, 2016). In more detail, timed pregnant Sprague Dawley E16 rats were anaesthetized with a ketamine xylazine cocktail administered intraperitoneally, and toe pinch was performed to ensure deep anesthesia. To avoid excessive heating loss during the surgical procedure, an external heating source was provided. For pain management buprenorphine and bupivacaine were administered subcutaneously, before the surgery. Abdominal cavity was opened and uterine horns exposed and trans-illuminated for clear identification of the embryonic brain ventricles. For easy visualization of the DNA in the brain ventricular space, a non-toxic dye (Sigma, F7252) was added to the DNA before surgery and injected with a sharpened glass needle. After injection, embryos were subjected to five electric impulses (50V, 50ms each, separated by 1s intervals) delivered by an electroporator (Harvard Apparatus ECM 830), to target the DNA to RGPs in the lateral neocortex. The embryos were returned to the abdominal cavity and the wound was closed. Rats were monitored every day post-surgery and buprenorphine was administered every 12h for the first 48h, for post-operative pain control.

Immunohistochemistry and live imaging

For embryonic brain harvesting, pregnant rats were re-anesthetized and the surgical wound was reopened 4 days post injection, at E20, to expose the uterus.

For fixed imaging, embryonic (E20) rat brains were harvested and immersed in PBS with 4% PFA overnight. They were then embedded in 4% of agarose (Sigma, A9539) and sliced in a vibratome (Leica, VT 1200S) in 100µm slices. After blocking in 5% normal donkey serum (Sigma, D9663) in PBS-Triton X-100 0.5% for 1 hour, slices were incubated with primary antibodies diluted in the blocking solution, overnight on a shaker, at 4°C. Secondary antibodies (1:500) and DAPI (4',6-diamidino-2-phenylindole, Thermo Scientific, 62248,

1:10.000 dilution) were diluted in PBS and incubated for 2 h at room temperature. Slices were mounted with Aqua-Poly mounting media (Polysciences, 18606).

For live imaging, the dissected embryonic rat brains were embedded in 4% low melting agarose (IBI Scientific, IB70057) diluted in artificial cerebrospinal fluid (Baffet *et al.*, 2016) and sliced into 300µm coronal sections. The slices were placed on porous filters (EMB Millipore, PICMORG50) in cortical culture medium containing 25% Hanks balanced salt solution (Life Technologies, 24020-117), 47% basal MEM (Life Technologies, 21010-046), 25% normal horse serum (Life Technologies, 26050-088), 1% penicillin/ streptomycin/glutamine (Life Technologies, 10378-016), and 2% of 30% glucose (Sigma, G5767) in a 50mm glass-bottom dish (MatTek Corporation, P50G-0-14-F) and imaged on an IX80 laser scanning confocal microscope (Olympus FV1000 Spectral Confocal System) at intervals of 10 min for up to 24 h.

RNAi and cDNA expressing constructs

For the *in utero* electroporation experiments in the embryonic brain, the shRNAs for BicD2, RanBP2 and LIC1 were previously described (Hu *et al.*, 2013; Baffet, Hu and Vallee, 2015; Gonçalves, Dantas and Vallee, 2019) and EGFP-C1 was used as control. The Mini N2G, N2G Spectrin Repeats (SR) 52-56, Mini N2G SR constructs were cloned into the pCAGIG vector (Addgene plasmid #11159)(Matsuda and Cepko, 2004) by PCR amplification using KOD Hot Start DNA Polymerase (Millipore, 71086). Previously described EGFP-C1-Mini N2G and pMSCV-N2G SR 52-56 constructs were used as templates (Zhu, Antoku and Gundersen, 2017) and an HA-tag coding sequence was introduced. Point mutagenesis was used to introduce LEAA mutation within the pCAGIG N2G SR construct. BicD2 CT (630-820aa) was PCR amplified from full length mouse BicD2 in pIRES2 DsRed-Express2 vector (Hu *et al.*, 2013) and inserted into pCAGIG and pCALNL-GFP (Addgene plasmid #13770)(Matsuda and Cepko, 2007) vectors. For the conditional expression of BicD2 CT, pNeuroD1-Cre (gift from Dr. Carlos Cardoso, Institut de Neurobiologie de la Méditerranée) was co-injected with pCALNL-GFP and pCALNL-BicD2 CT. C-terminal HA-tagged Kif5B tail (809-963 aa of rat Kif5B) and KLC-TPR (211-497 aa of rat KLC1) nucleotide sequences were gene synthesized and cloned into pCAGIG vector (Synbio Technologies, New Jersey, USA). To tag centrosomes, PACT domain (pericentrin-AKAP450 centrosomal targeting) sequence from rat pericentrin (2729-2933) was amplified and cloned into a pCAG-GFP vector (Addgene plasmid #11150)(Matsuda and Cepko, 2004), in which the GFP sequence was removed and it was C-terminal tagged with DsRed.

The constructs for bacterial expression GST-BicD2-CT (gift from Dr. Anna Akhmanova, Utrecht University)(Splinter *et al.*, 2010), His-BicD2-CT (Baffet, Hu and Vallee, 2015) GST-N2G (gift from Dr. Gregg Gundersen, Columbia University) (Zhu, Antoku and Gundersen, 2017) were described previously. For experiments in NIH 3T3 fibroblasts, pMSCV-puro GFP-Mini N2G and pMSCV-puro GFP-N2G SR (52-56) constructs were used. For experiments in HeLaM cells, pEGFP-C1 GFP-Mini N2G, pEGFP-C1 GFP-Mini N2G SR (51-56), pMSCV N2G SR (52-56) and pMSCV N2G SR (52-56) LEAA constructs were used. These constructs were a kind gift from Dr. Gregg Gundersen and they were described previously (Zhu, Antoku and Gundersen, 2017).

Cell Culture, Transfection, Immunostaining, and Drug Treatment

NIH3T3 fibroblasts (gift from Dr. Gregg Gundersen) and HeLaM cells (a gift from Dr. Viki Allan, University of Manchester) were cultured in DMEM supplemented with 10% FBS, 1% penicillin/streptomycin and maintained at 37°C with 5% CO_2. HeLaM cells transfection was performed with Effectene (Qiagen) as described by the manufacturer. NIH3T3 fibroblasts were transfected with adenovirus and then cells were serum starved for 2 days. Just before fixation, cells were treated with Nocodazole (5μM) for 1h for better nuclear envelope staining visualization. Then, cells were washed in PBS, and fixed in -20°C methanol for 10 min. Permeabilization was done with PBS-TritonX-100 (0.1% for 5min), and stained in PBS-Tween (0.05%) supplemented with donkey serum.

Western Blot and Co-Immunoprecipitation

For co-immunoprecipitation experiments in HeLaM cells, these were lysed on ice with RIPA buffer (pH=7.4, 50mM Tris-HCL, 125mM NaCl, 1mM EGTA, 0.5% NP-40) containing 1mM DTT and a protease inhibitor cocktail (Sigma, P8340). GST or GST-BicD2 CT were incubated with Glutathione magnetic beads (Thermo Scientific, 78601) for 30min at 4°C to allow binding of the protein to beads. Subsequently, pre-protein bound beads were incubated with the lysate expressing the desired constructs for 3 hrs at 4°C. For the pull-down with brain samples, rat brains were homogenized on ice using brain buffer (pH=7.4, HEPES 50mM, PIPES 50mM, MgCl 2mM, EDTA 1mM, NP-40 0.5%) containing 1mM DTT and a protease inhibitor cocktail (Sigma, P8340). Lysis proceeded for 30 min on ice, and then lysates were clarified removing the debris by centrifugation. Brain lysates were mixed with purified GST or GST-N2G proteins and incubated for 1 hr, at 4°C. After that, washed Glutathione magnetic beads were added and incubated for 2h, at 4°C. For

recombinant protein interaction studies, purified proteins were incubated for 1 hr, at 4°C, in a buffer solution (pH=7.5, 50mM Tris-HCL, 100mM NaCl, 1 mM DTT). Washed Glutathione magnetic Beads were added and incubated for 2h, at 4°C. Beads were pelleted, unbound proteins were collected, and beads were washed 4 times with brain buffer before elution. Eluate was obtained boiling the beads with Laemmli sample buffer.

Purified lysates were loaded on a polyacrylamide gel and transferred to a polyvinylidene difluoride membrane. The membrane was blocked in PBS with 5% milk, incubated with primary antibodies diluted in either PBS with 0.5% Tween or PBS with 1% milk, washed and incubated with secondary LI-COR antibodies in PBS. Imaging of the blots was carried out using an Odyssey system (LI-COR).

Antibodies

Antibodies used for immunofluorescence in brain slices include anti-Nesprin-2 (1:1000, gift from Dr. Gundersen, (Luxton *et al.*, 2010)), anti-HA (Sigma-Aldrich, H6908, 1:2000) and donkey fluorophore-conjugated secondary antibodies (Jackson Labs, 1:500).

Antibodies used for immunofluorescence in cells include anti-dynein intermediate chain clone 74.1 (University of Virginia, 1:250), anti-BicD1 (1:250, Abcam, ab170878), anti-BicD2 (1:250, Abcam, ab117818), anti-Nde1/L (1:250, (Stehman *et al.*, 2007)), anti-cyclin B1 (1:100, BD Biosciences, 554177), chicken polyclonal against GFP (1:150, Millipore, 16901), and Donkey fluorophore-conjugated secondary antibodies (Jackson Labs, 1:250 dilution).

Antibodies used for western blotting include anti GST (1:3000 Santa Cruz, sc-53909), anti GFP (1:3000 Invitrogen, A11122), anti-BicD2 (1:2000, Abcam, ab117818), anti BicD2 CT (1:2000, GeneTex, GTX120683). To develop in a LI-COR system, fluorescent secondary antibodies (1:10,000) were acquired from Invitrogen and Rockland.

Imaging and statistical analysis. The majority of the images were collected with an IX80 laser scanning confocal microscope (Olympus FV100 Spectral Confocal System). Brain sections were imaged using a 60x 1.42 N.A. oil objective or a 10x 0.40 N.A. air objective. Fixed cell images for the Figure 3 and Sup. Fig. 2 were collected using an IX83 Andor Revolution XD Spinning Disk Confocal System with a 1.49 N.A. 100x oil objective and a 2x magnifier coupled to an iXon Ultra 888 EMCCD Camera. All images were analyzed using ImageJ software (NIH, Bethesda, MD, USA).

Somal distribution control data was used in Fig. 1D and Fig. 5B. Somal distribution N2G SR data was used in Fig. 1D and Supp. Fig. 4C. N-C distance control data was used in Fig. 2B, Fig. 4D and Supp. Fig. 5B. N-C distance N2G SR data was used in Fig. 2B and Supp. Fig.4B.

All statistical analysis was performed using Prism (GraphPad Software, La Jolla, CA, USA). Values from the populations under analysis were subjected to the D'Agostino-Pearson omnibus normality test, to determine whether they followed a normal distribution. If the values respected a Gaussian distribution, the Two-tailed parametric unpaired T-test with Welch's correction was used. But, when the normality test failed, the non-parametric Mann-Whitney test was used. Significance was accepted at the level of $P < 0.05$.

ACKNOWLEDGEMENTS

We thank the members of the Vallee laboratory for technical expertise and productive discussions. We thank Dr. Aditi Falnikar and Paige Helmer for critical reading of the manuscript. We thank Dr. Tiago Dantas for the PACT-DsRed construct. We thank Dr. Gregg Gundersen for the very useful Nesprin-2 reagents and the extensive critical input. We thank Dr. Ruijun Zhu for the NIH3T3 cells infected with Nesprin constructs and helpful technical expertise. We thank Dr. Tiago Gil Oliveira for the critical input.

Funding

This project was supported by National Institutes of Health grants HD40182 and GM105536 to R.B. Vallee and the Fundação para Ciência e a Tecnologia MDPhD Scholarship PD/ BD/113766/2015 to J.C. Gonçalves. This work was also supported by the Columbia University Medical Center MDPhD program.

Competing interests

The authors declare no competing financial interests.

REFERENCES

Baffet, A. D. *et al.* (2016) 'Cellular and subcellular imaging of motor protein-based behavior in embryonic rat brain', *Methods in Cell Biology*, 131, pp. 349–363. doi: 10.1016/bs.mcb.2015.06.013.

Baffet, A. D., Hu, D. J. and Vallee, R. B. (2015) 'Cdk1 Activates Pre-mitotic Nuclear Envelope Dynein Recruitment and Apical Nuclear Migration in Neural Stem Cells', *Developmental Cell*. Elsevier Inc., 33(6), pp. 703–716. doi: 10.1016/j.devcel.2015.04.022.

Baudoin, J. P. *et al.* (2012) 'Tangentially Migrating Neurons Assemble a Primary Cilium that Promotes Their Reorientation to the Cortical Plate', *Neuron*, 76(6), pp. 1108–1122. doi: 10.1016/j.neuron.2012.10.027.

Bellion, A. *et al.* (2005) 'Nucleokinesis in tangentially migrating neurons comprises two alternating phases: forward migration of the Golgi/centrosome associated with centrosome splitting and myosin contraction at the rear.', *The Journal of neuroscience : the official journal of the Society for Neuroscience*, 25(24), pp. 5691–9. doi: 10.1523/JNEUROSCI.1030-05.2005.

Bertipaglia, C., Gonçalves, J. C. and Vallee, R. B. (2018) 'Nuclear migration in mammalian brain development', *Seminars in Cell & Developmental Biology*, 82, pp. 57–66. doi: 10.1016/j.semcdb.2017.11.033.

Bone, C. R. and Starr, D. A. (2016) 'Nuclear migration events throughout development', *Journal of Cell Science*, 129(10), pp. 1951–1961. doi: 10.1242/jcs.179788.

Carabalona, A., Hu, D. J.-K. and Vallee, R. B. (2016) 'KIF1A inhibition immortalizes brain stem cells but blocks BDNF-mediated neuronal migration', *Nature Neuroscience*, 19(2). doi: 10.1038/nn.4213.

Chang, W., Worman, H. J. and Gundersen, G. G. (2015) 'Accessorizing and anchoring the LINC complex for multifunctionality', *Journal of Cell Biology*, 208(1), pp. 11–22. doi: 10.1083/jcb.201409047.

Cooper, J. A. (2013) 'Mechanisms of cell migration in the nervous system', *The Journal of Cell Biology*, 202(5), pp. 725–734. doi: 10.1083/jcb.201305021.

Falnikar, A., Tole, S. and Baas, P. W. (2011) 'Kinesin-5, a mitotic microtubule-associated motor protein, modulates neuronal migration', *Molecular Biology of the Cell*, 22(9), pp. 1561–1574. doi: 10.1091/mbc.e10-11-0905.

Fridolfsson, H. N. and Starr, D. A. (2010) 'Kinesin-1 and dynein at the nuclear envelope mediate the bidirectional migrations of nuclei', *Journal of Cell Biology*, 191(1), pp. 115–128. doi: 10.1083/jcb.201004118.

Gillingham, A. K. and Munro, S. (2000) 'The PACT domain, a conserved centrosomal targeting motif in the coiled-coil proteins AKAP450 and pericentrin.', *EMBO reports*, 1(6), pp. 524–9. doi: 10.1093/embo-reports/kvd105.

Gomes, E. R., Jani, S. and Gundersen, G. G. (2005) 'Nuclear movement regulated by Cdc42, MRCK, myosin, and actin flow establishes MTOC polarization in migrating cells', *Cell*, 121(3), pp. 451–463. doi: 10.1016/j.cell.2005.02.022.

Gonçalves, J. C., Dantas, T. J. and Vallee, R. B. (2019) 'Distinct roles for dynein light intermediate chains in neurogenesis, migration, and terminal somal translocation.', *The Journal of cell biology*, 218(3), pp. 808–819. doi: 10.1083/jcb.201806112.

Grigoriev, I. *et al.* (2007) 'Rab6 Regulates Transport and Targeting of Exocytotic Carriers', *Developmental Cell*, 13(2), pp. 305–314. doi: 10.1016/j.devcel.2007.06.010.

Guerrier, S. *et al.* (2009) 'The F-BAR Domain of srGAP2 Induces Membrane Protrusions Required for Neuronal Migration and Morphogenesis', *Cell*, 138(5), pp. 990–1004. doi: 10.1016/j.cell.2009.06.047.

He, M. *et al.* (2010) 'Leading Tip Drives Soma Translocation via Forward F-Actin Flow during Neuronal Migration', *Journal of Neuroscience*, 30(32), pp. 10885–10898. doi: 10.1523/JNEUROSCI.0240-10.2010.

Hu, D. J.-K. *et al.* (2013) 'Dynein Recruitment to Nuclear Pores Activates Apical Nuclear Migration and Mitotic Entry in Brain Progenitor Cells', *Cell*, 154(6), pp. 1300–1313. doi: 10.1016/j.cell.2013.08.024.

Jaarsma, D. *et al.* (2014) 'A role for Bicaudal-D2 in radial cerebellar granule cell migration.', *Nature communications*. Nature Publishing Group, 5, p. 3411. doi: 10.1038/ncomms4411.

Jamuar, S. S. *et al.* (2014) 'Somatic Mutations in Cerebral Cortical Malformations', *New England Journal of Medicine*, 371(8), pp. 733–743. doi: 10.1056/NEJMoa1314432.

Jiang, J. *et al.* (2015) 'Spatiotemporal dynamics of traction forces show three contraction centers in migratory neurons', *Journal of Cell Biology*, 209(5), pp. 759–774. doi: 10.1083/jcb.201410068.

Konno, D. *et al.* (2008) 'Neuroepithelial progenitors undergo LGN-dependent planar divisions to maintain self-renewability during mammalian neurogenesis', *Nature Cell Biology*, 10(1), pp. 93–101. doi: 10.1038/ncb1673.

Luxton, G. W. G. *et al.* (2010) 'Linear arrays of nuclear envelope proteins harness retrograde actin flow for nuclear movement.', *Science (New York, N.Y.)*, 329(5994), pp. 956–9. doi: 10.1126/science.1189072.

Martini, F. J. and Valdeolmillos, M. (2010) 'Actomyosin Contraction at the Cell Rear Drives Nuclear Translocation in Migrating Cortical Interneurons', *Journal of Neuroscience*, 30(25), pp. 8660–8670. doi: 10.1523/JNEUROSCI.1962-10.2010.

Matanis, T. *et al.* (2002) 'Bicaudal-D regulates COPI-independent Golgi-ER transport by recruiting the dynein-dynactin motor complex', *Nature Cell Biology*, 4(12), pp. 986–992. doi: 10.1038/ncb891.

Matsuda, T. and Cepko, C. L. (2004) 'Electroporation and RNA interference in the rodent retina in vivo and in vitro', *Proceedings of the National Academy of Sciences*, 101(1), pp. 16–22. doi: 10.1073/pnas.2235688100.

Matsuda, T. and Cepko, C. L. (2007) 'Controlled expression of transgenes introduced by *in vivo* electroporation', *Proceedings of the National Academy of Sciences*, 104(3), pp. 1027–1032. doi: 10.1073/pnas.0610155104.

Metzger, T. *et al.* (2012) 'MAP and kinesin-dependent nuclear positioning is required for skeletal muscle function', *Nature*, 484(7392), pp. 120–124. doi: 10.1038/nature10914.

Noctor, S. C. *et al.* (2004) 'Cortical neurons arise in symmetric and asymmetric division zones and migrate through specific phases.', *Nature neuroscience*, 7(2), pp. 136–144. doi: 10.1038/nn1172.

Noell, C. R. *et al.* (2018) 'A Quantitative Model for BicD2/Cargo Interactions.', *Biochemistry*, 57(46), pp. 6538–6550. doi: 10.1021/acs.biochem.8b00987.

Poirier, K. *et al.* (2013) 'Mutations in TUBG1, DYNC1H1, KIF5C and KIF2A cause malformations of cortical development and microcephaly.', *Nature genetics*, 45(6), pp. 639–47. doi: 10.1038/ng.2613.

Rao, A. N. *et al.* (2016) 'Sliding of centrosome-unattached microtubules defines key features of neuronal phenotype', *Journal of Cell Biology*, 213(3), pp. 329–341. doi: 10.1083/jcb.201506140.

Reiner, O. *et al.* (1993) 'Isolation of a Miller-Dieker lissencephaly gene containing G protein beta-subunit-like repeats.', *Nature*. Nature Publishing Group, 364(6439), pp. 717–721. doi: 10.1038/364717a0.

Roux, K. J. *et al.* (2009) 'Nesprin 4 is an outer nuclear membrane protein that can induce kinesin-mediated cell polarization', *Proceedings of the National Academy of Sciences*, 106(7), pp. 2194–2199. doi: 10.1073/pnas.0808602106.

Schaar, B. T. and McConnell, S. K. (2005) 'Cytoskeletal coordination during neuronal migration', *Proceedings of the National Academy of Sciences*, 102(38), pp. 13652–13657. doi: 10.1073/pnas.0506008102.

Schneider, M. *et al.* (2011) 'Molecular mechanisms of centrosome and cytoskeleton anchorage at the nuclear envelope', *Cellular and Molecular Life Sciences*, 68(9), pp. 1593–1610. doi: 10.1007/s00018-010-0535-z.

Shu, T. *et al.* (2004) 'Ndel1 operates in a common pathway with LIS1 and cytoplasmic dynein to regulate cortical neuronal positioning', *Neuron*. Cell Press, 44(2), pp. 263–277. doi: 10.1016/j.neuron.2004.09.030.

Shubeita, G. T. *et al.* (2008) 'Consequences of Motor Copy Number on the Intracellular Transport of Kinesin-1-Driven Lipid Droplets', *Cell*. Elsevier Ltd, 135(6), pp. 1098–1107. doi: 10.1016/j.cell.2008.10.021.

Solecki, D. J. *et al.* (2009) 'Myosin II Motors and F-Actin Dynamics Drive the Coordinated Movement of the Centrosome and Soma during CNS Glial-Guided Neuronal Migration', *Neuron*, 63(1), pp. 63–80. doi: 10.1016/j.neuron.2009.05.028.

Splinter, D. *et al.* (2010) 'Bicaudal D2, dynein, and kinesin-1 associate with nuclear pore complexes and regulate centrosome and nuclear positioning during mitotic entry', *PLoS Biology*, 8(4). doi: 10.1371/journal.pbio.1000350.

Stehman, S. a. *et al.* (2007) 'NudE and NudEL are required for mitotic progression and are involved in dynein recruitment to kinetochores', *Journal of Cell Biology*, 178(4), pp. 583–594. doi: 10.1083/jcb.200610112.

Tanaka, T. *et al.* (2004) 'Lis1 and doublecortin function with dynein to mediate coupling of the nucleus to the centrosome in neuronal migration', *Journal of Cell Biology*, 165(5), pp. 709–721. doi: 10.1083/jcb.200309025.

Trivedi, N. *et al.* (2017) 'Drebrin-mediated microtubule-actomyosin coupling steers cerebellar granule neuron nucleokinesis and migration pathway selection.', *Nature communications*. Nature Publishing Group, 8, p.

14484. doi: 10.1038/ncomms14484.

Tsai, J.-W., Bremner, K. H. and Vallee, R. B. (2007) 'Dual subcellular roles for LIS1 and dynein in radial neuronal migration in live brain tissue.', *Nature neuroscience*, 10(8), pp. 970–979. doi: 10.1038/nn1934.

Tsai, J. W. *et al.* (2005) 'LIS1 RNA interference blocks neural stem cell division, morphogenesis, and motility at multiple stages', *Journal of Cell Biology*, 170(6), pp. 935–945. doi: 10.1083/jcb.200505166.

Umeshima, H., Hirano, T. and Kengaku, M. (2007) 'Microtubule-based nuclear movement occurs independently of centrosome positioning in migrating neurons', *Proceedings of the National Academy of Sciences*, 104(41), pp. 16182–16187. doi: 10.1073/pnas.0708047104.

Wilson, M. H. and Holzbaur, E. L. F. (2012) 'Opposing microtubule motors drive robust nuclear dynamics in developing muscle cells', *Journal of Cell Science*, 125(17), pp. 4158–4169. doi: 10.1242/jcs.108688.

Wilson, M. H. and Holzbaur, E. L. F. (2015) 'Nesprins anchor kinesin-1 motors to the nucleus to drive nuclear distribution in muscle cells', *Development*, 142(1), pp. 218–228. doi: 10.1242/dev.114769.

Wu, Y. K. *et al.* (2018) 'Nesprins and opposing microtubule motors generate a point force that drives directional nuclear motion in migrating neurons.', *Development (Cambridge, England)*, 145(5), p. dev158782. doi: 10.1242/dev.158782.

Zhang, X. *et al.* (2009) 'SUN1/2 and Syne/Nesprin-1/2 Complexes Connect Centrosome to the Nucleus during Neurogenesis and Neuronal Migration in Mice', *Neuron*. Elsevier Ltd, 64(2), pp. 173–187. doi: 10.1016/j.neuron.2009.08.018.

Zhu, R., Antoku, S. and Gundersen, G. G. (2017) 'Centrifugal Displacement of Nuclei Reveals Multiple LINC Complex Mechanisms for Homeostatic Nuclear Positioning', *Current Biology*. Elsevier Ltd., pp. 1–14. doi: 10.1016/j.cub.2017.08.073.

CHAPTER 2.2 – Supplemental material

Nesprin-2 recruits dynein via its adaptor BicD2 for nuclear transport during neuronal migration.

João Carlos Gonçalves, Sebastian Quintremil, Julie Yi, Richard B. Vallee

(Manuscript to be submitted)

Supplemental Figure 1

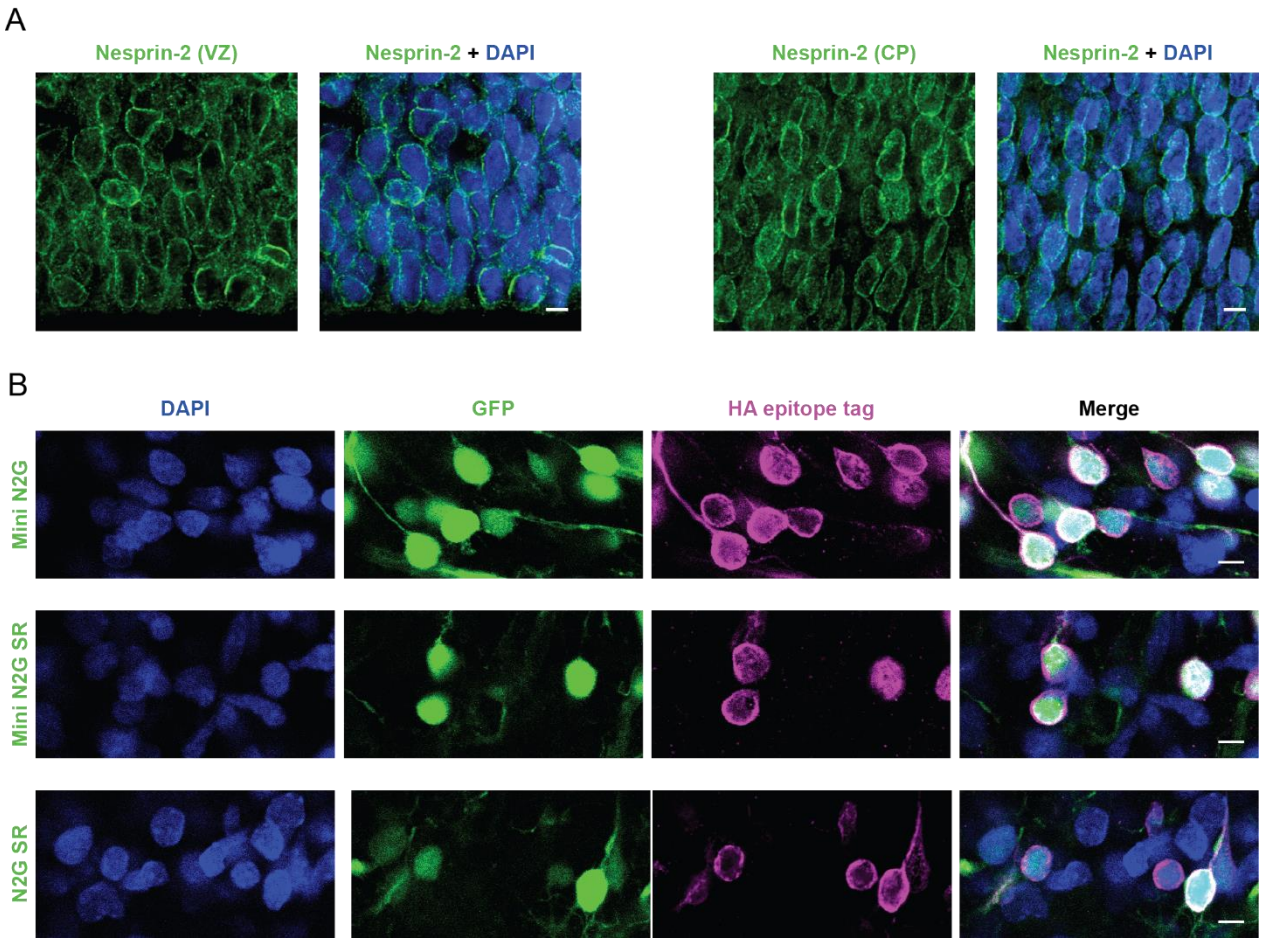

Supplemental Figure 1

Distribution of endogenous Nesprin-2 and localization of electroporated Nesprin-2 functional domains. (A) Embryonic day 20 (E20) rat brain slices were stained with DAPI and for endogenous Nesprin-2, and representative images from the Ventricular Zone (VZ) and Cortical Plate (CP) are depicted. **(B)** E16 rat brain was *in utero* electroporated with the Nesprin-2 constructs, and subsequently imaged, at E20. Electroporated brains were stained with DAPI and for HA epitope tag and fixed images from the Intermediate Zone (IZ) are shown. **A** and **B** scale bars, 5μm.

Supplemental Figure 2

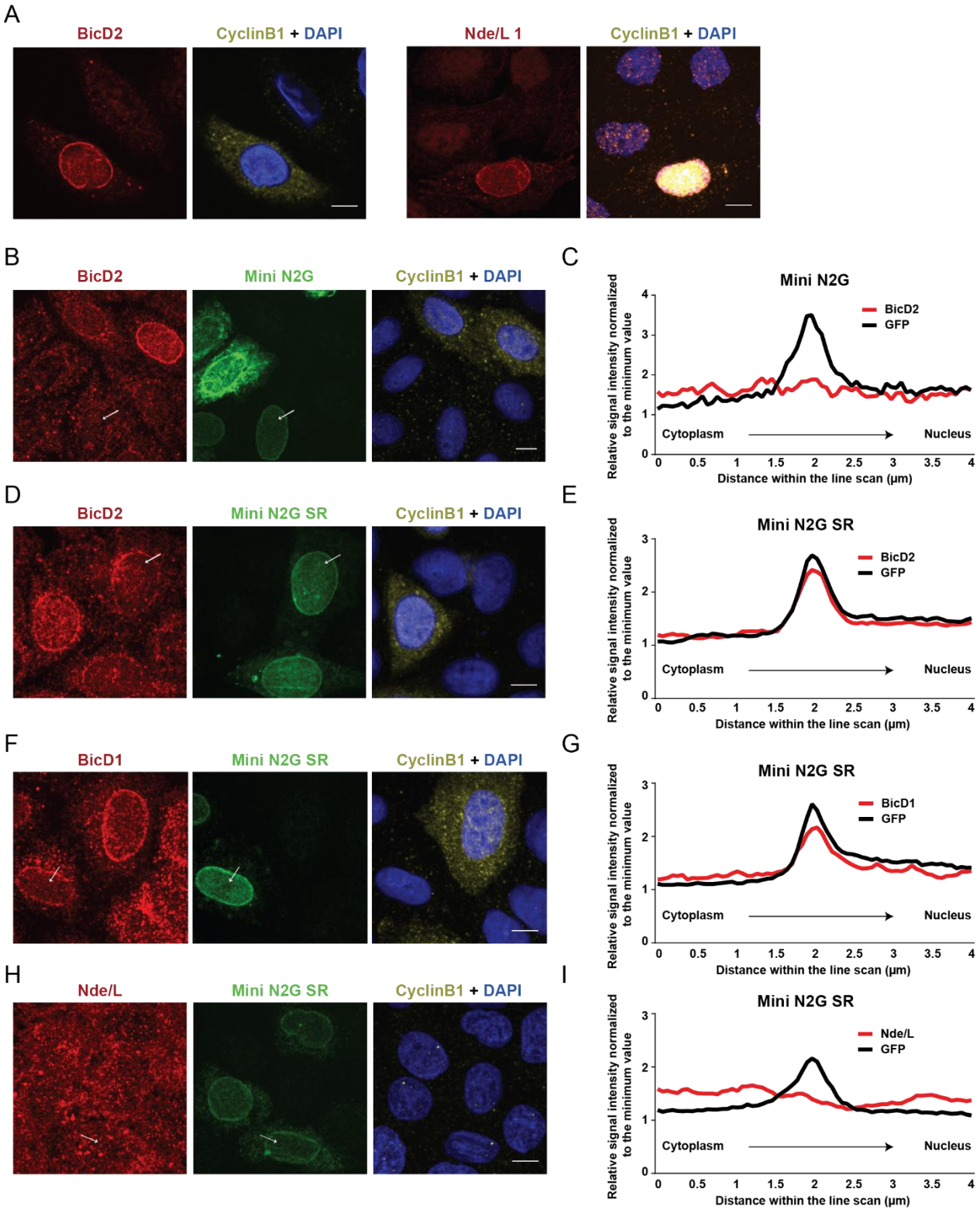

Supplemental Figure 2

BicD1, BicD2 and Ndel/L co-localization with Nesprin-2. (A) Representative images of fixed cultured HeLaM cells stained with DAPI for endogenous BicD2, Nde/L and Cyclin B1. **(B-E)** Cultured HeLaM cells transfected with GFP-Mini N2G and GFP-Mini N2G SR were stained with DAPI and for endogenous BicD2 and Cyclin B1. Arrows indicate the line scan position that was done for quantifications purposes. **(B, D)** Representative fixed images and **(C, E)** line scan quantifications are shown. **(F-I)** Cultured HeLaM cells transfected with GFP-Mini N2G SR were stained with DAPI and for endogenous BicD1, Nde/L and Cyclin B1. Arrows indicate the line scan position that was done for quantifications purposes. **(F, H)** Representative fixed images and **(G, I)** line scan quantifications are shown. Data presented as superimposed symbols at mean with a connecting line in **C, E, G** and **I**. Data in **C, E, G** and **I** includes line scan analysis from at least 7 cells. **A, B, D, F** and **H** scale bar, 10μm.

Supplemental Figure 3

A

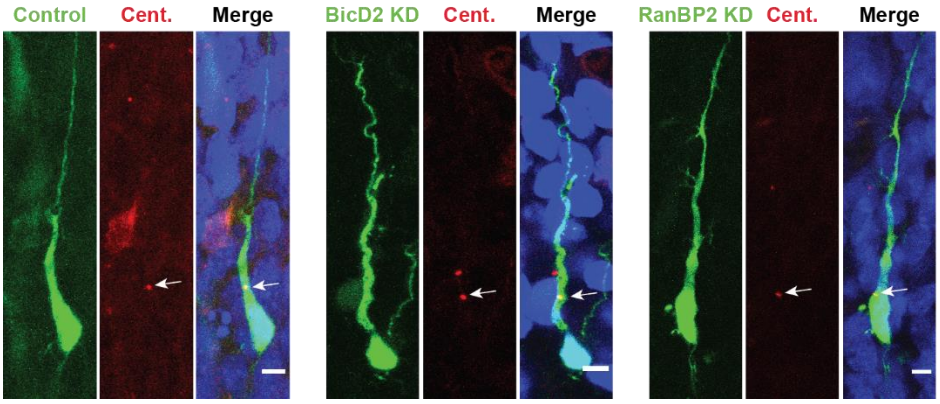

B

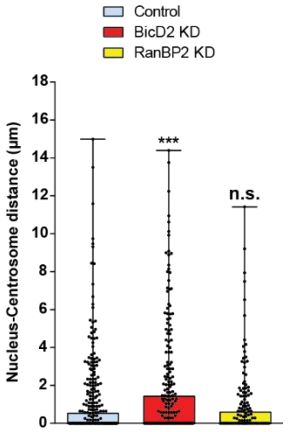

Supplemental Figure 3

Effects of BicD2 or RanBP2 shRNAs in Nucleus-Centrosome coupling. (A-B) E16 rat brain was *in utero* electroporated with control vector, BicD2 or RanBP2 shRNAs together with PACT-DsRed, and subsequently imaged fixed by E20. **(A)** Fixed images of electroporated neurons in the CP showing the centrosome (Cent.) position (arrows) relative to the soma. **(B)** Quantification of the N-C distance across conditions. Data presented as scatter dot plot with bar representing median with range in **B**. Mann Whitney test for non-parametric distributions was used in **B** (***P<0.001; n.s. non significant). Data in **B** includes at least 100 electroporated neurons from at least 2 embryos, per condition. **A** scale bar, 5μm.

Supplemental Figure 4

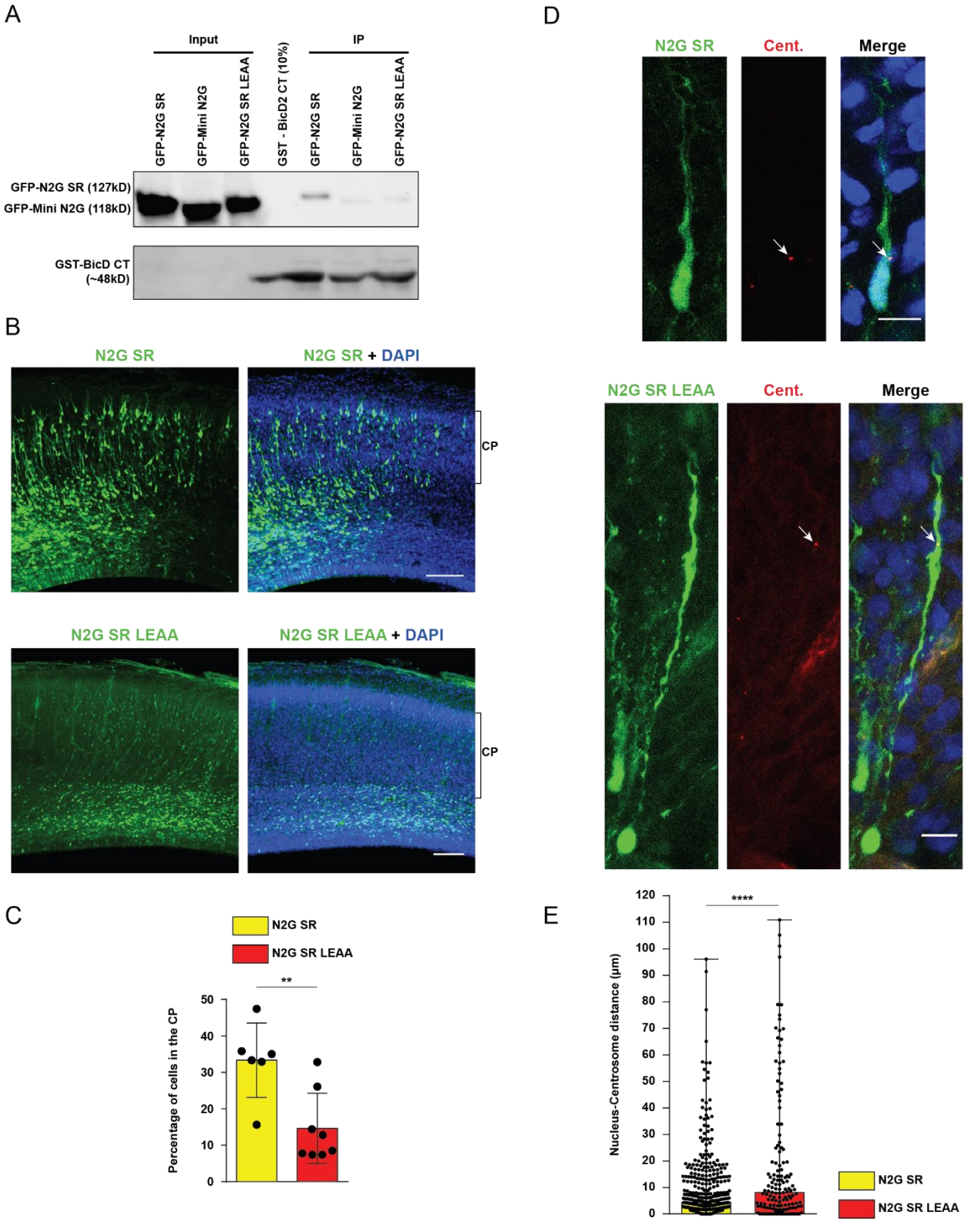

Supplemental Figure 4

Effect of LEAA mutation in Nesprin-2 interaction with BicD2. (A) GST-BicD2 CT pull downs from HeLaM cell lysates expressing GFP-N2G SR, GFP-Mini N2G or GFP-N2G SR LEAA were evaluated for GFP co-immunoprecipitation. **(B-C)** E16 rat brain was *in utero* electroporated with N2G SR or N2G SR LEAA, and subsequently imaged by E20. **(B)** Fixed images of the neocortex with electroporated cells in green and stained with DAPI. Brackets show CP margins. **(C)** Quantification of the proportion of cells reaching the CP. **(D-E)** E16 rat brain was *in utero* electroporated with N2G SR or N2G SR LEAA together with PACT-DsRed, and subsequently imaged by E20. **(D)** Fixed images of electroporated neurons in the CP showing the centrosome (Cent.) position (arrows) relative to the soma. **(E)** Quantification of the N-C distance. Data presented as scatter dot plot with bar representing mean±s.d. in **C**, and as scatter dot plot with bar representing median with range in **E**. Mann Whitney test for non-parametric distributions was used in **C** and **E** (**P<0.01; ****P<0.0001). Data in **C** includes at least 1666 electroporated cells from at least 6 embryos, per condition. Data in **E** includes at least 239 electroporated cells from at least 4 embryos, per condition. **B** scale bar, 100µm. **D** scale bar, 10µm.

Supplemental Figure 5

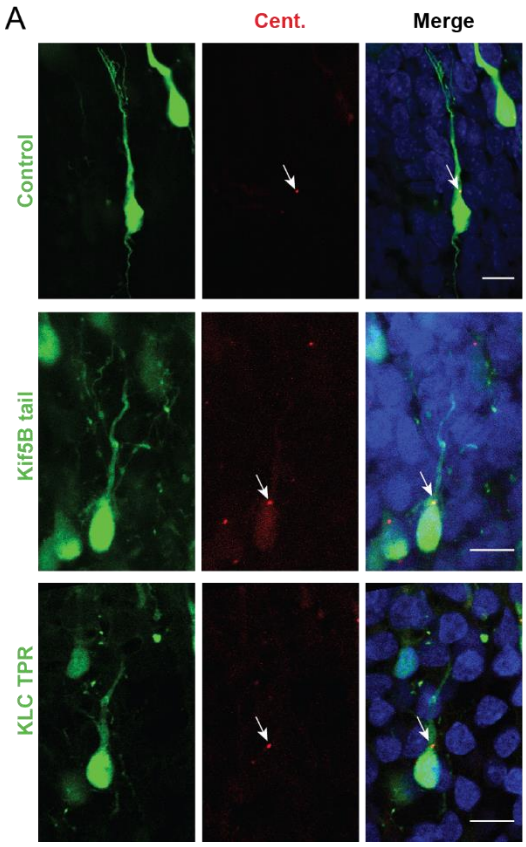

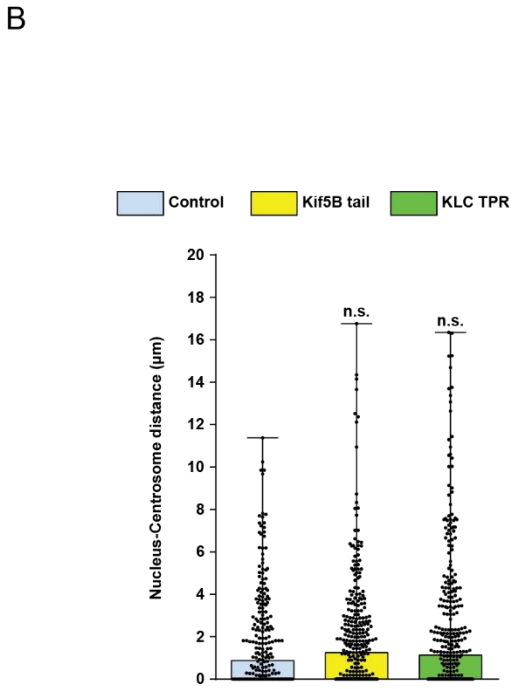

Supplemental Figure 5

Overexpression effects of the Kif5 tail or KLC TPR domains in nucleus-centrosome coupling. (A, B) E16 rat brain was *in utero* electroporated with control, Kif5 tail or KLC TPR, together with PACT-DsRed and subsequently imaged by E20. **(A)** Fixed images of electroporated neurons in the CP showing the centrosome (Cent.) position (arrows) relative to the soma. **(B)** Quantification of the N-C distance. Data presented as scatter dot plot with bar representing median with range in **B**. Mann Whitney test for non-parametric distributions was used in **B** (n.s. non-significant). Data in **B** includes at least 317 electroporated cells from at least 3 embryos, per condition. **B** scale bar, 10μm.

Supplementary Movie 1

Live imaging example of E20 embryonic rat brain electroporated with GFP control vector together with PACT-DsRed at E16. Transfected neurons were continuously imaged in the CP for 9hr50min at 10 min intervals. The arrow indicates the centrosome. Scale bar 10μm.

Supplementary Movie 2

Live imaging example of E20 embryonic rat brain electroporated with N2G SR expressing vector together with PACT-DsRed at E16. Transfected neurons were continuously imaged in the CP for 18hr at 10 min intervals. The arrow indicates the centrosome. Scale bar 10μm.

Supplementary Movie 3

Live imaging example of E20 embryonic rat brain electroporated with Mini N2G expressing vector together with PACT-DsRed at E16. Transfected neurons were continuously imaged in the CP for 12hr40min at 10 min intervals. The arrow and the arrowhead indicate the centrosome and the cell body, respectively. Scale bar 10μm.

Supplementary Movie 4

Live imaging example of E20 embryonic rat brain electroporated with BicD2 CT expressing vector together with PACT-DsRed at E16. Transfected neurons were continuously imaged in the CP for 15hr50min at 10 min intervals. The arrow and the arrowhead indicate the centrosome and the cell body, respectively. Scale bar 10μm.

Supplementary Movie 5

Live imaging example of E20 embryonic rat brain electroporated with GFP expressing vector at E16. Transfected neurons were continuously imaged in the CP for 13hr50min at 10 min intervals. Scale bar 10μm.

Supplementary Movie 6

Live imaging example of E20 embryonic rat brain electroporated with KLC TPR expressing vector at E16. Transfected neurons were continuously imaged in the CP for 12hr40min at 10 min intervals. Scale bar 10μm.

CHAPTER 3 - CONCLUSIONS, DISCUSSION AND FUTURE PERSPECTIVES

The experimental work in this thesis helps to dissect the mechanisms of dynein recruitment during neurogenesis and neuronal migration. In chapter 2.1, we found that LIC1- and LIC2-dynein subfractions have different functions during neocortical development. Although LIC1 and LIC2 are each essential for neurogenesis and migration, their functions are quite distinct. LIC1 is essential for INM of neural progenitors, and we link this observation to a stronger physical interaction with BicD2. In contrast, LIC2 was responsible for a newly identified dynein role in TST. Additionally, we found that expression of the LIC dynein-binding G-domains differentially interferes with neuronal migration, which suggests that the LICs may have somewhat distinct effects on dynein motor behavior.

We performed a more detailed analysis into the mechanisms governing dynein recruitment and function in post-mitotic migratory neurons. For that, in chapter 2.2, we investigated the role of Nesprin-2 in neuronal migration. Our data determined that Nesprin-2 represents a novel, and important, form of BicD2 and dynein cargo, which we have found to be independent of the cell cycle. In the brain, Nesprin-2 or BicD2 inhibition potently arrested the migration of post-mitotic neurons and disruption of this interaction dramatically interfered with nuclear, but not centrosome advance. This specific inhibitory effect in nuclear transport resulted in striking excursions of the centrosome toward the growing tip of the neuronal leading process, which accounted for the abnormally high distances (over 100μm) from the nucleus to the centrosome. Although Nesprin-2 interacts with components of both microtubule and actin cytoskeleton, our mutational analysis revealed that forces at the nucleus during neuronal migration are predominantly executed by microtubule motors. In contrast with other systems, such as migrating fibroblasts, we found a minor role, if any, for actin forces at the nucleus via Nesprin-2. Finally, although dynein and kinesin-1 have been reported to act cooperatively in nuclear behavior in some systems, we observed, surprisingly, that kinesin-1 inhibition dramatically stimulates neuronal migration. This result suggests a novel type of kinesin role in the migrating neuronal cells.

In the sections below, we discuss these findings further and their implications for the field. We also address the important questions that this thesis work raises for the future.

3.1 Roles of Nesprin-2 in neuronal migration

Nesprin-2 is an essential component in migrating neurons, and by the expression discrete functional domains, we were able to understand its role further. Our results in Chapter 2.2 define Nesprin-2 as the recruitment factor for dynein and the dynein adaptor BicD2 during neuronal migration (Figure 1). Perturbation of this dynein recruitment mechanism caused strong nuclear arrest, while centrosome transport seemed normal. Because of this, the centrosome migrated away from the nucleus. Further, we found that Nesprin-2 and BicD2 interact directly, which defines Nesprin-2 as a new form of BicD2 cargo, important in dynein recruitment to the NE (Figure 2). Finally, we show that dynein and kinesin-1 act during neuronal migration, apparently exerting oppositely-directed forces.

Post-mitotic neurons migrate from the IZ to the CP, and for that they require transport of both the centrosome and the nucleus. We have expressed Nesprin-2 chimeric constructs containing previously characterized functional domains in fibroblasts (Luxton *et al.*, 2010; Zhu, Antoku and Gundersen, 2017). The Calponin Homology domain, which had been shown to interact with actin filaments for rearward nuclear positioning (Luxton *et al.*, 2010); the microtubule-motor binding domain, situated between the spectrin repeats 53 and 54 of the Nesprin molecule, which had been shown to recruit dynein and kinesin-1 (Schneider *et al.*, 2011; Wilson and Holzbaur, 2015; Zhu, Antoku and Gundersen, 2017); and the KASH domain that targeted the chimeric constructs to the NE, competing with the endogenous protein for SUN binding (Luxton *et al.*, 2010). We first tested whether expression of the Mini N2G SR, which contains the calponin homology and the microtubule-motor binding domains, could provide a useful system to mimic and dissect the role of Nesprin-2 in neuronal migration. Neurons expressing Mini N2G SR were able to migrate to the CP in substantial number. Interestingly, removal of the microtubule motor-binding domain by the expression of the Mini N2G construct caused a drastic decrease in the number of cells that could reach the CP. This suggested that the Mini N2G SR construct is sufficient for migration, which was impaired when we further removed its capacity to bind to microtubule motors. More clues came from the expression of N2G SR, which is incapable of binding to actin filaments. Brains expressing this construct had levels of migration comparable to the Mini N2G SR, suggesting that the actin-interacting domain had no apparent function in the migrating neurons. Our findings are in agreement with a role for Nesprin-2 in neuronal migration (Zhang *et al.*, 2009; Hu *et al.*, 2013; Wu *et al.*, 2018), and substantially increase our mechanistic understanding in this behavior.

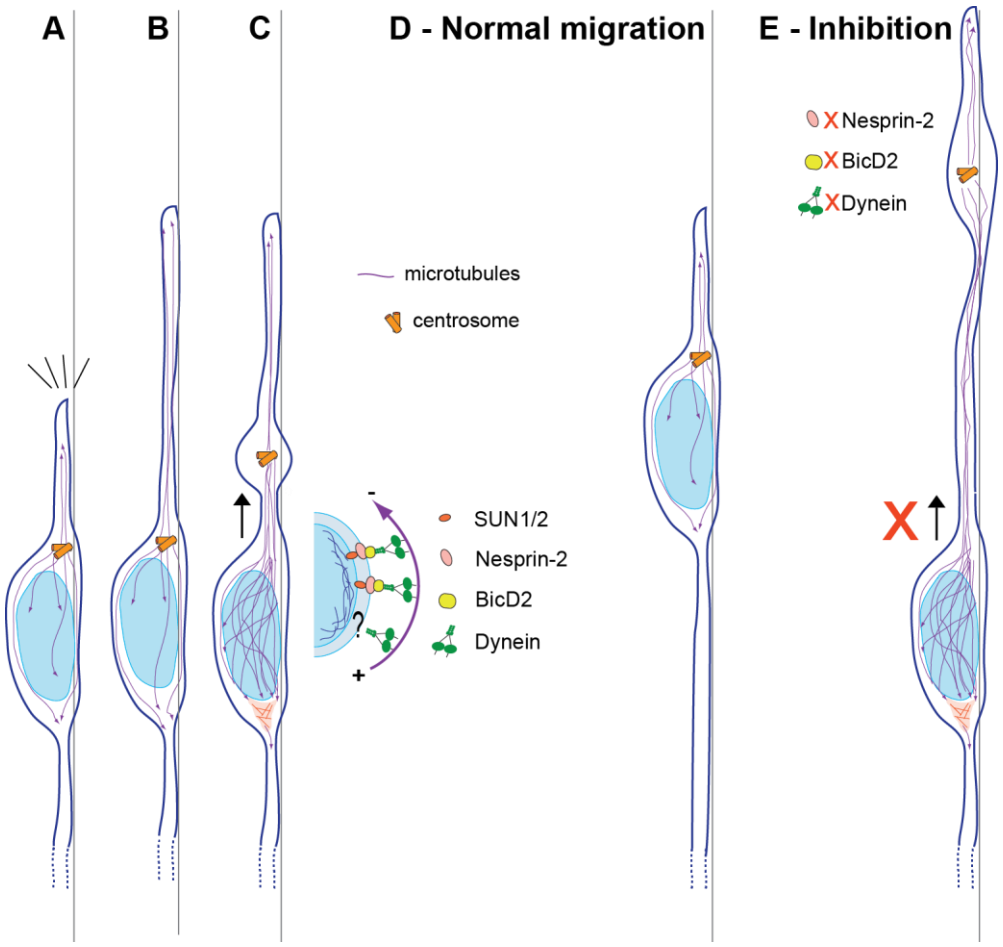

Figure 1: Nesprin-2/BicD2/Dynein mechanism in neuronal migration. Schematic illustration showing the mechanisms of nuclear transport during neuronal migration. (A) Neurons migrate along the radial glial fibers, and the centrosome is the microtubule organizing center at this stage. (B) Migration occurs in a saltatory fashion and neurons, first, extend the leading process toward the direction of migration and (C) the centrosome advances into the leading process. Then, neurons recruit BicD2/dynein via Nesprin-2 to the NE to displace the nucleus, which advances toward the centrosome (D). In this study, we show that Nesprin-2, BicD2 or dynein inhibition arrests nuclear movement (E), but centrosome transport appears intact. Adapted from Bertipaglia et al. 2018.

The cell bodies of neurons expressing the Mini N2G construct were arrested in the IZ, but the long leading processes of these cells reached as far as the CP. The LINC complex is involved in many forms of nuclear transport (Lee and Burke, 2018), and the observed phenotype was very suggestive of an impairment in its

behavior. Because the LINC complex mediates N-C coupling, we decided to analyze centrosomal dynamics across conditions. By fixed and live imaging, we observed that in cells expressing the Mini N2G construct, the centrosome migrated into the leading process, while the nucleus remained arrested. The distances that the centrosome could separate from the nucleus were very high, sometimes above 100µm. Interestingly, the centrosome and the centrosome-associated dilations were unable to progress once they were separated from the nucleus by such large distances. Centrosomes remained dynamic within the leading process, but without net forward advance. This suggests that the centrosomal transport mechanisms are not affected by the disruption of Nesprin-2 function at the NE, whereas nuclear displacement was specifically impaired. These data also support the idea that when the centrosome is separated from the nucleus by very large distances, the transport machinery of the former becomes compromised.

An interesting remaining question is what governs centrosomal displacement during neuronal migration. Centrosomes typically migrate ahead of the nucleus into the dilations formed in the proximal leading process (Bellion *et al.*, 2005; Schaar and McConnell, 2005; Tsai, Bremner and Vallee, 2007). Evidence obtained from migrating neurons *in vitro* has suggested that dynein accumulates in these dilations (Tsai, Bremner and Vallee, 2007). This raises the hypothesis that dynein, presumably anchored at the cell cortex (Dujardin *et al.*, 2003; Grabham *et al.*, 2007), powers centrosome transport through forces generated on the centrosome-anchored microtubules. In support of a role for dynein in centrosome transport, DHC or LIS1 KD were shown to hinder both nuclear and centrosomal displacement (Tsai, Bremner and Vallee, 2007)., One of the challenges in dissecting the mechanisms of nuclear *vs* centrosome transport was the lack of understanding of each individually. This was because KD of genes involved in nuclear movement ultimately affect that of the centrosome as well (Shu *et al.*, 2004; Tsai, Bremner and Vallee, 2007; Doobin *et al.*, 2016). More experiments are needed to determine the cellular apparatus for centrosome transport. Because inhibiting Nesprin function directly at the NE completely uncouples the nucleus from the centrosome, this may be an appropriate tool to study these behaviors separately.

Although it had previously been suggested that Nesprin-2 might recruit dynein during neuronal migration (Zhang et al., 2009), direct evidence in vivo was lacking. Our results show that nuclear movement in migratory neurons involves the microtubule motor-binding domain of Nesprin-2 acting from the NE. Importantly, our data more firmly establish cytoplasmic dynein in particular as a major contributor to neuronal migration in developing brain (Bertipaglia, Gonçalves and Vallee, 2018). We have now also tested how Nesprin-2-mediated

kinesin-1 recruitment to the NE might contribute to this process. We found, remarkably, that kinesin-1 inhibition increases the number of cells that reach the CP, and this is likely explained by faster migration. The insights on the role of kinesin-1 in neuronal migration are scarce. One recent study found that inhibition of kinesin-1, by expressing its tail domain disrupts cerebellar granular cell migration in vivo (Wu et al., 2018). The basis for the disparity between those results and ours is uncertain. Nuclear movement in the cerebellar neurons has been reported to be independent from that of the centrosome (Umeshima, Hirano and Kengaku, 2007), in contrast with migration in the neocortex in which nuclear movement substantially depends on centrosome advance (Tsai, Bremner and Vallee, 2007). Importantly, another study focusing on kinesin-5 found that its inhibition resulted in an increase in cells reaching the CP and in migration velocity (Falnikar, Tole and Baas, 2011; Rao et al., 2016). The basis for the differential kinesin isoform-specific behavior remains unknown.

How kinesin-1 controls nuclear behavior has been studied in myoblasts (Metzger *et al.*, 2012; Wilson and Holzbaur, 2012, 2015). Two models exist to explain kinesin-1 dependent nuclear positioning, one that results from the sliding of antiparallel microtubules by this motor (Metzger *et al.*, 2012) and another that depends on a Nesprin-2-dependent recruitment of kinesins to the nuclear envelope (Wilson and Holzbaur, 2012, 2015). Our results indicate that kinesin-1 opposes dynein forces during nuclear transport, presumably both acting from the NE. In line with a role for kinesin-1 at the NE counter-balancing dynein forces for nuclear position, expression of Nesprin-4, which recruits kinesin-1 to the NE, induces movement of the nuclei away from the centrosome (Roux *et al.*, 2009). Further, in G2 cells, dynein disruption by injection of a functional inhibitory antibody causes nucleus separation from the centrosome (Splinter *et al.*, 2010). Overall this evidence supports a model in which kinesin-1 inhibition could release dynein, thus favoring nuclear minus-end net displacement (Shubeita *et al.*, 2008).

Analysis of neuronal migration in isolated neuronal precursors suggested that the actin cytoskeleton is also important in neuronal migration (Bellion *et al.*, 2005; Schaar and McConnell, 2005). Actin was reported to exert forces at 3 discrete sites using traction force microscopy experiments (Jiang *et al.*, 2015; Umeshima *et al.*, 2019). These are the growing tip of the leading process, the proximal region of the leading process and the rear of the nucleus. Actin forces from the leading process tip seem to contribute to its extension, but not nuclear or centrosome transport (Jiang *et al.*, 2015; Umeshima *et al.*, 2019). There is also substantial evidence indicating that actomyosin, both at the front and at the rear of the nucleus, is important for nuclear

(Bellion *et al.*, 2005; Schaar and McConnell, 2005; Tsai, Bremner and Vallee, 2007; Solecki *et al.*, 2009; Jiang *et al.*, 2015; Trivedi *et al.*, 2017) and centrosome transport (Solecki *et al.*, 2009; Trivedi *et al.*, 2017). In fibroblasts, Nesprin-2 anchors the actin cables, flowing retrogradely, to move the nucleus rearward. Two actin contact sites within Nesprin-2 have been found, specifically the calponin homology domain and a second one involving the Formin FODH1, which binds the Spectrin Repeats 9-13 of Nesprin-2. Therefore molecular manipulation of the Nesprin-2 molecule has emerged as an appealing means to test how actin filaments participate in nuclear transport during neuronal migration. In our studies we have tested the role of the calponin homology domain in migrating neurons, which in fibroblasts was necessary and sufficient to move nuclei rearward. We found that this domain alone does not participate in nuclear displacement in post-mitotic migrating neurons. These results indicate that actin forces during neuronal migration are not transferred to the nucleus for its transport using Nesprin-2. We note that in post-mitotic neurons the nucleus is transported forward, toward the centrosome. In fibroblasts, these actin cable structures participate in rearward displacement of nuclei, away from the centrosome. A possible model is that actin "pulls" the nucleus and the centrosome from the proximal leading process (Solecki *et al.*, 2009; Jiang *et al.*, 2015), perhaps by linking to the microtubule cytoskeleton (Trivedi *et al.*, 2017). However, more studies are needed to understand the exact mechanisms by which actin filaments contribute to this function.

3.2 Roles for BicD2 in brain development

Dynein is responsible for all known forms of retrograde microtubule motor activity in interphase cells, and performs a wide array of cellular roles (Vallee, McKenney and Ori-McKenney, 2012; Reck-Peterson *et al.*, 2018). BicD2 is one member of a group of structurally related dynein cargo adaptor proteins, which coordinate the assembly of its regulators dynactin and LIS1 into a supercomplex for enhanced transport (Splinter *et al.*, 2012; Liu *et al.*, 2013; McKenney *et al.*, 2014). Using co-immunoprecipitation and immunofluorescence approaches, we identified Nesprin-2 as a novel BicD2 interactor, specifically with its C-terminal portion, which was also show to bind the Golgi GTPase Rab6 (Matanis *et al.*, 2002) and the nucleoporin RanBP2 (Splinter *et al.*, 2010). These results support the multivalence of BicD2 in cargo binding, presumably associated with a remarkable degree of functional diversity.

A study in the *C. elegans* worm revealed that the KASH protein UNC-83 interacted physically with dynein through BICD-1 and NUD-2 (Fridolfsson *et al.*, 2010). We found that in mammalian cells BicD2 interacts directly and colocalizes at the NE with Nesprin-2 through its microtubule motor-biding domain. Experiments in the developing brain revealed that BicD2, as for Nesprin-2, was required for nuclear transport in post-mitotic migrating neurons. These results further supported our *in vitro* findings and revealed a novel interaction between BicD2 and Nesprin-2.

One interesting and still unanswered question is how BicD2 shifts from its cytoplasmic functions to the NE. Based on current evidence we know that BicD2 can be recruited to the NE during G2 phase of the cell cycle by RanBP2 (Splinter *et al.*, 2010; Hu *et al.*, 2013; Baffet, Hu and Vallee, 2015). This requires Cdk1 phosphorylation of RanBP2, which increases its affinity for BicD2 and targets it to the NE. Specifically in RGPs, this recruitment mechanism is necessary for apical INM (Baffet, Hu and Vallee, 2015). Here, we report Nesprin-2 as protein with the novel capacity of recruiting BicD2 to the NE, independent of cell cycle stage (Figure 2). This pathway has an important function during neuronal migration and it is possible that there is a mechanism that increases the BicD2/dynein recruitment capacity of Nesprin-2 at this stage. However, this has to be tested.

Significantly, we find another role for BicD2 in brain development. BicD2 had been implicated in RGP behavior and in the multipolar-to-bipolar transition of post mitotic neurons (Hu *et al.*, 2013). Evidence from *BicD2* KO mice also suggested a role for this protein in neuronal migration, as these animals displayed severe layering

defects in the neocortex and cerebellum. The authors concluded that abnormalities in the secretion of factors from Bergmann glial cells in the cerebellum caused a non-cell autonomous arrest on migrating neurons (Jaarsma *et al.*, 2014). We now find an additional, and fundamental, cell autonomous role for BicD2 in cortical neuronal migration, which further elucidates the importance of this protein in brain development. These data should be of considerable interest in understanding the broad range of pathological consequences associated with human BicD2 mutations (Lipka *et al.*, 2013; Fiorillo *et al.*, 2016; Ravenscroft *et al.*, 2016).

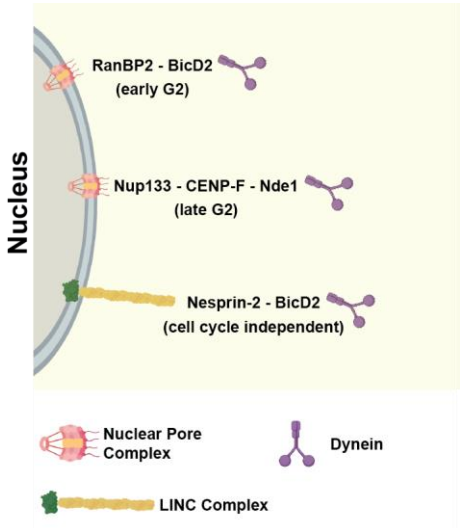

Figure 2: Schematic diagram depicting mechanisms for dynein NE recruitment mechanisms in G2 vs Non-G2 phase of the cell cycle. During G2 in RGP cells dynein is recruited by two consecutive Nuclear Pore Complex-dependent pathways (Hu et al., 2013; Baffet, Hu and Vallee, 2015), the "early-pathway", via nucleoporin RanBP2/BicD2 and the "late-pathway" via the nucleoporin Nup133/CENP-F/Nde1. Our data revealed that BicD2 and dynein are recruited by the microtubule motor-binding domain of Nesprin-2, part of the LINC complex, independent of the cell cycle stage. Diagram created using BioRender.

3.3 Roles for the LICs in brain development

The results from Chapter 2.1 establish differential physiological roles for LIC1 and LIC2 dynein populations during the rodent brain development (Figure 1). We observe evidence of this in embryonic neurogenesis and post-mitotic neuronal migration with consequences for the post-natal brain. Our results find LIC1 to be required for apical INM recruited by BicD2, and later in development for the multipolar-to-bipolar transition and locomotion. On the other hand, LIC2 was dispensable for the previous processes, but necessary for the little-studied mechanism of neuronal TST (Figure 3).

Our experiments revealed discrete roles for LIC1 and LIC2 in the embryonic brain. Using KD approaches and expression of truncated LICs we determined that LIC1-, but not LIC2-containing dynein is essential for apical INM in RGP cells. Judging by the position of the nuclear arrest when we interfere with LIC1, we hypothesized that this effect could be due to inability of dynein to bind to BicD2. In fact, when we overexpressed a version of LIC1 lacking the region that could bind to BicD2, or other dynein adaptors, we mimicked the effects seen with LIC1 KD. In addition, overexpression of BicD2 on a LIC1 KD background failed to restore nuclei position, suggesting an interdependence between these molecules.

Notable, however, was the apparent lack of function of LIC2 in apical INM. We inhibited LIC2 using RNAi and overexpression of truncated proteins, but we did not observe an apparent effect on RGP nuclei distribution. Yet, abundant amounts of LIC2 were able to compensate for LIC1 loss, and restored nuclei position to control levels. Based on these results, we reasoned that BicD2 might bind the LICs differentially. Using pull down assays, we, indeed, observed that BicD2 could bind more LIC1 than LIC2. These results are consistent with a more dominant role of LIC1 in BicD2-mediated apical INM.

Previous work in the Vallee laboratory had shown a role for dynein and dynein-associated proteins in the multipolar-to-bipolar transition. In particular, inhibition of DHC, LIS1 or BicD2 all caused accumulation of cells in the IZ in the multipolar stage, preventing subsequent neuronal migration toward the CP (Tsai *et al.*, 2005; Tsai, Bremner and Vallee, 2007; Hu *et al.*, 2013). Consistently, we saw that LIC1 KD caused an arrest of cells in the IZ of the developing neocortex. A more careful morphological analysis revealed that the proportion of accumulated neurons that had multiple processes was increased, in line with a role for LIC1 in the multipolar-to-bipolar transition. Also, in support of a preferential role for LIC1 in BicD2-mediated functions, LIC2 had no effect on the multipolar-to-bipolar transition.

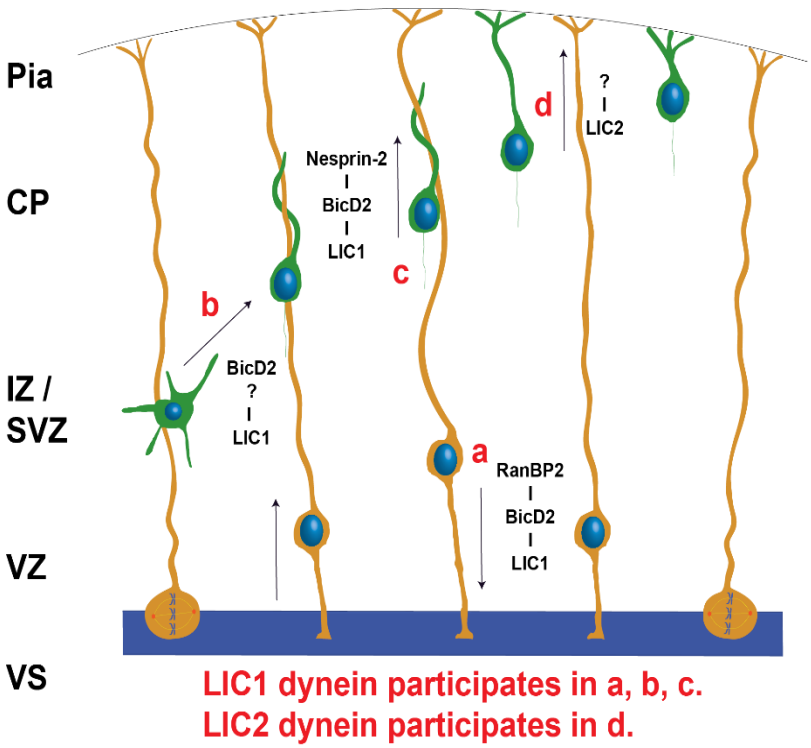

Figure 3: Roles for the LICs during neocortical development. Schematic illustration showing the pathways involving LIC1 and LIC2 in neural progenitor proliferation and neuronal migration. After division, RGPs (yellow) undergo INM, during which the nucleus migrates basally, and then apically for the next division. Neurons (green), originated from RGP division, assume a multipolar morphology in the SVZ/IZ. Then, they become bipolar and initiate migration toward the CP, using RGPs processes as scaffold. Closer to the MZ, neurons switch to TST. In this mode of migration neurons become detached from RGP fibers and attach their leading processes to the MZ so they can translocate their cell bodies toward their final destination. **LIC1-dependent pathways:** Apical nuclear migration of RGPs (a) is arrested and cells can no longer divide, as they are unable to reach the VS. In later stages, LIC1 also has a fundamental role in the multipolar-to-bipolar transition (b) and glial-guided migration (c), arresting neurons before they reach the CP. In (b) the specific requirement for the BicD2/LIC1 dynein mechanism remains undetermined, indicated with a question mark. **LIC2-dependent pathway:** There was no noticeable effect on RGP INM, the multipolar-to-bipolar transition and glial-guided migration. However, LIC2 is essential for the later stage of neuronal migration, TST of neurons in the upper CP (d). The dynein adaptor for LIC2 at this stage remains to be addressed, indicated with a question mark. Adapted from Chapter 2.1.

An interesting and still-outstanding question at this stage is the precise contribution of dynein during the multipolar-to-bipolar transition (Dantas *et al.*, 2016; Bertipaglia, Gonçalves and Vallee, 2018). This is a stage in which processes extend and retract dynamically, until one process becomes the axon and the other becomes the migratory leading process (Okamoto *et al.*, 2013; Namba *et al.*, 2014; Sakakibara *et al.*, 2014b). It has been shown that dynein helps to organize the polarity of the microtubule cytoskeleton for proper axonogenesis (del Castillo *et al.*, 2015). Presumably dynein participates in the multipolar-to-bipolar transition by helping to remodel the microtubule network (van Beuningen and Hoogenraad, 2016; Lu and Gelfand, 2017). Additionally, multipolar neurons are in a very dense environment with various signaling molecules sending important intracellular signals. Neurons have to interpret these clues and another possible role in which dynein might be important, is to mediate the transport of signaling vesicles from the periphery, i.e. from the extended processes, to the cell body (Fu and Holzbaur, 2014; Olenick, Dominguez and Holzbaur, 2019). Therefore, an impairment in dynein function could lead to an arrest in the multipolar stage as cells cannot receive the signals controlling their transition to a polarized state. We also note that inhibition of molecules involved on the recruitment of dynein to the NE in RGPs, such as RanBP2, Nup133, and CENP-F arrest post-mitotic neurons in a multipolar stage (Tsai *et al.*, 2005; Hu *et al.*, 2013). Although these proteins are involved in nuclear transport during G2, a relevant question is whether these mechanisms are still active in post-mitotic neurons. Thus, dynein might participate in neuronal polarization by regulating nuclear position (Tabata and Nakajima, 2003). Nonetheless, the role of dynein in the multipolar-to-bipolar transition remains unclear and future experiments will be needed to dissect it.

After becoming bipolar, neurons migrate from the IZ to the CP, where they will establish the layers of the neocortex. At first they migrate in a glial-guided fashion, also called locomotion. Then, once they are closer to the pial surface, neurons switch migration modes to a glial independent mode, called terminal somal translocation (Cooper, 2013). We have analyzed neuronal migration in brains inhibited for LIC1 and LIC2, which showed clear phenotypic differences. Expression of a truncated version of LIC1, incapable of cargo binding, caused a decrease in the number of neurons reaching the CP, without affecting the total number of bipolar neurons. This suggested an impairment in locomotion, and more detailed analysis by live imaging confirmed an arrest of bipolar migratory neurons, establishing a role for LIC1 at this stage. This was consistent with previous evidence that dynein was required for migration of neurons out of the IZ (Shu *et al.*, 2004; Tsai *et al.*, 2005; Tsai, Bremner and Vallee, 2007). Brains inhibited for LIC2 had cells in the CP in numbers comparable to the control, suggesting that locomotion depends on LIC1-, but not LIC2-containg dynein. This

finding further confirmed our observations that LICs have different roles during neocortical development. Additionally, our work in Chapter 2.2 found a role for BicD2 in locomotion, as this protein was required for neuronal migration out of the IZ. Thus, these results also support our judgment that BicD2 function depends on LIC1 more than LIC2 dynein, in line with what we had observed in apical INM and multipolar-to-bipolar transition.

Interestingly, although LIC2 had no noticeable function in locomotion, LIC2 inhibition caused a marked accumulation of migratory neuron somata at an abnormally large distance from the pial surface. Neurons were arrested mid-way in the CP, but still extended long processes that contacted the MZ. This was observed with using both LIC2 RNAi and expression of the inhibitory LIC2 G-domain. Using live imaging, we confirmed that these cells were unable to move their cell bodies toward the CP revealing a crucial function for LIC2 and dynein in neuronal TST. We note that we cannot rule out a contribution for LIC1 in TST, due to the severe effects of LIC1 inhibition prior to this stage. Nonetheless, to our knowledge, this is the first report of a microtubule motor role in neuronal TST.

How dynein acts in detail in neuronal TST is not clear, however our observations appear to phenocopy the effects of the Reelin downstream effector, Dab1, depletion on migratory neurons in the mouse brain (Olson and Walsh, 2006; Franco *et al.*, 2011; Sekine *et al.*, 2011; Gil-Sanz *et al.*, 2013). Reelin is secreted by the Cajal-Retzius cells, and provides a migratory gradient for neurons. Interestingly, Dab1 was shown to co-immunoprecipitate with LIS1, a dynein regulatory subunit, and this interaction was enhanced in a reelin-induced phosphorylation-dependent manner (Assadi *et al.*, 2003). Since Dab1 has been shown to regulate the actin cytoskeleton (Pramatarova *et al.*, 2003; Suetsugu *et al.*, 2004; Chai *et al.*, 2009) it is plausible that it also modulates microtubule cytoskeleton and affects dynein function. Perhaps, when neurons are about to reach the pial surface, Reelin levels trigger signaling cascades in neurons that ultimately require LIC2-dynein. Yet, future evidence will be important to address whether there is cross-talk between the reelin signaling pathway and dynein for TST.

Mutations in dynein genes have been shown to cause malformations of cortical development (Lipka *et al.*, 2013; Poirier *et al.*, 2013; Fiorillo *et al.*, 2014; Jamuar *et al.*, 2014) and our laboratory has contributed for the understanding of such diseases at the cellular level. To our knowledge, so far, no mutations in the LIC coding genes have been demonstrated to directly cause human neurodevelopmental disease, however our results clearly show fundamental roles for these two subunits in the process of neocortex formation at

embryonic stages with phenotypic consequences in the post-natal brain. Of note, a mouse model harboring a mutation in the *Dync1li1* (LIC1) gene presented disrupted brain development and behavioral defects (Banks *et al.*, 2011).

Seeking to explain the differential phenotypes for LIC1 and LIC2 in neocortical development that we had observed, we investigated whether LIC1 and LIC2 relative levels would change from the embryo to the adult. One would expect that if the phenotypic differences were due to more expression of LIC1 in RGPs and less in neurons, compared to LIC2, the levels of these proteins would fluctuate across the conditions analyzed. We did not verify this, as LIC1 *vs* LIC2 relative levels were unchanged in late embryonic stage and in the adult. We also stained brain slices with specific LIC1 and LIC2 antibodies and we did not find a noticeable difference in layer distribution. These data suggest that the differential roles for each LIC are due to functional differences, rather than differential expression levels. As noted before, BicD2-dependent functions appear to be mediated preferentially by LIC1 rather by LIC2. This might underlie the functional differences between the LICs that we observe during neocortical development.

BicD2 and other dynein adaptors bind to the C-terminal portion of the LICs, which is least conserved region between LIC1 and LIC2. This might affect how the LICs interact with dynein adaptors and explain why LIC1 is preferentially recruited by BicD2. In support of a cargo-binding functional difference for the LICs, discrete cargoes have been characterized for each one of them. Pericentrin was shown to exclusively bind LIC1, and PAR3 only interacted with LIC2 (Tynan *et al.*, 2000; Schmoranzer *et al.*, 2009). However, more studies will be needed to determine the cargo-binding functional difference between LIC1 and LIC2, as these seem to influence the specific roles that each LIC has within the cell.

Recent studies have elucidated the structure of dynein LICs and the functional domains responsible for dynein and cargo binding (Schroeder *et al.*, 2014; Lee *et al.*, 2018). We have expressed in the brain a truncated version of each LIC, specifically the G-domain that binds to dynein. Because both LICs bind to the same region of the DHC (Tynan, Gee and Vallee, 2000) one would expect similar phenotypes with the expression of either LIC1 or LIC2 G-domain. Our results clearly showed that LIC1 expression lacking the adaptor domain strongly interfered with dynein function, as shown by the effects on neurogenesis and neuronal migration in embryonic rat brain. Nevertheless, this was clearly different from the phenotype seen with the LIC2 G-domain, which showed a significant effect only in later stages of neuronal migration. This led us to speculate that distinct populations of dynein complexes exist, in which different subunit components and/or regulatory

mechanisms might either depend on or dictate LIC composition on dynein molecule. In support of this idea, pull-down experiments with LIC1 vs LIC2 followed by analysis by mass spectrometry revealed that each LIC pulled down a different composition of LCs (Redwine *et al.*, 2017). Similar to the LICs, the LCs per se can also form mutually exclusive populations of dynein (Tynan *et al.*, 2000; Tynan, Gee and Vallee, 2000; Tai, Chuang and Sung, 2001). Thus, one interesting possibility is that the LCs and LICs might influence each other's behavior, and determine the composition of different dynein subfractions, but further experiments are needed to address this interesting question.

3.4 Final remarks

In summary, the work done for this PhD thesis has advanced our knowledge on the roles of molecular motors during brain development. In particular, we have made important findings on the mechanims that govern neocortical neuronal migration. Our results have shown that nuclear transport in migratory neurons depends on the recruitment of the dynein/BicD2 complex by Nesprin-2. Additionally, we have gained significant insight into the nuclear *vs* centrosome transport dynamics and that dynein and kinesin-1 act cooperatively during neuronal migration. Furthermore, we have identified two distinct dynein populations with discrete roles in brain development, and we found that dynein is required for TST, an unexplored neuronal migration mechanism. Our results in the brain also help to better define the basis of molecular motor regulation. Finally, this work contributes for the understanding of brain neurodevelopmental diseases arising from genetic mutations in dynein and dynein-associated genes.

References:

Assadi, A. H. *et al.* (2003) 'Interaction of reelin signaling and Lis1 in brain development', *Nature Genetics*, 35(3), pp. 270–276. doi: 10.1038/ng1257.

Baffet, A. D., Hu, D. J. and Vallee, R. B. (2015) 'Cdk1 Activates Pre-mitotic Nuclear Envelope Dynein Recruitment and Apical Nuclear Migration in Neural Stem Cells', *Developmental Cell*. Elsevier Inc., 33(6), pp. 703–716. doi: 10.1016/j.devcel.2015.04.022.

Banks, G. T. *et al.* (2011) 'Behavioral and other phenotypes in a cytoplasmic Dynein light intermediate chain 1 mutant mouse.', *The Journal of neuroscience : the official journal of the Society for Neuroscience*, 31(14), pp. 5483–5494. doi: 10.1523/JNEUROSCI.5244-10.2011.

Bellion, A. *et al.* (2005) 'Nucleokinesis in tangentially migrating neurons comprises two alternating phases: forward migration of the Golgi/centrosome associated with centrosome splitting and myosin contraction at the rear.', *The Journal of neuroscience : the official journal of the Society for Neuroscience*, 25(24), pp. 5691–9. doi: 10.1523/JNEUROSCI.1030-05.2005.

Bertipaglia, C., Gonçalves, J. C. and Vallee, R. B. (2018) 'Nuclear migration in mammalian brain development', *Seminars in Cell & Developmental Biology*, 82, pp. 57–66. doi: 10.1016/j.semcdb.2017.11.033.

van Beuningen, S. F. and Hoogenraad, C. C. (2016) 'Neuronal polarity: remodeling microtubule organization', *Current Opinion in Neurobiology*. Elsevier Ltd, 39, pp. 1–7. doi: 10.1016/j.conb.2016.02.003.

del Castillo, U. *et al.* (2015) 'Interplay between kinesin-1 and cortical dynein during axonal outgrowth and microtubule organization in Drosophila neurons.', *eLife*, 4(12), p. e10140. doi: 10.7554/eLife.10140.

Chai, X. *et al.* (2009) 'Reelin Stabilizes the Actin Cytoskeleton of Neuronal Processes by Inducing n-Cofilin Phosphorylation at Serine3', *Journal of Neuroscience*, 29(1), pp. 288–299. doi: 10.1523/JNEUROSCI.2934-08.2009.

Cooper, J. A. (2013) 'Mechanisms of cell migration in the nervous system', *The Journal of Cell Biology*, 202(5), pp. 725–734. doi: 10.1083/jcb.201305021.

Dantas, T. J. *et al.* (2016) 'Emerging roles for motor proteins in progenitor cell behavior and neuronal

migration during brain development', *Cytoskeleton*, 73(10), p. Spc1. doi: 10.1002/cm.21337.

Doobin, D. J. *et al.* (2016) 'Severe NDE1-mediated microcephaly results from neural progenitor cell cycle arrests at multiple specific stages', *Nature Communications*. Nature Publishing Group, 7, pp. 1–14. doi: 10.1038/ncomms12551.

Dujardin, D. L. *et al.* (2003) 'A role for cytoplasmic dynein and LIS1 in directed cell movement', *Journal of Cell Biology*, 163(6), pp. 1205–1211. doi: 10.1083/jcb.200310097.

Falnikar, A., Tole, S. and Baas, P. W. (2011) 'Kinesin-5, a mitotic microtubule-associated motor protein, modulates neuronal migration', *Molecular Biology of the Cell*, 22(9), pp. 1561–1574. doi: 10.1091/mbc.e10-11-0905.

Fiorillo, C. *et al.* (2014) 'Novel dynein DYNC1H1 neck and motor domain mutations link distal spinal muscular atrophy and abnormal cortical development', *Human Mutation*, 35(3), pp. 298–302. doi: 10.1002/humu.22491.

Fiorillo, C. *et al.* (2016) 'Beyond spinal muscular atrophy with lower extremity dominance: Cerebellar hypoplasia associated with a novel mutation in BICD2', *European Journal of Neurology*, 23(4), pp. e19–e21. doi: 10.1111/ene.12914.

Franco, S. J. *et al.* (2011) 'Reelin Regulates Cadherin Function via Dab1/Rap1 to Control Neuronal Migration and Lamination in the Neocortex', *Neuron*, 69(3), pp. 482–497. doi: 10.1016/j.neuron.2011.01.003.

Fridolfsson, H. N. *et al.* (2010) 'UNC-83 coordinates kinesin-1 and dynein activities at the nuclear envelope during nuclear migration', *Developmental Biology*, 338(2), pp. 237–250. doi: 10.1016/j.ydbio.2009.12.004.

Fu, M. M. and Holzbaur, E. L. F. (2014) 'Integrated regulation of motor-driven organelle transport by scaffolding proteins', *Trends in Cell Biology*. Elsevier Ltd, pp. 1–11. doi: 10.1016/j.tcb.2014.05.002.

Gil-Sanz, C. *et al.* (2013) 'Cajal-Retzius cells instruct neuronal migration by coincidence signaling between secreted and contact-dependent guidance cues', *Neuron*, 79(3), pp. 461–477. doi: 10.1016/j.neuron.2013.06.040.

Grabham, P. W. *et al.* (2007) 'Cytoplasmic dynein and LIS1 are required for microtubule advance during growth cone remodeling and fast axonal outgrowth.', *The Journal of neuroscience : the official journal of the*

Society for Neuroscience, 27(21), pp. 5823–5834. doi: 10.1523/JNEUROSCI.1135-07.2007.

Hu, D. J.-K. *et al.* (2013) 'Dynein Recruitment to Nuclear Pores Activates Apical Nuclear Migration and Mitotic Entry in Brain Progenitor Cells', *Cell*, 154(6), pp. 1300–1313. doi: 10.1016/j.cell.2013.08.024.

Jaarsma, D. *et al.* (2014) 'A role for Bicaudal-D2 in radial cerebellar granule cell migration.', *Nature communications*. Nature Publishing Group, 5, p. 3411. doi: 10.1038/ncomms4411.

Jamuar, S. S. *et al.* (2014) 'Somatic Mutations in Cerebral Cortical Malformations', *New England Journal of Medicine*, 371(8), pp. 733–743. doi: 10.1056/NEJMoa1314432.

Jiang, J. *et al.* (2015) 'Spatiotemporal dynamics of traction forces show three contraction centers in migratory neurons', *Journal of Cell Biology*, 209(5), pp. 759–774. doi: 10.1083/jcb.201410068.

Lee, I.-G. *et al.* (2018) 'A conserved interaction of the dynein light intermediate chain with dynein-dynactin effectors necessary for processivity', *Nature Communications*, 9(1), p. 986. doi: 10.1038/s41467-018-03412-8.

Lee, Y. L. and Burke, B. (2018) 'LINC complexes and nuclear positioning', *Seminars in Cell & Developmental Biology*. Elsevier Ltd, 82, pp. 67–76. doi: 10.1016/j.semcdb.2017.11.008.

Lipka, J. *et al.* (2013) 'Mutations in cytoplasmic dynein and its regulators cause malformations of cortical development and neurodegenerative diseases.', *Biochemical Society transactions*, 41(6), pp. 1605–12. doi: 10.1042/BST20130188.

Liu, Y. *et al.* (2013) 'Bicaudal-D uses a parallel, homodimericcoiled coil with heterotypic registry tocoordinate recruitment of cargos to dynein', *Genes and Development*, 27(11), pp. 1233–1246. doi: 10.1101/gad.212381.112.

Lu, W. and Gelfand, V. I. (2017) 'Moonlighting Motors: Kinesin, Dynein, and Cell Polarity', *Trends in Cell Biology*. Elsevier Ltd, xx, pp. 1–10. doi: 10.1016/j.tcb.2017.02.005.

Luxton, G. W. G. *et al.* (2010) 'Linear arrays of nuclear envelope proteins harness retrograde actin flow for nuclear movement.', *Science (New York, N.Y.)*, 329(5994), pp. 956–9. doi: 10.1126/science.1189072.

Matanis, T. *et al.* (2002) 'Bicaudal-D regulates COPI-independent Golgi-ER transport by recruiting the dynein-dynactin motor complex', *Nature Cell Biology*, 4(12), pp. 986–992. doi: 10.1038/ncb891.

McKenney, R. J. *et al.* (2014) 'Activation of cytoplasmic dynein motility by dynactin-cargo adapter complexes.', *Science (New York, N.Y.)*, 345(6194), pp. 337–41. doi: 10.1126/science.1254198.

Metzger, T. *et al.* (2012) 'MAP and kinesin-dependent nuclear positioning is required for skeletal muscle function', *Nature*, 484(7392), pp. 120–124. doi: 10.1038/nature10914.

Namba, T. *et al.* (2014) 'Pioneering axons regulate neuronal polarization in the developing cerebral cortex', *Neuron*. Elsevier Inc., 81(4), pp. 814–829. doi: 10.1016/j.neuron.2013.12.015.

Okamoto, M. *et al.* (2013) 'TAG-1-assisted progenitor elongation streamlines nuclear migration to optimize subapical crowding.', *Nature neuroscience*, 16(11), pp. 1556–66. doi: 10.1038/nn.3525.

Olenick, M. A., Dominguez, R. and Holzbaur, E. L. F. (2019) 'Dynein activator Hook1 is required for trafficking of BDNF-signaling endosomes in neurons.', *The Journal of cell biology*, 218(1), pp. 220–233. doi: 10.1083/jcb.201805016.

Olson, E. C. and Walsh, C. A. (2006) 'Impaired Neuronal Positioning and Dendritogenesis in the Neocortex after Cell-Autonomous Dab1 Suppression', *Journal of Neuroscience*, 26(6), pp. 1767–1775. doi: 10.1523/JNEUROSCI.3000-05.2006.

Poirier, K. *et al.* (2013) 'Mutations in TUBG1, DYNC1H1, KIF5C and KIF2A cause malformations of cortical development and microcephaly.', *Nature genetics*, 45(6), pp. 639–47. doi: 10.1038/ng.2613.

Pramatarova, A. *et al.* (2003) 'Nck beta interacts with tyrosine-phosphorylated disabled 1 and redistributes in Reelin-stimulated neurons.', *Molecular and cellular biology*, 23(20), pp. 7210–21. doi: PMC230306.

Rao, A. N. *et al.* (2016) 'Sliding of centrosome-unattached microtubules defines key features of neuronal phenotype', *Journal of Cell Biology*, 213(3), pp. 329–341. doi: 10.1083/jcb.201506140.

Ravenscroft, G. *et al.* (2016) 'Recurrent de novo BICD2 mutation associated with arthrogryposis multiplex congenita and bilateral perisylvian polymicrogyria', *Neuromuscular Disorders*. Elsevier B.V., 26(11), pp. 744–748. doi: 10.1016/j.nmd.2016.09.009.

Reck-Peterson, S. L. *et al.* (2018) 'The cytoplasmic dynein transport machinery and its many cargoes', *Nature Reviews Molecular Cell Biology*. Springer US, 19(6), pp. 382–398. doi: 10.1038/s41580-018-0004-3.

Redwine, W. B. *et al.* (2017) 'The human cytoplasmic dynein interactome reveals novel activators of motility',

eLife, 6, pp. 1–27. doi: 10.7554/eLife.28257.

Roux, K. J. *et al.* (2009) 'Nesprin 4 is an outer nuclear membrane protein that can induce kinesin-mediated cell polarization', *Proceedings of the National Academy of Sciences*, 106(7), pp. 2194–2199. doi: 10.1073/pnas.0808602106.

Sakakibara, A. *et al.* (2014) 'Dynamics of centrosome translocation and microtubule organization in neocortical neurons during distinct modes of polarization', *Cerebral Cortex*, 24(5), pp. 1301–1310. doi: 10.1093/cercor/bhs411.

Schaar, B. T. and McConnell, S. K. (2005) 'Cytoskeletal coordination during neuronal migration', *Proceedings of the National Academy of Sciences*, 102(38), pp. 13652–13657. doi: 10.1073/pnas.0506008102.

Schmoranzer, J. *et al.* (2009) 'Par3 and Dynein Associate to Regulate Local Microtubule Dynamics and Centrosome Orientation during Migration', *Current Biology*, 19(13), pp. 1065–1074. doi: 10.1016/j.cub.2009.05.065.

Schneider, M. *et al.* (2011) 'Molecular mechanisms of centrosome and cytoskeleton anchorage at the nuclear envelope', *Cellular and Molecular Life Sciences*, 68(9), pp. 1593–1610. doi: 10.1007/s00018-010-0535-z.

Schroeder, C. M. *et al.* (2014) 'A Ras-like domain in the light intermediate chain bridges the dynein motor to a cargo-binding region.', *eLife*, 3, p. e03351. doi: 10.7554/eLife.03351.

Sekine, K. *et al.* (2011) 'The Outermost Region of the Developing Cortical Plate Is Crucial for Both the Switch of the Radial Migration Mode and the Dab1-Dependent "Inside-Out" Lamination in the Neocortex', *Journal of Neuroscience*, 31(25), pp. 9426–9439. doi: 10.1523/JNEUROSCI.0650-11.2011.

Shu, T. *et al.* (2004) 'Ndel1 operates in a common pathway with LIS1 and cytoplasmic dynein to regulate cortical neuronal positioning', *Neuron*. Cell Press, 44(2), pp. 263–277. doi: 10.1016/j.neuron.2004.09.030.

Shubeita, G. T. *et al.* (2008) 'Consequences of Motor Copy Number on the Intracellular Transport of Kinesin-1-Driven Lipid Droplets', *Cell*. Elsevier Ltd, 135(6), pp. 1098–1107. doi: 10.1016/j.cell.2008.10.021.

Solecki, D. J. *et al.* (2009) 'Myosin II Motors and F-Actin Dynamics Drive the Coordinated Movement of the Centrosome and Soma during CNS Glial-Guided Neuronal Migration', *Neuron*, 63(1), pp. 63–80. doi: 10.1016/j.neuron.2009.05.028.

Splinter, D. *et al.* (2010) 'Bicaudal D2, dynein, and kinesin-1 associate with nuclear pore complexes and regulate centrosome and nuclear positioning during mitotic entry', *PLoS Biology*, 8(4). doi: 10.1371/journal.pbio.1000350.

Splinter, D. *et al.* (2012) 'BICD2, dynactin, and LIS1 cooperate in regulating dynein recruitment to cellular structures', *Molecular Biology of the Cell*, 23(21), pp. 4226–4241. doi: 10.1091/mbc.E12-03-0210.

Suetsugu, S. *et al.* (2004) 'Regulation of actin cytoskeleton by mDab1 through N-WASP and ubiquitination of mDab1.', *The Biochemical journal*, 384(Pt 1), pp. 1–8. doi: 10.1042/BJ20041103.

Tabata, H. and Nakajima, K. (2003) 'Multipolar migration: the third mode of radial neuronal migration in the developing cerebral cortex.', *The Journal of neuroscience : the official journal of the Society for Neuroscience*, 23(31), pp. 9996–10001.

Tai, A. W., Chuang, J. Z. and Sung, C. H. (2001) 'Cytoplasmic dynein regulation by subunit heterogeneity and its role in apical transport', *Journal of Cell Biology*, 153(7), pp. 1499–1509. doi: 10.1083/jcb.153.7.1499.

Trivedi, N. *et al.* (2017) 'Drebrin-mediated microtubule-actomyosin coupling steers cerebellar granule neuron nucleokinesis and migration pathway selection.', *Nature communications*. Nature Publishing Group, 8, p. 14484. doi: 10.1038/ncomms14484.

Tsai, J.-W., Bremner, K. H. and Vallee, R. B. (2007) 'Dual subcellular roles for LIS1 and dynein in radial neuronal migration in live brain tissue.', *Nature neuroscience*, 10(8), pp. 970–979. doi: 10.1038/nn1934.

Tsai, J. W. *et al.* (2005) 'LIS1 RNA interference blocks neural stem cell division, morphogenesis, and motility at multiple stages', *Journal of Cell Biology*, 170(6), pp. 935–945. doi: 10.1083/jcb.200505166.

Tynan, S. H. *et al.* (2000) 'Light intermediate chain 1 defines a functional subfraction of cytoplasmic dynein which binds to pericentrin', *Journal of Biological Chemistry*, 275(42), pp. 32763–32768. doi: 10.1074/jbc.M001536200.

Tynan, S. H., Gee, M. A. and Vallee, R. B. (2000) 'Distinct but overlapping sites within the cytoplasmic dynein heavy chain for dimerization and for intermediate chain and light intermediate chain binding', *Journal of Biological Chemistry*, 275(42), pp. 32769–32774. doi: 10.1074/jbc.M001537200.

Umeshima, H. *et al.* (2019) 'Local traction force in the proximal leading process triggers nuclear translocation during neuronal migration.', *Neuroscience research*. Elsevier Ireland Ltd and Japan Neuroscience Society, 142, pp. 38–48. doi: 10.1016/j.neures.2018.04.001.

Umeshima, H., Hirano, T. and Kengaku, M. (2007) 'Microtubule-based nuclear movement occurs independently of centrosome positioning in migrating neurons', *Proceedings of the National Academy of Sciences*, 104(41), pp. 16182–16187. doi: 10.1073/pnas.0708047104.

Vallee, R. B., McKenney, R. J. and Ori-McKenney, K. M. (2012) 'Multiple modes of cytoplasmic dynein regulation', *Nature Cell Biology*. Nature Publishing Group, 14(3), pp. 224–230. doi: 10.1038/ncb2420.

Wilson, M. H. and Holzbaur, E. L. F. (2012) 'Opposing microtubule motors drive robust nuclear dynamics in developing muscle cells', *Journal of Cell Science*, 125(17), pp. 4158–4169. doi: 10.1242/jcs.108688.

Wilson, M. H. and Holzbaur, E. L. F. (2015) 'Nesprins anchor kinesin-1 motors to the nucleus to drive nuclear distribution in muscle cells', *Development*, 142(1), pp. 218–228. doi: 10.1242/dev.114769.

Wu, Y. K. *et al.* (2018) 'Nesprins and opposing microtubule motors generate a point force that drives directional nuclear motion in migrating neurons.', *Development (Cambridge, England)*, 145(5), p. dev158782. doi: 10.1242/dev.158782.

Zhang, X. *et al.* (2009) 'SUN1/2 and Syne/Nesprin-1/2 Complexes Connect Centrosome to the Nucleus during Neurogenesis and Neuronal Migration in Mice', *Neuron*. Elsevier Ltd, 64(2), pp. 173–187. doi: 10.1016/j.neuron.2009.08.018.

Zhu, R., Antoku, S. and Gundersen, G. G. (2017) 'Centrifugal Displacement of Nuclei Reveals Multiple LINC Complex Mechanisms for Homeostatic Nuclear Positioning', *Current Biology*. Elsevier Ltd., pp. 1–14. doi: 10.1016/j.cub.2017.08.073.